KoG

SCIENTIFIC - PROFESSIONAL JOURNAL
OF CROATIAN SOCIETY FOR GEOMETRY AND GRAPHICS

No. 27. (2023)
ISSN 1331-1611

ISSN 1331-1611
9 771331 161005

KoG

Official publication of the Croatian Society for Geometry and Graphics publishes scientific and professional papers from the fields of geometry, applied geometry and computer graphics.

Founder and Publisher

Croatian Society for Geometry and Graphics

Design

Miroslav Ambruš-Kiš

Layout

Sonja Gorjanc, Ema Jurkin

Cover Illustration

Marija Šimić Horvath, photography

Print

SAND d.o.o., Zagreb

URL address

http://www.hdgg.hr/kog
http://hrcak.srce.hr

Edition

150

Published annually

Guide for authors
Please, see the page 60.

KoG is reviewed by zbMATH.

This issue has been financially supported by the Ministry of Science and Education.

ISSN 1331–1611

KoG

No. 27

Zagreb, 2023

SCIENTIFIC AND PROFESSIONAL JOURNAL OF
CROATIAN SOCIETY FOR GEOMETRY AND GRAPHICS

CONTENTS

ORIGINAL SCIENTIFIC PAPERS

R. Garcia, D. Tejada: Principal Lines on an Ellipsoid in a Minkowski Three-Dimensional Space ... 3

B. Odehnal: A Miquel-Steiner Transformation ... 14

W. Jank, G. Glaeser, B. Odehnal: On the Geometry of Spherical Trochoids ... 25

I. Kodrnja, H. Koncul: Locus Curves in Triangle Families ... 35

PROFESSIONAL PAPERS

M. Đuzel, I. Filipan, Lj. Primorac Gajčić: Curves in 3-dimensional Minkowski Space ... 43

V. Volenec, E. Jurkin, M. Šimić Horvath: Circles Related to a Complete Quadrangle ... 51

ISSN 1331–1611

KoG

BROJ 27
Zagreb, 2023

ZNANSTVENO-STRUČNI ČASOPIS
HRVATSKOG DRUŠTVA ZA GEOMETRIJU I GRAFIKU

SADRŽAJ

ORIGINALNI ZNANSTVENI RADOVI

R. Garcia, D. Tejada: Glavne krivulje zakrivljenosti elipsoida u trodimenzionalnom prostoru Minkowskog 3

B. Odehnal: Miquel-Steinerova transformacija 14

W. Jank, G. Glaeser, B. Odehnal: O geometriji sfernih trohoida 25

I. Kodrnja, H. Koncul: Lokus krivulje u familijama trokuta 35

STRUČNI RADOVI

M. Đuzel, I. Filipan, Lj. Primorac Gajčić: Krivulje u 3-dimenzionalnom Minkowskijevom prostoru 43

V. Volenec, E. Jurkin, M. Šimić Horvath: Kružnice pridružene potpunom četverovrhu 51

https://doi.org/10.31896/k.27.1
Original scientific paper
Accepted 15. 9. 2023.

RONALDO GARCIA
DIMAS TEJADA

Principal Lines on an Ellipsoid in a Minkowski Three-Dimensional Space

Principal Lines on an Ellipsoid in a Minkowski Three-Dimensional Space

ABSTRACT

The description of principal lines of the ellipsoid on the 3-dimensional Minkowski space is established. A global principal parametrization of a triple orthogonal system of quadrics is also achieved, and the focal set of the ellipsoid is sketched.

Key words: principal lines, configuration principal, Minkowski three-dimensional space, ellipsoid, triple orthogonal system

MSC2010: 53C12, 53C50, 37C86, 37E35

Glavne krivulje zakrivljenosti elipsoida u trodimenzionalnom prostoru Minkowskog

SAŽETAK

U radu su opisane glavne krivulje zakrivljenosti (crte krivine) elipsoida u trodimenzionalnom Minkowskijevom prostoru. Navedena je i globalna parametrizacija trostruko ortogonalnog sustava te je prikazan fokalni skup elipsoida.

Ključne riječi: glavne krivulje zakrivljenosti (crte krivine), glavna konfiguracija, trodimenzionalni prostor Minkowskog, elipsoid, trostruko ortogonalni sustav

1 Introduction

The goal of this work is to describe the global behavior of principal lines of the ellipsoid in the three dimensional Minkwoswki space $\mathbb{R}^{2,1}$. We recall that the concept of principal lines were introduced by G. Monge [11] and geometrically they can be characterized as the curves on the surface such that the ruled surface having the rules being the normal straight lines along the curve is a developable surface [18, page 93].

The principal lines of the ellipsoid with three different axes in the Euclidean space $\mathbb{R}^3$ are as illustrated in Fig. 1. In this case, the principal lines of the triaxial ellipsoid are obtained by Dupin's theorem. The ellipsoid belongs to a triple orthogonal family of surfaces, formed by the ellipsoid and two hyperboloids (one of one leaf and the other of two leaves).

For more recent and historical developments of principal lines on surfaces see [4], [13], [14], [15] and [16]. This work is organized as follows. In section 2 we recall the basic properties of the Minkowski 3-space and principal lines. In section 3 we describe the global behavior of principal lines in the ellipsoid. In section 4 we will describe the topological equivalence of the principal configuration of the ellipsoid. In section 5 we will show that the geometric inversion in Minkowski 3-space preserves lines of curvature. In section 6 we obtain a triple orthogonal system of quadrics. Finally, in section 7 the focal set of the ellipsoid is analyzed.

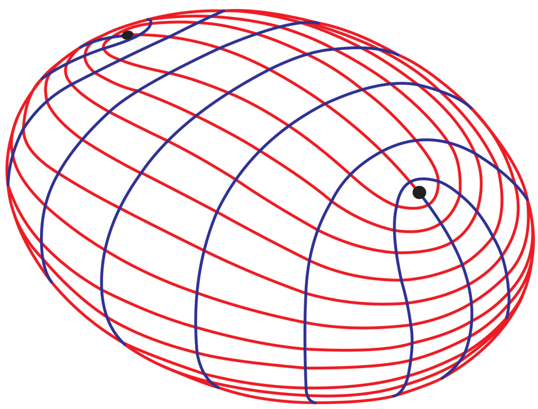

Figure 1: *Principal lines on the triaxial ellipsoid. There are four umbilic points, the singularities. Also, there are four umbilic separatrices and other principal lines are closed.*

2 Preliminaries

The Minkowski 3-space $\mathbb{R}^{2,1} = (\mathbb{R}^3, \langle , \rangle)$ is the vector space $\mathbb{R}^3$ endowed with the inner product $\langle u, v\rangle = u_1v_1 + u_2v_2 - u_3v_3$, where $u = (u_1,u_2,u_3)$ and $v = (v_1,v_2,v_3)$. The norm is $\|v\| = \sqrt{|\langle v, v\rangle|}$.

The vector product $u\times v$, is a vector such that $\langle u\times v,u\rangle = \langle u\times v, v\rangle = 0$. Then

$$u\times v = \begin{vmatrix} i & j & -k \\ u_1 & u_2 & u_3 \\ v_1 & v_2 & v_3 \end{vmatrix}.$$

A vector v is said to be

- spacelike, if $\langle v, v\rangle > 0$ or $v = 0$,
- timelike, if $\langle v, v\rangle < 0$,
- lightlike, if $\langle v, v\rangle = 0$ and $v \neq 0$.

A plane is called spacelike (resp. timelike, lightlike), if the normal vector is timelike (resp. spacelike, lightlike).

A regular curve is spacelike (resp. timelike, lightlike) if the tangent vector is spacelike (resp. timelike, lightlike). A smooth surface is called spacelike (resp. timelike) if the tangent planes are spacelike (resp. timelike).

Let $\alpha\colon M \to \mathbb{R}^{2,1}$ be a C^r ($r \geq 4$) immersion of a smooth and oriented surface M of dimension two in $\mathbb{R}^{2,1}$. Let $X(u,v)\colon \mathbb{R}^2 \to M$ be a local parametrization. The first fundamental form is

$$I = Edu^2 + 2Fdudv + Gdv^2,$$

where $E = \langle Xu,Xu\rangle$, $F = \langle Xu,Xv\rangle$ and $G = \langle Xv,Xv\rangle$.

Given $p\in M$, if $det(I_p) = EG - F^2$ is positive (resp. negative), the surface is spacelike or Riemannian (resp. timelike or Lorentzian) in the point p. This is equivalent to say that tangent plane is spacelike or timelike. The metric induced on M can be degenerate; this happens at the points p on M where the tangent space TM_p is lightlike, or equivalently that $det(I_p) = EG - F^2 = 0$. We call this set of points the *tropic* and will be denoted by LD (Locus of Degeneracy).

On a spacelike (resp. timelike) surface, we define the *Gauss map*

$$N(u,v) = \varepsilon\cdot \frac{\alpha_u\times\alpha_v}{\|\alpha_u\times\alpha_v\|}(u,v)$$

such that $N\colon M \to H^{2,1}$ with $\varepsilon = 1$ (resp. $N\colon M \to S^{2,1}$ with $\varepsilon = -1$), where $H^{2,1} = \{(x,y,z)\in\mathbb{R}^3 : x^2+y^2-z^2 = -1\}$ and $S^{2,1} = \{(x,y,z)\in\mathbb{R}^3 : x^2+y^2-z^2 = 1\}$.

The sign $\varepsilon = \pm 1$ is only necessary to define the base positively oriented $\{\alpha_u, \alpha_v, N\}$ in all over the surface (except in the tropic), this is,
$det(\alpha_u,\alpha_v,N) = \dfrac{\varepsilon}{\|\alpha_u\times\alpha_v\|}\langle\alpha_u\times\alpha_v, \alpha_u\times\alpha_v\rangle > 0$,
[9, page 50].

The second fundamental form is

$$II = edu^2 + 2fdudv + gdv^2,$$

where $e = \langle X_{uu},N\rangle$, $f = \langle X_{uv},N\rangle$ and $g = \langle X_{vv},N\rangle$.

The mean curvature H and Gauss curvature K are defined by

$$H = \frac{Eg+Ge-2Ff}{2(EG-F^2)} \text{ and } K = \frac{eg-f^2}{EG-F^2},$$

and the principal curvatures k_1 and k_2 are defined by

$$k_1 = H+\sqrt{H^2-K} \text{ and } k_2 = H-\sqrt{H^2-K}.$$

In general, a surface $M\subset\mathbb{R}^{2,1}$ has a Riemannian part and a Lorentzian part. On the Riemannian part, dN_p does have real eigenvalues; on Lorentzian part, dN_p does not always have real eigenvalues. These eigenvalues are the principal curvatures k_1 and k_2 in each point and the respective eigendirections of dN_p are called principal directions and they define two line fields $\mathcal{L}_1$ and $\mathcal{L}_2$ mutually orthogonal in M. They are determined by non-zero vectors on $T_p(M)$ which satisfy the implicit differential equation

$$(Fg-Gf)\,dv^2 + (Eg-Ge)\,dudv + (Ef-Fe)\,du^2 = 0. \tag{1}$$

The integral curves of the equation (1) are called *lines of curvature or principal lines*. The families of principal lines $\mathcal{F}_1$ and $\mathcal{F}_2$ associated with $\mathcal{L}_1$ and $\mathcal{L}_2$, respectively, are called principal foliations of M. An umbilic point is defined as a point where $II = cI$ for some constant c. It is called a spacelike (resp. timelike) umbilic point when it is on Riemannian (resp. Lorentzian) part of M. The set of umbilic points is denoted by $\mathcal{U}$.

The map N is not defined on the tropic, but since the equation (1) is homogeneous, we can multiply the coefficients of (1) by $\|\alpha_u\times\alpha_v\|$. Let $L_1 = \|\alpha_u\times\alpha_v\|\,(Fg-Gf)$, $M_1 = \|\alpha_u\times\alpha_v\|\,(Eg-Ge)$ and $N_1 = \|\alpha_u\times\alpha_v\|\,(Ef-Fe)$.

So, *the equation of curvature lines (or principal lines)* can be extended to the tropic by

$$L_1 dv^2 + M_1 dv du + N_1 du^2 = 0. \tag{2}$$

The tropic $LD = (EG - F^2)^{-1}(0)$ is generically a curve that is solution of the equation (2), [21, Lemma 1.31]. The discriminant of the equation (2), define the set of points where it determines a unique direction or an umbilic point, the first set is denoted by *LPL* (Ligthlike Principal Locus). On the Riemannian part $LPL = \emptyset$, and on the Lorentzian part the set *LPL* is generically a curve that divide locally the surface into two regions, in one of them there are no real principal directions and in the other there are two real principal directions at each point, [7].

Definition 1 *The quintuple $\mathbb{P}_M = \{\mathcal{F}_1, \mathcal{F}_2, \mathcal{U}, LD, LPL\}$ is called the* ***principal configuration*** *of M, or rather of the immersion α of M in $\mathbb{R}^{2,1}$.*

Definition 2 *Two principal configurations $\mathbb{P}_{M_1}$ and $\mathbb{P}_{M_2}$ are C^0-principally equivalent if there exists a homeomorphism $h : M_1 \to M_2$ which is a topological equivalence between them, i.e., h sends principal foliations, umbilic set, LD and LPL of M_1 in the correspondent of M_2.*

Remark 1 *The umbilic points can also be seen as the points where $L_1 = M_1 = N_1 = 0$.*

Remark 2 *A smooth curve c is a principal line, if this curve satisfies the equation (2) and there are no umbilic points on c.*

Remark 3 *Let $X(u,v)$ be a local parametrization of M. If $F = f = 0$ then $L_1 = N_1 = 0$ and (u,v) is a principal curvature coordinate system. It is called a principal chart.*

Triply orthogonal system (see [8, 18]).

In this subsection, it will be introduced a triple orthogonal systems of surfaces in the Minkowski space $\mathbb{R}^{2,1}$.

Definition 3 *A triply orthogonal system of surfaces is a differentiable map $X\colon W \to \mathbb{R}^{2,1}$, defined on an open set $W \subset \mathbb{R}^{2,1}$, satisfying:*

a) The linear map $dX_{(u,v,w)} : T_{(u,v,w)}\mathbb{R}^{2,1} \to T_{X(u,v,w)}\mathbb{R}^{2,1}$ is bijective for all $(u,v,w) \in W$.

b) $\langle X_u, X_v\rangle = \langle X_u, X_w\rangle = \langle X_w, X_v\rangle = 0.$

Let $p = (u_0, v_0, w_0) \in W$. Consider the three surfaces

$$(u,v) \longmapsto X(u,v,w_0)$$

$$(u,w) \longmapsto X(u,v_0,w)$$

$$(v,w) \longmapsto X(u_0,v,w),$$

we denote these surfaces by M_{w_0}, M_{v_0} and M_{u_0}, respectively. They are regular surfaces by the condition a).

Notice that by condition b), $F = 0$ on each of them. Furthermore, $X_w(u,v,w_0)$ is normal to M_{w_0} at (u,v,w_0) (similarly to other two surfaces) and differentiating,

$$\langle X_u, X_v\rangle_w = \langle X_u, X_w\rangle_v = \langle X_w, X_v\rangle_u = 0.$$

Therefore,

$$\langle X_{uv}, X_w\rangle = \langle X_{uw}, X_v\rangle = \langle X_{vw}, X_u\rangle = 0,$$

which means that $f = 0$ on each of the surfaces. By remark (3), we may conclude that:

Theorem 1 *The coordinate curves on a surface belonging to a triply orthogonal system in a Minkowski three-dimensional space are principal curvature lines.*

3 The Ellipsoid in the Minkowski space

Consider the family of surfaces

$$\mathbb{F}_u = \{(x,y,z) : \frac{x^2}{a^2-u} + \frac{y^2}{b^2-u} + \frac{z^2}{c^2+u} = 1\}$$

$$\mathbb{G}_v = \{(x,y,z) : \frac{x^2}{a^2-v} + \frac{y^2}{b^2-v} + \frac{z^2}{c^2+v} = 1\}$$

$$\mathbb{H}_w = \{(x,y,z) : \frac{x^2}{a^2-w} + \frac{y^2}{b^2-w} + \frac{z^2}{c^2+w} = 1\}$$

where $a > b > 0$ (the case $b > a > 0$ is similar) and $c > 0$.

Let $U_E := \{(u,v,w) \in (-c^2, b^2) \times (b^2, a^2) \times (-c^2, b^2)\}$. For $(u,v,w) \in U_E$, $\mathbb{F}_u$, $\mathbb{H}_w$ are ellipsoids and $\mathbb{G}_v$ is a hyperboloid of one leaf.

Theorem 2 *The surfaces $\mathbb{F}_u$, $\mathbb{G}_v$ and $\mathbb{H}_w$ define a triple orthogonal system for $(u,v,w) \in U_E$, $u \neq w$.*

Proof. Solving the system below in the variables $\{x,y,z\}$

$$\frac{x^2}{a^2-u}+\frac{y^2}{b^2-u}+\frac{z^2}{c^2+u}-1=0$$
$$\frac{x^2}{a^2-v}+\frac{y^2}{b^2-v}+\frac{z^2}{c^2+v}-1=0$$
$$\frac{x^2}{a^2-w}+\frac{y^2}{b^2-w}+\frac{z^2}{c^2+w}-1=0,$$

it is obtained in the positive octant:

$$x(u,v,w)=\sqrt{\frac{(a^2-u)(a^2-v)(a^2-w)}{(a^2-b^2)(a^2+c^2)}}$$
$$y(u,v,w)=\sqrt{\frac{-(b^2-u)(b^2-v)(b^2-w)}{(a^2-b^2)(b^2+c^2)}}$$
$$z(u,v,w)=\sqrt{\frac{(c^2+u)(c^2+v)(c^2+w)}{(a^2+c^2)(b^2+c^2)}}.$$

A long and straightforward calculations show that

$$X(u,v,w)=(x(u,v,w),y(u,v,w),z(u,v,w)) \tag{3}$$

satisfies $\langle X_u,X_v\rangle=\langle X_u,X_w\rangle=\langle X_v,X_w\rangle=0$. Moreover,

$$\det(DX(u,v,w))=$$
$$\frac{(u-v)(u-w)(v-w)}{8x(u,v,w)y(u,v,w)z(u,v,w)(a^2-b^2)(a^2+c^2)(b^2+c^2)}\neq 0.$$

□

Since $\{\mathbb{F}_u,\mathbb{G}_v,\mathbb{H}_w\}$ is a triple orthogonal system, these surfaces intersect along their curvature lines. The curvature lines can be obtained globally by symmetry in relation to the coordinates planes.

Now, we fixed w and defined the ellipsoid $\mathbb{E}_w=\mathbb{H}_w$ with $(u,v,w)\in U_E$, so we have that the principal lines on $\mathbb{E}_w$ are the intersection curves, with the hyperboloid of one leaf $\mathbb{G}_v$ and with the other ellipsoid $\mathbb{F}_u$ (See Fig. 2).

In each octant, we have that for $\mathbb{E}_w$ the parametrization (3) is a principal chart, i.e., $f=F=0$. So, the principal lines are $u=constant$ and $v=constant$, and these curves are exactly the intersection between surfaces.

Remark 4 *The triply orthogonal system of quadratic surfaces in the Euclidean space is make up by an ellipsoid, a hyperboloid of one leaf and a hyperboloid of two leaves* [4, Chapter 2]. *See also* [12, Chapter 7] *for more details about the geometric properties of confocal quadrics.*

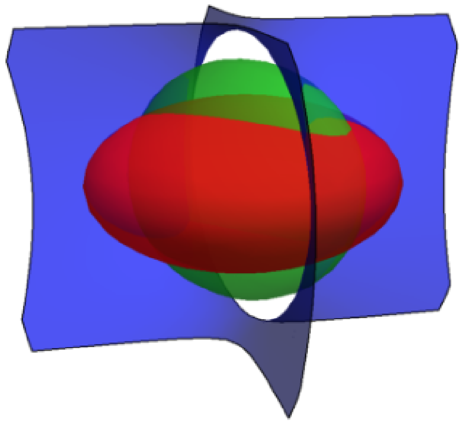

Figure 2: *Triply orthogonal system defined by two ellipsoids and one hyperboloid of one leaf.*

To complete the description, the principal configuration is necessary to analyze the curves of the intersections of the ellipsoid with the coordinates planes. Without loss of generality, we do $w=0$, i.e., we analyze

$$\mathbb{E}_0=\left\{(x,y,z):\frac{x^2}{a^2}+\frac{y^2}{b^2}+\frac{z^2}{c^2}=1\right\}$$

with $a>b>0$ and $c>0$ (it is allowed $a=c$ or $b=c$).

The parametrization below is inspired in the Euclidean case. See also Section 6 where a global parametrization will be obtained in a triple orthogonal system of quadrics.

Lemma 1 *The parametrization*

$$X(u,v)=(a\cos(u)A(v),b\sin(u)\sin(v),c\cos(v)B(u))$$
$$A(v)=\sqrt{A_1\cos^2(v)+\sin^2(v)},$$
$$B(u)=\sqrt{B_1\cos^2(u)+\sin^2(u)} \tag{4}$$

with $(u,v)\in U_1=[0,\pi]\times[0,2\pi]$ *or* $(u,v)\in U_2=[0,2\pi]\times[0,\pi]$, *where* $A_1=\frac{a^2-b^2}{a^2+c^2}$ *and* $B_1=\frac{b^2+c^2}{a^2+c^2}$, *defines a principal chart* (u,v) *on the ellipsoid* $\mathbb{E}_0$.

Proof. Calculating of the coefficients of the first and second fundamental form, we have

$$E = -\frac{\left((a^2-b^2)\cos^2 u - a^2\right)\left((a^2-b^2)\cos^2 u + (b^2+c^2)\cos^2 v - a^2 - c^2\right.}{(a^2-b^2)\cos^2 u - a^2 - c^2}$$

$$F = 0$$

$$G = -\frac{\left((a^2-b^2)\cos^2 u + (b^2+c^2)\cos^2 v - a^2 - c^2\right)\left((b^2+c^2)\cos^2 v - c^2\right.}{-(b^2+c^2)\cos^2 v + a^2 + c^2}$$

$$e = \frac{abc\left((a^2-b^2)\cos^2 u + (b^2+c^2)\cos^2 v - a^2 - c^2\right)^2}{\sqrt{(b^2+c^2)\cos^2 v - c^2 - a^2}\left((a^2-b^2)\cos^2 u - a^2 - c^2\right)^{\frac{3}{2}}}$$

$$f = 0$$

$$g = \frac{b\left((a^2-b^2)\cos^2 u + (b^2+c^2)\cos^2 v - a^2 - c^2\right)^2 ac}{\left((b^2+c^2)\cos^2 v - c^2 - a^2\right)^{\frac{3}{2}}\sqrt{(a^2-b^2)\cos^2 u - a^2 - c^2}}.$$

Since that, $F = f = 0$ then $L_1 = N_1 = 0$ in the equation (2). So, by Remark 3, we have that X defines a parametrization by principal lines, i.e., (u, v) is a principal chart.

The parametrization (X, U_1) (resp. (X, U_2)) cover all the ellipsoid and is smooth, except in the curves $X(0, v)$ and $X(\pi, v)$ (resp. $X(u, 0)$ and $X(u, \pi)$). $\square$

Proposition 1 *On the ellipsoid $\mathbb{E}_0$, we have that:*

a. The curves $c_x = \{(x,y,z) : x = 0\} \cap \mathbb{E}_0$ and $c_z = \{(x,y,z) : z = 0\} \cap \mathbb{E}_0$ are principal lines.

b. $\mathbb{E}_0$ has exactly four spacelike umbilic points,

$$\left(\pm a\sqrt{\frac{a^2-b^2}{a^2+c^2}}, 0, \pm c\sqrt{\frac{b^2+c^2}{a^2+c^2}}\right).$$

c. The umbilic points are of type D_1.

d. The curve $c_y = \{(x,y,z) : y = 0\} \cap \mathbb{E}_0$ is the union of principal lines. Moreover, these are the separatrices of the umbilic points.

e. The tropic is composed by two disjoint regular closed curves. Moreover, these curves are principal lines.

f. The principal lines are globally defined, i.e., the set $LPL = \emptyset$.

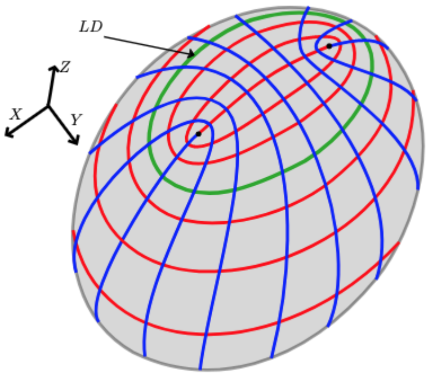

Figure 3: *Principal lines on the Ellipsoid in the Minkowski space. Parameters $a = 2.0$, $b = 1.5$, $c = 2.2$.*

Proof.
a) Consider the principal chart (X, U_1) (resp. (X, U_2)) given by Lemma 1. We have $c_x = X(\frac{\pi}{2}, v)$ (resp. $c_z = X(u, \frac{\pi}{2})$).

The principal chart (X, U_1) (resp. (X, U_2)) is smooth, except in the curves $X(0, v)$ and $X(\pi, v)$ (resp. $X(u, 0)$ and $X(u, \pi)$), but this curves not intersect with c_x (resp. c_z). Therefore, c_x (resp. c_z) is a principal line of the ellipsoid.

b) Consider the parametrization,

$$X(u, v) = \left(au, bv, \pm c\sqrt{1 - u^2 - v^2}\right). \tag{5}$$

Then the differential equation of principal lines (2) with X is

$$\begin{aligned} &E(u, v, du : dv) = \\ &-uv(a^2+c^2)du^2 + uv(b^2+c^2)dv^2 \\ &+(u^2(a^2+c^2) - v^2(b^2+c^2) - a^2 + b^2)dudv = 0. \end{aligned} \tag{6}$$

We have that $L_1 = N_1 = 0$ when $u = 0$ or $v = 0$. If $u = 0$ then $M_1 = -v^2(b^2+c^2) - a^2 + b^2 \neq 0$. If $v = 0$, we have that $M_1 = u^2(a^2+c^2) - a^2 + b^2 = 0$ if and only if

$$u_0 = \pm\sqrt{\frac{a^2-b^2}{a^2+c^2}}.$$

So, there are four umbilic points. Moreover,

$$(EG - F^2)(u_0, 0) = \frac{b^4(a^2+c^2)}{b^2+c^2} > 0,$$

and then the umbilic points are in the Riemannian part of E_0, i.e., they are spacelike umbilic points.

c) For completeness, it will be included a detailed sketch of proof. We take $p = \frac{dv}{du}$ in the equation (6), so

$$\begin{aligned} F(u,v,p) = &- uv(a^2+c^2) \\ &+ (u^2(a^2+c^2) - v^2(b^2+c^2) - a^2 + b^2)p \\ &+ uv(b^2+c^2)p^2 = 0. \end{aligned}$$

Under the hypothesis, the implicit surface $F^{-1}(0)$ is a regular surface, contain the projective line, and is topologically a cylinder. The map $\pi : F^{-1}(0) \to \mathbb{R}^2$, $\pi(x,y,p) = (x,y)$ is a ramified double covering and $\pi^{-1}(u_0,0)$ is the projective line parametrized by $[du:dv]$. The umbilic point $P_1 = \left(a\sqrt{\frac{a^2-b^2}{a^2+c^2}}, 0, c\sqrt{\frac{b^2+c^2}{a^2+c^2}}\right)$ has coordinates $u_0 = \sqrt{\frac{a^2-b^2}{a^2+c^2}}$ and $v = 0$. The Lie-Cartan line field associated to the implicit equation $F(u,v,p) = 0$ is $Y = (F_p, pF_p, -(F_x + pF_y))$ on the surface $M = F^{-1}(0)$, $M \subset \mathbb{R}^2 \times \mathbb{RP}^1$. The solutions of the implicit differential equation $F(u,v,p) = 0$ are the projections of the integral curves of Y. See [1] and [4].

We have that

$$Y(u_0,0,p) = \left(0,0,-\sqrt{\frac{a^2-b^2}{a^2+c^2}}\,p(b^2p^2+c^2p^2+a^2+c^2)\right) = (0,0,0)$$

if and only if $p = 0$.

Moreover, the eigenvalues of $DY(u_0,0,0)$ are,

$$\lambda_1 = 2\sqrt{\frac{a^2-b^2}{a^2+c^2}}(a^2+c^2), \quad \lambda_2 = -2\sqrt{\frac{a^2-b^2}{a^2+c^2}}(a^2+c^2).$$

Therefore, $(u_0,0,0)$ is a hyperbolic saddle point of Y. To complete the analysis, it is also necessary to consider the chart $q = du/dv$ in the equation (6) to obtain an implicit surface $G(u,v,q) = 0$. Now the Lie-Cartan vector field is $Z = (qG_q, G_q, -(qG_u + G_v))$. We have that $Z(u_0,0,q) \neq 0$. Gluing the phase portraits of Y and Z near the projective line $[du:dv]$ we obtain a line field on the cylinder with a unique hyperbolic singular point. The projections of the leaves (integral curves of X and Y) are the principal lines of the ellipsoid near the umbilic point. See Fig. 4.

Therefore, the umbilic point P_1 is Darbouxian of type D_1 (see also [4]). By symmetry, all the other umbilic points are also of type D_1.

d) Using the parametrization (5), a curve c_y satisfies the equation the principal lines (6). Furthermore, the umbilic points are on c_y, so this curve is a union of principal lines and the umbilic points. Since the umbilic points are D_1, we obtain the result as stated.

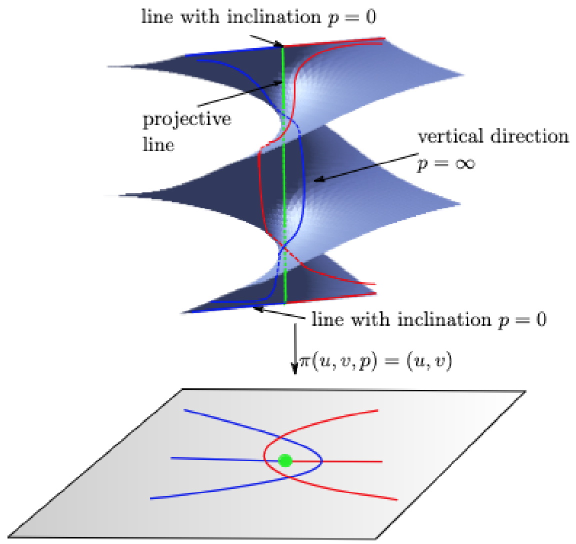

Figure 4: *Implicit surface $F(u,v,p) = 0$ (cylinder) and a ramified double covering π with $\pi^{-1}(u_0,0)$ being the projective line. The top and bottom lines with inclination $p = 0$ are identified.*

e) Using the chart defined by equation (4) with $(u,v) \in U_1$, we have that

$$EG - F^2 = \left((b^2+c^2)\cos^2(v) - c^2\right)\left((a^2-b^2)\cos^2(u) - a^2\right)$$
$$\left((a^2-b^2)\cos^2(u) + (b^2+c^2)\cos^2(v) - a^2 - c^2\right)^2 = 0.$$

if, and only if, $v_1 = \arccos\left(\frac{c}{\sqrt{c^2+b^2}}\right)$ or $v_2 = \arccos\left(-\frac{c}{\sqrt{c^2+b^2}}\right) = \pi - v_1$.

The tropic is the union of the closed curves $c_1(u) = X(u,v_1)$ and $c_2(u) = X(u,v_2)$. As $v = constant$ and (X,U_1) is a principal chart, then c_1 and c_2 are principal lines.

f) Since the parametrization (4) is defined globally on $\mathbb{E}_0$ and defines a principal chart, it follows that $L_1 = N_1 = 0$ and $LPL = M_1^2 \geq 0$. Therefore, the principal lines are globally defined. □

Confocal and orthogonal family of conics

Performing the change of coordinates by $u = \sqrt{\frac{b^2+c^2}{a^2+c^2}}\,x$ and $v = y$, then equation (6) is given by

$$-xydx^2 + \left(x^2 - y^2 - \lambda^2\right)dxdy + xydy^2 = 0$$

with $\lambda^2 = \frac{a^2-b^2}{b^2+c^2}$. The coordinates axes, the family of ellipses

$$u(t) = R\cos(t), \quad v(t) = r\sin(t), \quad R^2 = r^2 + \lambda^2$$

and the family of hyperbolas

$$u(t) = R\cosh(t), \quad v(t) = r\sinh(t), \quad R^2 - r^2 = \lambda^2$$

are the solutions of the differential equation above. This is similar to Euclidean case, see [4].

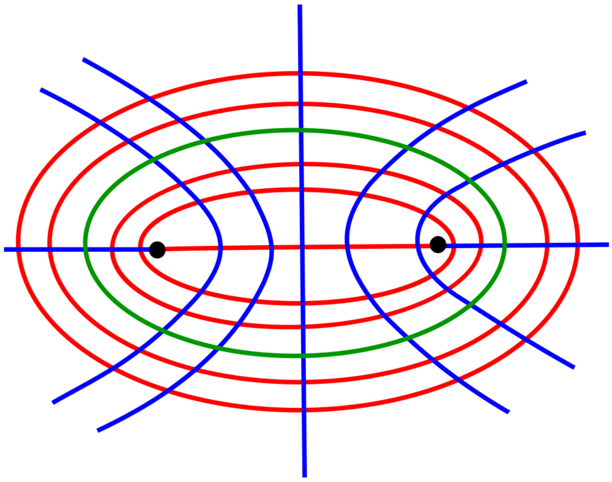

Figure 5: *Confocal and orthogonal family of conics. The tropic is shown in green and is parametrized by* $\cos^2 v = c/(b+c)$.

Horizontal ellipsoid of revolution.

When $a = c$ or $b = c$, we have four spacelike umbilic points of type D_1, while with the Euclidean scalar product only have two umbilic points of center type.

Vertical ellipsoid of revolution and Euclidean sphere.

When $a = b$ and $c > 0$, the parametrization (4) is reduced to

$$X(u,v) = (a\sin(v)\cos(u), a\sin(v)\sin(u), c\cos(v)).$$

The equation of principal lines is

$$a^2c(a^2\cos^2(v) + c^2\cos^2(v) - a^2 - c^2)^4 du dv = 0.$$

Therefore, the principal lines are $u = constant$ and $v = constant$. We have only two spacelike umbilic points $(0,0,\pm c)$ of type center.

On ellipsoid of revolution with $a = b$ and $c \neq a$, the principal lines are the same in the two geometries (Euclidean and Lorentzian).

With the Euclidean scalar product the Eucidean sphere is a umbilic surface, while with the Lorentzian scalar product the Euclidean sphere has only two spacelike umbilic points of type center.

Umbilic surfaces.

The umbilic surfaces with Euclidean inner scalar are the Euclidean sphere and planes, while with Lorentzian inner scalar the umbilic surfaces are planes, the vertical hyperboloid of one leaf $\mathbb{S}^2_1(c,r) = \{p \in \mathbb{R}^{2,1} : \langle p - p_0, p - p_0\rangle = r^2\}$ and vertical hyperboloid of two leaves $\mathbb{H}^2_1(c,r) = \{p \in \mathbb{R}^{2,1} : \langle p - p_0, p - p_0\rangle = -r^2\}$, see [3, page 191] and [9, page 85].

Remark 5 *For the study of geodesics on an ellipsoid in the Minkowski space* $\mathbb{R}^{2,1}$ *see* [5]. *The analysis of umbilic points in smooth surfaces in* $\mathbb{R}^{2,1}$ *of the form* $f_\varepsilon(x,y,z) = x^2/a^2 + y^2/b^2 + z^2/c^2 + h.o.t = \varepsilon$ *was developed in* [6].

4 Topological equivalence of principal foliations

In this section we will obtain that the principal configurations of the ellipsoids of three distinct axes are all principal topologically equivalent. The Euclidean case was established by J. Sotomayor [15].

Proposition 2 *Consider an ellipsoid* $E(x,y,z) = ax^2 + by^2 + cz^2 + 2dxy + 2exz + 2fyz + gx + hy + kz + l = 0$. *Then there exists an isometry* $h\colon \mathbb{R}^{2,1} \to \mathbb{R}^{2,1}$ *such that* $E(h(u,v,w)) = \lambda_1 u^2 + \lambda_2 v^2 + \lambda_3 w^2 = 1$, *with* $\lambda_i > 0$ *for* $(i = 1,2,3)$.

Proof. The rotation group of $\mathbb{R}^{2,1}$ is $SO(2,1)$ of dimension 3 and is generated by the Euclidean and Hyperbolic rotations defined by:

$$\begin{aligned} R(u,v,w) &= (u\cos\theta + v\sin\theta, -u\sin\theta + v\cos\theta, w) \\ S(u,v,w) &= (u\cosh\alpha + w\sinh\alpha, v, u\sinh\alpha + w\cosh\alpha) \\ T(u,v,w) &= (u, v\cosh\beta + w\sinh\beta, v\sinh\beta + w\cosh\beta) \end{aligned}$$

The quadric form $q(x,y,z) = ax^2 + by^2 + cz^2 + 2dxy + 2exz + 2fyz$ is positive definite when one of the following conditions holds:

$a > 0,\ ab - d^2 > 0,\ abc - af^2 - be^2 - cd^2 + 2def = \Delta > 0,$

$b > 0,\ bc - f^2 > 0,\ \Delta > 0,$

$c > 0,\ ac - e^2 > 0,\ \Delta > 0.$

In this case the eigenvalue problem

$$\det\begin{pmatrix} a-x & d & e \\ d & b-x & f \\ e & f & c+x \end{pmatrix} = 0$$

has three real eigenvalues $x_1 \leq x_2 \leq x_3$ and the correspondent eigenvectors e_1, e_2, e_3 are orthonormal relative to the Minkowski inner product. Therefore, one of the eigenvectors, say e_3, is timelike and the other two $\{e_1, e_2\}$ are spacelike. There exists an isometry h (composition of hyperbolic rotations) such that $h(0,0,-1) = e_3$. In the new coordinates we have that $q_1(u,v,w) = q(h(u,v,w)) = a_1u^2 + b_1v^2 + c_1w^2 + d_1uv$.

Also, there exists an isometry H (Euclidean rotation) such that

$$q_1(H(u_1,v_1,w_1)) = a_2u_1^2 + b_2v_1^2 + c_1w_1^2, a_2 > 0,$$

$$b_2 > 0,\ c_1 > 0.$$

Finally, with a translation we obtain the result stated. □

Remark 6 *In general, a hyperboloid is not isometric to one given in a diagonal form. The classification of conics in Minkowski plane is carried out in* [10].

Theorem 3 *Consider the set of ellipsoids $\mathcal{E}$ with three distinct axes in the space of quadrics $\mathcal{Q}$ of $\mathbb{R}^3$. Then the principal configurations of any two elements of $\mathcal{E}$ are principal topologically equivalent.*

Proof. The principal configuration of an ellipsoid with three different axes in the diagonal form $x^2/a^2 + y^2/b^2 + z^2/c^2 = 1$ has the following properties.

i) There are four umbilic points of Darbouxian type D_1.

ii) The set LD is the union of two regular curves.

iii) The set LPL is empty.

iv) The principal foliations $\mathcal{F}_1$ and $\mathcal{F}_2$ have all leaves closed, with the exception of the umbilic separatrices. See Fig. 3.

The construction of the topological equivalence can be done explicitly using the method of canonical regions defined by the union of two topological disks and a cylinder; the boundary being the tropics. See [17] and Fig. 6. By Proposition 2, any ellipsoid is isometric to an ellipsoid in the diagonal form. This ends the proof. □

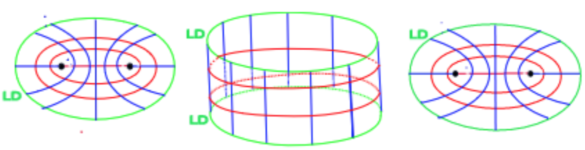

Figure 6: *Decomposition of the ellipsoid in three canonical regions foliated by principal lines; the boundary of each region is formed by the tropic lines.*

5 Geometric Inversion in Minkowski space

In this section, we will show that the principal lines are the same when we consider the inversion of the surface with respect to a given point in the space. Recall that the inversion is defined by:

$$I_q(p) = \frac{p-q}{\langle p-q, p-q\rangle}.$$

Proposition 3 *Consider a regular surface S and a point $q \in \mathbb{R}^{2,1} \setminus S$. Let $S_q = I_q(S)$, where I_q is the inversion with respect to the point q. The principal lines on S are the same that on S_q.*

Proof. Consider the local parametrization

$$X(u,v) = (u,v,h(u,v)).$$

Calculating the equation of principal lines of X, we have that:

$$\begin{aligned}&(h_{uv}h_v^2 - h_{vv}h_uh_v - h_{uv})dv^2\\ &+(h_{uu}h_v^2 + h_{vv} - h_{vv}h_u^2 - h_{uu})dvdu \\ &+(h_{uv} + h_uh_vh_{uu} - h_{uv}h_u^2)du^2 = 0.\end{aligned} \tag{7}$$

The local parametrization of the inverted surface in the relation to the point $q = (q_1, q_2, q_3)$, is given by:

$$\begin{aligned}\bar{X}(u,v) &= \frac{1}{\langle X(u,v)-q, X(u,v)-q\rangle}(X(u,v)-q)\\ &= \frac{1}{(u-q_1)^2 + (v-q_2)^2 - (h(u,v)-q_3)^2}\cdot\\ &\quad \cdot(u-q_1, v-q_2, h(u,v)-q_3).\end{aligned}$$

Calculating the first fundamental form of $\bar{X}$ it follows that

$$E = -\frac{h_u^2-1}{Q_0^2},\ F = -\frac{h_uh_v}{Q_0^2},\ G = -\frac{h_v^2-1}{Q_0^2},$$

with $Q_0 = \langle X(u,v)-q, X(u,v)-q\rangle$. Similarly, we calculate the coefficients of the second fundamental form:

$$\begin{aligned}e =& \frac{1}{Q_0^4}\big[2(q_1-u)h_u^3 + 2((q_2-v)h_v + h - q_3)h_u^2\\ &+2(u-q_1)h_u + 2(v-q_2)h_v + 2q_3 - 2h\\ &+(h^2 - 2hq_3 - q_1^2 + 2q_1u - q_2^2 + 2q_2v + q_3^2 - u^2 - v^2)h_{uu}\big]\\ f =& \frac{1}{Q_0^4}\big[2(q_1-u)h_vh_u^2 + 2((q_2-v)h_v^2 + (h-q_3)h_v)h_u\\ &+h^2h_{uv} - 2hh_{uv}q_3 - h_{uv}q_1^2 + 2h_{uv}q_1u - h_{uv}q_2^2\\ &+2h_{uv}q_2v + h_{uv}q_3^2 - h_{uv}u^2 - h_{uv}v^2\big]\\ g =& \frac{1}{Q_0^4}\big[2((q_1-u)h_v^2 + u - 2q_1)h_u + 2(q_2-2v)h_v^3\\ &+2(h-q_3)h_v^2 + 2(v-q_2)h_v + 2q_3 - 2h\\ &+(h^2 - 2hq_3 - q_1^2 + 2q_1u - q_2^2 + 2q_2v + q_3^2 - u^2 - v^2)h_{vv}\big].\end{aligned}$$

Then, the coefficients of the differential equation of the principal lines are given by:

$$L = Fg - Gf = \frac{h_u h_v h_{vv} - h_{uv} h_v^2 + h_{uv}}{\langle X-q, X-q\rangle^5},$$
$$M = Eg - Ge = \frac{h_u^2 h_{vv} - h_{uu} h_v^2 + h_{uu} - h_{vv}}{\langle X-q, X-q\rangle^5},$$
$$N = Ef - Fe = \frac{h_u^2 h_{uv} - h_u h_{uu} h_v - h_{uv}}{\langle X-q, X-q\rangle^5}.$$

So, the differential equation of the principal lines of $\bar{X}$ is exactly (7). The analysis, with local parametrization $(u, h(u,v), v)$ or $(h(u,v), u, v)$ are analog.

Therefore, the principal lines of the surface S and of the inverted surface S_q are related by the inversion I_q, i.e., if $\gamma(s)$ is a principal line of S, then $I_q(\gamma(s))$ is a principal line of S_q. □

6 Triple Orthogonal System in Minkowski space

In this section a global parametrization of a triple orthogonal system of quadrics in the Minkowski 3-space will be established.

Let $Z(u,v,w) = (A(u,v,w), B(u,v,w), C(u,v,w))$ defined by:

$$
\begin{aligned}
A(u,v,w) &= \cos u \cosh w \sqrt{(\varepsilon n^2 + m^2)\cos^2 v + m^2 \sin^2 v}\\
B(u,v,w) &= m \sin u \sin v \sinh w\\
C(u,v,w) &= \\
&\cos(v) \sqrt{\frac{\left(\varepsilon n^2 \cos^2 u - m^2 \sin^2 u\right)\left(\varepsilon n^2 \cosh^2 w + m^2 \sinh^2 w\right)}{\varepsilon n^2 + m^2}}
\end{aligned}
\tag{8}
$$

Here $\varepsilon = \pm 1$.

Theorem 4 *The map Z defined by equation (8) is a triple orthogonal system of quadrics in $\mathbb{R}^{2,1}$ (Minkowski 3-space). More precisely, the quadrics are given by:*

$$\mathcal{E}_1 : \frac{x^2}{m^2\cosh^2 w} + \frac{y^2}{m^2 \sinh^2 w} + \frac{z^2\left(m^2+\varepsilon n^2\right)}{(\varepsilon n^2 \cosh^2 w - m^2 \sinh^2 w)m^2} = 1$$
$$\mathcal{E}_2 : \frac{x^2\left(m^2+\varepsilon n^2\right)}{m^2\left(m^2+\varepsilon n^2\cos^2 v\right)} + \frac{\left(m^2+\varepsilon n^2\right)y^2}{\varepsilon m^2 n^2 \sin^2 v} + \frac{z^2\left(m^2+\varepsilon n^2\right)}{\varepsilon m^2 n^2 \cos^2 v} = 1$$
$$\mathcal{H}_1 : \frac{x^2}{m^2\cos^2 u} - \frac{y^2}{m^2\sin^2 u} + \frac{z^2\left(m^2+\varepsilon n^2\right)}{m^2\left(m^2\sin^2 u + \varepsilon n^2 \cos^2 u\right)} = 1.$$

Proof. The map Z defined by equation (8) was inspired in [19] where a similar map was obtained in the Euclidean case. The main idea is to try a parametrization with separation of variables as

$Z(u,v,w) =$
$(h_1 \cos u \cos w\, a(v), h_2 \sin u \sin v \sinh w, h_3\, c(u)\, d(w) \cos v)$.

A long, and straightforward calculation, using the equation (8), leads to

$$\langle Z_u, Z_v\rangle = \langle Z_u, Z_w\rangle = \langle Z_v, Z_w\rangle = 0.$$

The quadrics defined by equation (8) was obtained by the method of elimination of variables from the equations

$$A(u,v,w) - x = 0,\ \ B(u,v,w) - y = 0,\ \ C(u,v,w) - z = 0.$$

□

Remark 7 *For $\varepsilon = -1$, $m = \sqrt{a^2-b^2}$, $n = \sqrt{(b^2+c^2)(a^2-b^2)}/\sqrt{a^2+c^2}$ and $\cosh w = a/\sqrt{a^2-b^2}$ it follows that $Z_w(u,v) = Z(u,v,w)$ is a parametrization of the ellipsoid $x^2/a^2 + y^2/b^2 + z^2/c^2 = 1$.*

7 Focal set of a surface in the Minkowski space

The focal set of a surface M can be defined as the singular set of the congruence of lines given by

$$L(u,v,t) = \alpha(u,v) + tN(u,v)$$

where α is a parametrization of M and N is the normal vector to the surface. Also, the focal set can be seen as the locus of the centers of curvature of the given surface.

$\mathcal{F}_i :\ \alpha(u,v) + \frac{1}{k_i(u,v)} N(u,v), \quad (i = 1,2).$

See [2] and [20].

Proposition 4 *The focal set $\mathcal{F}_1$ of the ellipsoid is parametrized by*

$$(A_1(u,v), B_1(u,v), C_1(u,v))$$

where:

$$
\begin{aligned}
A_1(u,v) &= \frac{\cos^3 u\left(a^2-b^2\right)}{a\sqrt{a^2+b^2}} \sqrt{\left(a^2-b^2\right)\cos^2 v + \left(a^2+c^2\right)\sin^2 v}\\
B_1(u,v) &= -\frac{\sin^3 u \sin v\left(a^2-b^2\right)}{b}\\
C_1(u,v) &= \frac{\cos v}{c\sqrt{a^2+c^2}} \left[\left(b^2+c^2\right)\cos^2 u + \left(a^2+c^2\right)\sin^2 u\right]^{\frac{3}{2}}.
\end{aligned}
$$

The focal set $\mathcal{F}_2$ of the ellipsoid is parametrized by $(A_2(u,v), B_2(u,v), C_2(u,v))$ where:

$$A_2(u,v) = \frac{\cos u}{a\sqrt{a^2+c^2}}\left[(a^2-b^2)\cos^2 v + (a^2+c^2)\sin^2 v\right]^{\frac{3}{2}}$$
$$B_2(u,v) = \frac{\sin u \sin^3 v\left(b^2+c^2\right)}{b}$$
$$C_2(u,v) = \frac{(b^2+c^2)\cos^3 v}{c\sqrt{a^2+c^2}}\sqrt{(b^2+c^2)\cos^2 u + (a^2+c^2)\sin^2 u}$$

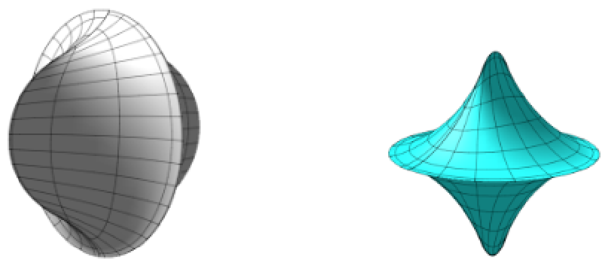

Figure 7: *The focal surfaces $\mathcal{F}_1$ and $\mathcal{F}_2$ of the ellipsoid. Both are singular on two arcs of ellipses connecting the umbilic points and each is singular in an ellipse contained in a coordinate plane. At the umbilic points the singularities are of type D_4^+ (Arnold's notation).*

Proof. It follows directly from the parametrization of the ellipsoid Z_w given by Remark 7. It is worth to observe that at the tropics defined by $\cos v = \pm c/\sqrt{b^2+c^2}$ the principal curvatures k_i are unbounded but at these sets the normal N has norm zero and the product $(1/k_i)N$ has a finite limit. See [20]. □

Acknowledgments

The first author is fellow of CNPq (313724/2021-0) and coordinator of Project PRONEX/ CNPq/ FAPEG 2017 10 26 7000 508.

References

[1] BRUCE, J.W., FIDAL, D.L., On binary differential equations and umbilics, *Proc. Roy. Soc. Edinburgh Sect. A mathematics* **111**(1-2) (1989), 147–168, https://doi.org/10.1017/S0308210500025087

[2] CAYLEY, A., On the centro-surface of an ellipsoid, *Trans. Camb. Phi. Soc.* **63** (1873), 319–365.

[3] COUTO, I.T., LYMBEROPOULOS, A., *Introduction to Lorentz Geometry: Curves and Surfaces*, Chapman and Hall/CRC Press, 2020, https://doi.org/10.1201/9781003031574

[4] GARCIA, R., SOTOMAYOR, J., *Differential equations of classical geometry, a qualitative theory*, Publicações Matemáticas do IMPA. IMPA, Rio de Janeiro, 2009.

[5] GENIN, D., KHESIN, B., TABACHNIKOV, S., Geodesics on an ellipsoid in Minkowski space, *Enseign. Math.* (2), **53**(3-4) (2007), 307–331, https://doi.org/10.5169/seals-109549

[6] HASEGAWA, M., TARI, F., On umbilic points on newly born surfaces, *Bull. Braz. Math. Soc., New Series* **48**(4) (2017), 679–696, https://doi.org/10.1007/s00574-017-0037-9

[7] ISUMIYA, S., TARI, F., Self-adjoint operators on surfaces with singular metrics, *J. Dyn. Control Syst.* **16**(3) (2010), 329–353, https://doi.org/10.1007/s10883-010-9096-6

[8] KLINGENBERG, W., *A Course in differential geometry*, Springer Science+Bussiness Media, 1978, https://doi.org/10.1007/978-1-4612-9923-3

[9] LÓPEZ, R., Differential geometry of curves and surfaces in Lorentz-Minkowski space, *Int. Electron. J. Geom.* **7**(1) (2014), 44–107, https://doi.org/10.36890/iejg.594497

[10] MENDES, C.M., MARIA APARECIDA SOARES RUAS, Hyperbolic motions of conics, *Amer. Math. Monthly* **94**(9) (1987), 825–845, https://doi.org/10.2307/2322815

[11] MONGE, G., Sur les lignes de courbure de la surface de l'ellipsoide, *Journ. Ecole Polytech.*, II cah. (1796), 145–165.

[12] ODEHNAL, B., STACHEL, H., GLAESER, G., *The universe of quadrics*, Springer, Berlin, 2020, https://doi.org/10.1007/978-3-662-61053-4

[13] SOTOMAYOR, J., An encounter of classical differential geometry with dynamical systems in the realm of structural stability of principal curvature configurations, *São Paulo J. Math. Sci.* **16** (2022), 256–279, https://doi.org/10.1007/s40863-021-00231-6

[14] SOTOMAYOR, J., El elipsoide de Monge y las líneas de curvatura, *Materials Matemátics* **1** (2007), 1–25.

[15] SOTOMAYOR, J., O elipsóide de Monge, *Revista Matemática Universitária* **15** (1993), 33–47.

[16] SOTOMAYOR, J., GARCIA, R., Historical comments on Monge's ellipsoid and the confgurations of lines of curvature on surfaces, *Antiquitates Mathematicae* **10** (2016), 169–182, https://doi.org/10.14708/am.v10i0.1918

[17] SOTOMAYOR, J., GUTIERREZ, C., Structurally stable configurations of lines of principal curvature, in *Bifurcation, ergodic theory and applications 1981*, *Astérisque* **98-99**, 195–215.

[18] STRUIK, D.J., *Lectures on classical differential geometry*, Dover Publications, Inc., New York, second edition, 1988.

[19] TABANOV, M.B., New ellipsoidal confocal coordinates and geodesics on an ellipsoid, *J. Math. Sci.* **82**(6) (1996), 3851–3858, https://doi.org/10.1007/BF02362647

[20] TARI, F., Caustics of surfaces in the Minkowski 3-space, *Q. J. Math.* **63**(1) (2012), 189–209, https://doi.org/10.1093/qmath/haq030

[21] TEJADA, D., *Linhas de curvaturas principais e geodésicas nulas em superfícies imersas no espaço de Minkowski 3-dimensionald*, Tese - UFG - Goiânia, 2018.

Ronaldo Garcia
orcid.org/0000-0001-8876-6956
e-mail: ragarcia@ufg.br

Instituto de Matemática e Estatística
Universidade Federal de Goiás
Goiânia-GO, Brazil

Dimas Tejada
orcid.org/0009-0005-2513-5424
e-mail: dimas.tejada@ues.edu.sv

Facultad de Ciencias Naturales y Matemática
Universidad de El Salvador
San Salvador, El Salvador

https://doi.org/10.31896/k.27.2
Original scientific paper
Accepted 12. 10. 2023.

BORIS ODEHNAL

A Miquel-Steiner Transformation

A Miquel-Steiner Transformation

ABSTRACT

Each complete quadrilateral has three Miquel-Steiner points. Any triangle together with an arbitrarily chosen point not on a triangle side also defines a complete quadrilateral, and thus, this pivot point defines three Miquel-Steiner points. These three Miquel points form a triangle which is perspective with the base triangle. The mapping that assigns to the pivot point the uniquely defined perspector is a quadratic and not involutive Cremona transformation and shall be called Miquel-Steiner transformation. We shall study the action of the Miquel-Steiner transformation and its inverse.

Key words: Miquel points, quadrilateral, triangle, quadratic Cremona transformation

MSC2020: 14A25, 51N15

Miquel-Steinerova transformacija

SAŽETAK

Svaki potpuni četverokut ima tri Miquel-Steinerove točke. Bilo koji trokut zajedno s po volji odabranom točkom koja ne leži na stranicama trokuta također definira potpuni četverokut, pa stoga ova točka određuje tri Miquel-Steinerove točke. Te tri Miquelove točke tvore trokut koji je perspektivan polaznom trokutu. Preslikavanje koje točki pridružuje jedinstveno definirano središte perspektiviteta je kvadratna neinvolutivna Cremonina transformacija koju ćemo zvati Miquel-Steinerova transformacija. Proučavat ćemo djelovanje Miquel-Steinerove transformacije i njen inverz.

Ključne riječi: Miquelove točke, četverokut, trokut, kvadratna Cremonina transformacija

1 Introduction

There are several theorems in geometry that are ascribed to the French geometer AUGUSTE MIQUEL (1816-1851). The most common of his results (originally published in [10]) may be the following (see Figure 1):

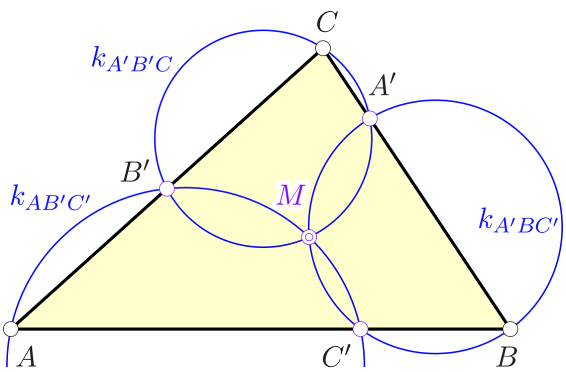

Figure 1: *Miquel's theorem as a theorem in triangle geometry.*

Let A, B, C be the vertices of a triangle and let A', B', C' be arbitrary points (different from A, B, C and not collinear) on the sides lines $[B,C]$, $[C,A]$, $[A,B]$. Then, the three circles $k_{AB'C'}$, $k_{A'BC'}$, $k_{A'B'C}$ have a common point M, the Miquel point. Here and in the following, k_{XYZ} denotes the circle on the (non-collinear) points X, Y, and Z. Sometimes, this theorem is also called the *Pivot Theorem* (see [5]).

There are other results on geometric configurations ascribed to Miquel:

(i) Miquel's *Five Circles Theorem* (cf. Figure 2, top) states that consecutive circumcircles of the spikes of a pentagonal star intersect in five concyclic points (see [3, pp. 151–152]).

(ii) Miquel's *Six Circles Theorem* (cf. Figure 2, bottom) states that if five circles meet four times in three points, then the remaining four common points are concyclic. This circle configuration can be viewed as an image of the stereographic projection of all circumcircles of the faces of a cube under a Möbius transformation. (cf. [1, 11]).

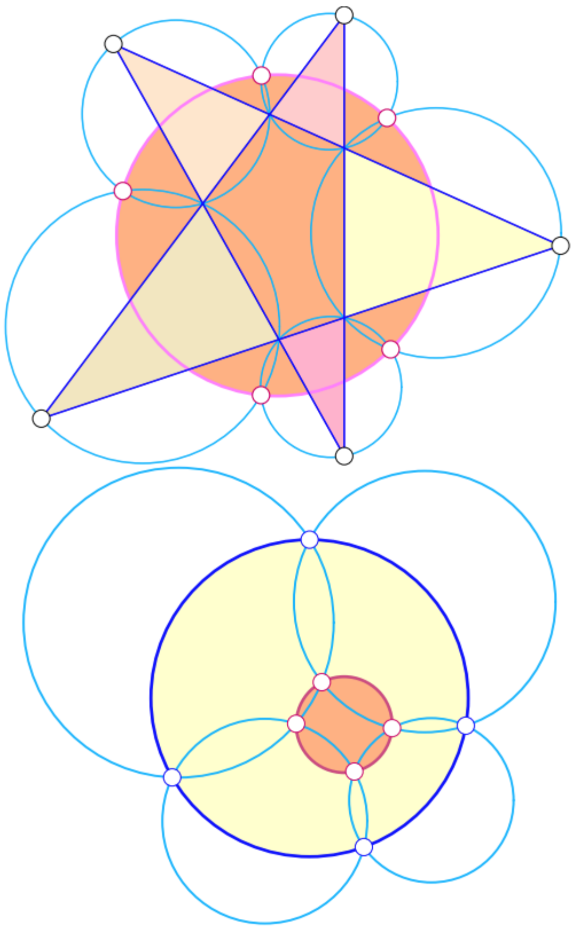

Figure 2: *Top:* MIQUEL*'s Five Circles Theorem. Bottom:* MIQUEL*'s Six Circles Theorem.*

In this article, we make use of the *Miquel-Steiner Quadrilateral Theorem*: We assume that $Q = ABCD$ is a quadrilateral, *i.e.*, no three of these points are collinear. The totality of the six lines $[A,B]$, ..., $[C,D]$ joining these points forms a complete quadrilateral. The points

$$\begin{aligned} D_1 &:= [A,B] \cap [C,D], \\ D_2 &:= [B,C] \cap [D,A], \\ D_3 &:= [C,A] \cap [B,D], \end{aligned}$$

are usually referred to as the diagonal points of Q. In the complete quadrilateral built on Q, we can find the following three quadruples of subtriangles

$$\begin{aligned} &ABD_3, \ CDD_3, \ ACD_1, \ BDD_1; \\ &ADD_1, \ BCD_1, \ ABD_2, \ CDD_2; \\ &ACD_2, \ BDD_2, \ ADD_3, \ BCD_3; \end{aligned}$$

each of which defining its own circumcircle. Then, the Miquel-Steiner Theorem reads:

Theorem 1 *The following quadruples of circumcircles of subtriangles in a complete quadrilateral share a single point:*

$$\begin{aligned} k_{ABD_3} \cap k_{CDD_3} \cap k_{ACD_1} \cap k_{BDD_1} &=: M_1, \\ k_{ADD_1} \cap k_{BCD_1} \cap k_{ABD_2} \cap k_{CDD_2} &=: M_2, \\ k_{ACD_2} \cap k_{BDD_2} \cap k_{ADD_3} \cap k_{BCD_3} &=: M_3. \end{aligned} \tag{1}$$

The *quadruple points*

$$M_1, \quad M_2, \quad M_3$$

are called the *Miquel-Steiner points* of Q, see [12, 13]. Figure 3 illustrates the contents of Thm. 1. (It is well-known, but nonetheless surprising that the four centers of the circles defining a Miquel point are concyclic, cf. [13].) As outlined in [12], the triangle $\Delta_M = M_1M_2M_3$ of Miquel points is perspective to the triangle $\Delta_D = D_1D_2D_3$ of diagonal points. Further, Δ_M is also perspective to $\Delta = ABC$ (see Figure 4). The perspector P of the triangles Δ and Δ_M shall be called *Miquel perspector*. Later, we shall replace the point D by an arbitrarily chosen point Z and consider the mapping $\mu : Z \mapsto P$ which shall be called the Miquel-Steiner transformation.

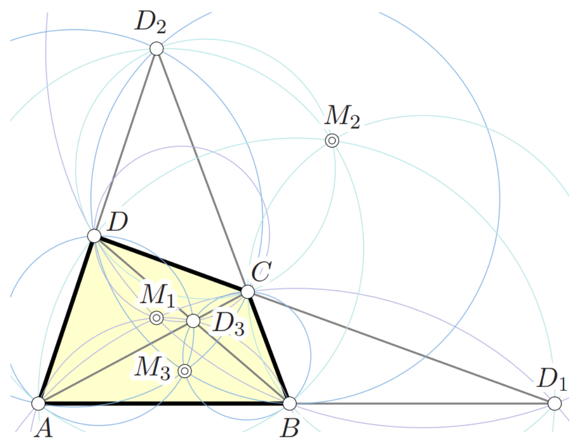

Figure 3: *The triple of Miquel points of a quadrilateral.*

In the following, we derive an analytical description of the Miquel-Steiner transformation μ. This will allow us to study its properties (cf. Section 2). Further, we derive the inverse which turns out to be different from the initial mapping. The Miquel-Steiner transformation is one of the rare examples of quadratic Cremona transformation that is not involutive as we shall see in Section 3. This is a good reason to have a closer look onto its properties and its action on objects which are occurring frequently in triangle geometry. In Section 3.3, we shall also investigate the six-parameter manifold of triangle cubics attached to the base triangle Δ which is left fixed as a whole under the Miquel-Steiner transformation. Besides that, we want to give a geometric meaning to at least some known triangle centers that show up in the inflationarily increasing *Encyclopedia of Triangle Centers* (cf. [9]).

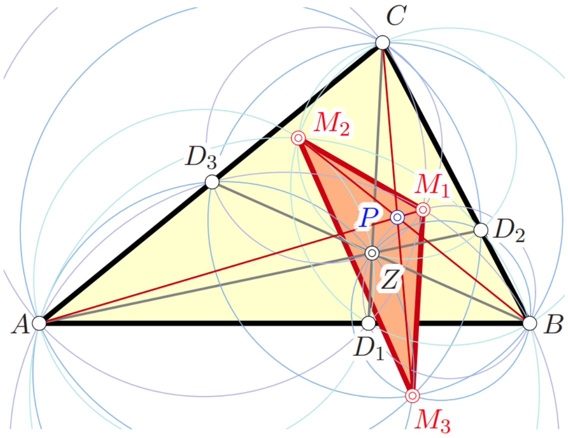

Figure 4: *Miquel points of a point Z with respect to a triangle $\Delta = ABC$ and the Miquel perspector P.*

2 A quadratic Miquel-Steiner transformation

Let us now assume that we are given a triangle $\Delta = ABC$ in the Euclidean plane. Any point Z that does not lie on a side line of Δ gives rise to a quadrilateral $Q = ABCZ$, *i.e.*, in comparison to Sec. 1, we have replaced D by Z, and the diagonal points are as defined above. Hence, the Miquel points are the quadruple points given in (1). Provided that Z is a triangle center (in the sense of [8, 9]), the Miquel perspector P is also a triangle center.

In order to study the mapping $\mu: Z \to P$, we shall derive an analytic description. For that purpose, we use homogeneous trilinear coordinates in the plane of Δ. The side lengths of Δ are

$$c := \overline{AB}, \quad a := \overline{BC}, \quad b := \overline{CA}.$$

We use the vertices of the triangle $\Delta = ABC$ as the base points of the projective frame and the incenter X_1 as the unit point. (Here and in the following, we use C. KIMBERLING's notation for triangle centers, cf. [8, 9]). Thus, we have

$$A = 1:0:0, \quad B = 0:1:0,$$
$$C = 0:0:1, \quad X_1 = 1:1:1.$$

With this coordinatization, the line at infinity (ideal line) ω is given by the homogeneous equation $a\xi + b\eta + c\zeta = 0$, or in terms of homogeneous trilinear line coordinates, as $a:b:c$.

We may assume that the fourth point Z has the homogeneous trilinear coordinates

$$\xi:\eta:\zeta \neq 0:0:0.$$

It is rather elementary to compute the three Miquel points M_1, M_2, M_3 as the intersections of the circumcircles mentioned in (1) and we find

$$\begin{aligned} M_1 := a(-a^2+b^2+c^2)\xi^2 - b(a^2-b^2)\xi\eta \\ -abc\eta\zeta + c(c^2-a^2)\zeta\xi : \\ : b(a\xi+b\eta)(a\xi+b\eta+c\zeta) : \\ : c(c\zeta+a\xi)(a\xi+b\eta+c\zeta), \\ M_2 := a(a\xi+b\eta)(a\xi+b\eta+c\zeta) : \\ : a(a^2-b^2)\xi\eta + b(a^2-b^2+c^2)\eta^2 \\ -abc\zeta\xi + c(c^2-b^2)\eta\zeta : \\ : c(b\eta+c\zeta)(a\xi+b\eta+c\zeta), \\ M_3 := a(c\zeta+a\xi)(a\xi+b\eta+c\zeta) : \\ : b(b\eta+c\zeta)(a\xi+b\eta+c\zeta) : \\ : c(a^2+b^2-c^2)\zeta^2 + a(a^2-c^2)\zeta\xi \\ +b(b^2-c^2)\eta\zeta - abc\xi\eta. \end{aligned}$$

With this it is easily verified that the triangles Δ and $\Delta_M = M_1M_2M_3$ are perspective. The Miquel perspector can be given in terms of trilinear coordinates

$$P = a(a\xi+b\eta)(a\xi+c\zeta) ::= \frac{1}{bc(b\eta+c\zeta)} ::, \qquad (2)$$

where the :: indicates that the subsequent coordinate functions are obtained by cyclically replacing all variables, *i.e.*, $a \to b \to c \to a$ and $\xi \to \eta \to \zeta \to \xi$.

The cyclic symmetry of the coordinate functions of the Miquel perspector indicates that the Miquel perspector assigned to a triangle center is also a triangle center (in the sense of C. KIMBERLING, see [8, 9]).

We can state:

Theorem 2 *The mapping $\mu: Z \mapsto P \notin \Delta_a$ that assigns to each point $Z = \xi:\eta:\zeta$ which does not lie on a side line of Δ's anticomplementary triangle Δ_a the Miquel perspector P as given in (2) is a quadratic Cremona transformation. The orthocenter X_4 of Δ is fixed under μ.*

Proof. The fact that μ from (2) is quadratic is obvious. We have to show that this mapping meets the requirements of a quadratic mapping to be invertible, *i.e.*, the (not necessarily regular) base conics defined by the three (homogeneous) quadratic coordinate functions (set equal to zero) share three points (cf. [4, 7]).

For that end, we look at the polynomial representation of μ given in (2) (in the middle). The two linear factors set equal to zero yield the equations of two straight lines: $a\xi + b\eta = 0$ is parallel to $[A,B]$ and passes through C, while $a\xi + c\zeta = 0$ is parallel to $[C,A]$ and passes through B. The latter lines meet in $A_a = -bc : ca : ab$. By virtue of the cyclic symmetry of μ's coordinate functions, we see that the exceptional set of μ consists of the lines

$$a\xi + b\eta = 0, \quad b\eta + c\zeta = 0, \quad c\zeta + a\xi = 0$$

which meet in the points

$$\begin{aligned} A_a &= -bc : \ ca : \ ab, \\ B_a &= \ bc : -ca : \ ab, \\ C_a &= \ bc : \ ca : -ab. \end{aligned}$$

The latter lines and points are the side lines and vertices of the anticomplementary triangle Δ_a of Δ. (Sometimes, Δ_a is called the *antimedial triangle*, see, *e.g.*, [6]).
The fact that $\mu(X_4) = X_4$ can easily be shown by inserting the orthocenters trilinear representation into (2). □

It is clear that no further point (different from X_4) can be fixed under μ. The Miquel-Steiner image of a point X can be found as the isogonal conjugate (with respect to Δ) of a collinear image of X (see Thm. 3). Under the isogonal conjugation ι, Δ's incenter X_1 is the only fixed point.
The base conics of the quadratic mapping μ are singular as is the case with the base conics in the isogonal and isotomic conjugation (cf. [7, 8]), and in the case of any inversion in a conic (see [7]).
According to Thm. 2, μ is a quadratic Cremona transformation, and as such, it is invertible. However, μ differs from the well-known quadratic Cremona transformations that occur frequently in triangle geometry. So, we state and prove:

Theorem 3 *The Miquel-Steiner transformation μ is not involutive. Its inverse is not defined on the side lines of Δ. The Miquel-Steiner transformation is the composition of the isogonal conjugation ι with respect to Δ and the central similarity α with Δ's centroid X_2 as the center and the scaling factor* 2, i.e., $\mu = \iota \circ \alpha$. *Δ's orthocenter is also fixed under μ^{-1}.*

Proof. The mapping μ is not involutive, since $\mu^2 \neq \mathrm{id}$ as can easily be verified.
By virtue of the right-hand side of (2), we set

$$\rho x = \frac{1}{bc(b\eta + c\zeta)}, \quad \rho y = \frac{1}{ca(c\zeta + a\xi)}, \quad \rho z = \frac{1}{ab(a\xi + b\eta)},$$

where $\rho \neq 0$ (is the complex but constant homogenizing factor). By applying the isogonal conjugation ι, we can rewrite the latter equations in the form

$$\begin{aligned} \rho^{-1}x^{-1} &= bc(b\eta + c\zeta), \\ \rho^{-1}y^{-1} &= ca(c\zeta + a\xi), \\ \rho^{-1}z^{-1} &= ab(a\xi + b\eta). \end{aligned}$$

Finally, we have to solve this system of three linear equations in the three unknowns ξ, η, ζ. By replacing x, y, z with ξ, η, ζ, we find

$$\mu^{-1}(\xi,\eta,\zeta) = bc(-a\eta\zeta + b\zeta\xi + c\xi\eta) :: . \quad (3)$$

The inverse of μ is not defined on the side lines of the base triangle. The coordinate functions of μ^{-1} describe three independent regular conics in the plane of Δ which share Δ's vertices.
The coordinate representation (2) of μ shows that μ can be considered as the composition of the isogonal transformation $\iota: (\xi,\eta,\zeta) \mapsto (\xi^{-1},\eta^{-1},\zeta^{-1})$ with respect to the base triangle Δ and a collineation α with the transformation matrix

$$\mathbf{T} = \begin{pmatrix} 0 & b^2c & bc^2 \\ a^2c & 0 & ac^2 \\ a^2b & ab^2 & 0 \end{pmatrix}.$$

The collineation α has Δ's centroid $X_2 = bc ::$ as fixed point and the ideal line $\omega = a ::$ of the projectively closed Euclidean plane of the initial triangle Δ is an axis of α. In order to show that α is a central similarity with the scaling factor -2, we compute the characteristic crossratio. For that end, we impose a projective frame on a fixed line (different from the axis, passing through the center X_2) and assign the coordinates $1:0$ to the center X_2 and $0:1$ to a generic point $Q \neq X_2$ and $Q \notin \omega$. We assume that the generic point Q has the homogeneous trilinear coordinates

$$m : n : o \neq 0 : 0 : 0$$

with respect to Δ. Then, the homogeneous coordinates of $\alpha(Q)$ and $U = [Q,\alpha(Q)] \cap \omega$ with respect to the frame on $[X_2,Q]$ are equal to

$$am + bn + co : -abc \text{ and } am + bn + co : -3abc.$$

Hence, we have

$$\mathrm{cr}(X_2,U,Q,\alpha(Q)) = -2.$$

The orthocenter of Δ is fixed under μ^{-1}. □

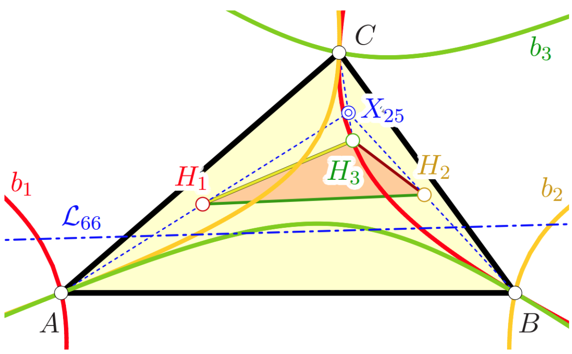

Figure 5: *The centers H_i of the three base conics b_i of μ^{-1} form a triangle perspective with Δ. X_{25} serves as the perspector, $\mathcal{L}_{66}$ is the perspectrix.*

Further, we can show what is illustrated in Figure 5:

Theorem 4 *The triangle of the centers of the three base conics of μ^{-1} is perspective with Δ. The perspector is the center triangle center X_{25} (of Δ).*

Proof. The centers H_1, H_2, H_3 of the conics given in (3) are found by multiplying the inverses of their coefficient matrices with a coordinate vector of the ideal line, *i.e.*, for example with (a,b,c). This yields

$$\begin{aligned} H_1 &= \sigma : 2b^2\cos C : 2c^2\cos B,\\ H_2 &= 2a^2\cos C : \sigma : 2c^2\cos A,\\ H_3 &= 2a^2\cos B : 2b^2\cos A : \sigma, \end{aligned}$$

where

$$\sigma := a^2+b^2+c^2$$

and

$$\cos A = \frac{b^2+c^2-a^2}{2bc} \quad \text{(cyclic)}$$

is the cosine of Δ's interior angle at A (cyclic). The perspector between Δ and $\Delta_H = H_1H_2H_3$ has the trilinear center function

$$a(-a^2+b^2+c^2)^{-1}$$

which belongs to the triangle center X_{25} in KIMBERLING's list (cf. [8, 9]). It is the homothetic center of the orthic triangle and the tangential triangle of Δ. □

The perspectrix p of Δ and Δ_H is the line carrying the triangle centers $X_{8673} \in \omega$ as well as the proper centers X_{2485}, X_{14396}, X_{52950}, *i.e.*, $p = [X_{2485}, X_{8673}] = \mathcal{L}_{66}$ (after canonical identification of line coordinates with point coordinates).

2.1 The square of μ

Since μ is not involutive, the square of the Miquel-Steiner transformation is a non-trivial and quartic Cremona transformation. It is obvious that μ^2 is a Cremona transformation, *i.e.*, it is invertible, since $(\mu^{-1})^2 \circ \mu^2 = \text{id}$. In terms of trilinear coordinates the *square* of μ reads

$$\mu^2(\xi,\eta,\zeta) = \big(bc(b\eta+c\zeta)(a(b^2+c^2)\xi+b^3\eta+c^3\zeta)\big)^{-1} :: .$$

The mapping μ^2 is not defined on the sides of the excentral triangle Δ_a of Δ and on the sides of further triangle Δ_f which is perspective with Δ. Here, X_4 (of Δ) serves as the perspector, while the perspectrix between Δ and Δ_f is the line with homogeneous coordinates $a^3 : b^3 : c^3$. The canonical identification of point and line coordinates assigns the perspectrix to the 3rd power point X_{32} (cf. [8, 9]).

3 Action of μ and μ^{-1}

Since μ is a quadratic mapping, it sends algebraic curves c of degree n to algebraic curves of degree $2n$. Degree reductions occur if c passes through a base point of the transformation. The same holds true for its inverse. In what follows, we shall have a look at the μ-images and μ^{-1}-images of some geometric objects related to the base triangle.
In order to increase the readability of equations, we shall write the coordinates ξ, η, ζ with bold characters.

3.1 Images of straight lines

We restrict ourselves to the μ-images and μ^{-1}-images of some very special lines related to a triangle. It is clear that images and pre-images of straight lines under the Miquel-Steiner transformations are conics in general, and straight lines only if the lines under consideration pass through at most one base point of the transformation.

3.1.1 Antiorthic axis

The antiorthic axis $\mathcal{L}_1 = 1:1:1$ is the harmonic conjugate of X_1 with respect to the base triangle Δ. Its μ-image is the central conic

$$\mu(\mathcal{L}_1) : \sum_{\text{cyclic}} c\,(bc+ca-ab)\,\xi\eta = 0$$

passing through the triangle centers X_i with

$$i \in \{100, 34071, 52923\}.$$

The center of the conic $\mu(\mathcal{L}_1)$ is the yet unnamed, and thus, unlabelled triangle center defined by the homogeneous trilinear center function

$$\begin{aligned} &a(ab+ac-bc)\cdot\\ &\cdot\big(a^3(b+c)-a^2bc-a(b+c)(b-c)^2-bc(b^2+c^2)\big). \end{aligned}$$

The μ-pre-image of the antiorthic axis is again a conic and has the trilinear equation

$$\mu^{-1}(\mathcal{L}_1) : \sum_{\text{cyclic}} a^3\xi^2 + ab(a+b+c)\xi\eta = 0.$$

It is centered at the Gergonne point X_7 and houses the centers

$$i \in \{149, 4440, 20355, 20533, 21220, 21221, 30578, 37781\}.$$

Figure 6 shows a triangle with its antiorthic axis $\mathcal{L}_1$ the conics $\mu(\mathcal{L}_1)$ and $\mu^{-1}(\mathcal{L}_1)$.

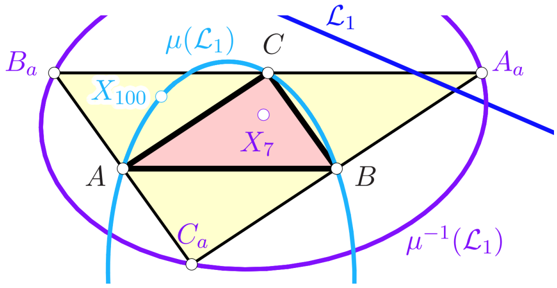

Figure 6: *Image and pre-image of the antiorthic axis $\mathcal{L}_1$.*

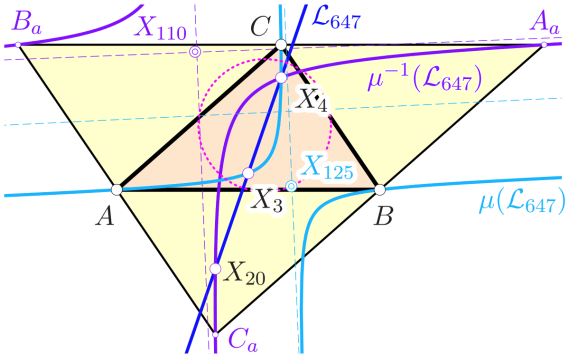

Figure 7: *The Euler line and its μ-image and μ^{-1}-image.*

3.1.2 Euler line

The μ-pre-image of the Euler line (cf. Figure 7)

$$\mathcal{L}_{647} = [X_2, X_3] = a(b^2 - c^2)(a^2 - b^2 - c^2) ::$$

is the central conic with the trilinear equation

$$\mu^{-1}(\mathcal{L}_{647}) : \sum_{\text{cyclic}} a^4(b^2-c^2)(a^2-b^2-c^2)\xi^2 = \\ = 2 \prod_{\text{cyclic}} (a^2-b^2) \sum_{\text{cyclic}} ab\xi\eta$$

centered at X_{110}, the focus of the Kiepert parabola.
The conic $\mu^{-1}(\mathcal{L}_{647})$ passes through the proper triangle centers X_i with the Kimberling indices

$$i \in \{4, 20, 69, 146, 193, 2888, 2889, 2892, 3868, 3869, 5596, 6193, 6225, 10340, 11061, 11271, 11469, 12383, 17220, 18387, 22647, 32354, 37889, 39355\}$$

and carries also the centers X_{2574} and X_{2575} located on the line at infinity.
The μ-image of the Euler line is the conic

$$\mu(\mathcal{L}_{647}) : \sum_{\text{cyclic}} c(a^2-b^2)(a^2+b^2-c^2)\xi\eta = 0$$

centered at X_{125} which is the center of the Jeřabek hyperbola. The latter conic carries 272 known triangle center of which X_{2574} and X_{2575} are points at infinity while the proper points have the Kimberling indices

$$i \in \{3, 4, 6, 54, 64-74, 248, 265, 290, 695, 879, 895, 1173, 1175-1177, 1242-1246, 1439, 1798, 1903, 1942, 1987, 2213, 2435, 3426, 3431, 3519, 3521, 3527, 3531, 3532, 3657, 4846, 5486, 5504, 5505, 5900, 6145, 6391, 8044, 8612, 8795, 8811, 8814, 9399, 9513, 10097, 10099, 10100, 10262, 10293, 10378, 10693, 11270, 11559, 11564, 11738, 11744, 12023, 13418, 13452, 13472, 13603, 13622, 13623, 14220, 14374, 14375, 14380, 14457, 14483, 14487, 14490, 14491, 14498, 14528, 14542, 14841, 14843, 14861, 15002, 15077, 15232, 15316, 15317, 15320, 15321, 15328, 15453, 15460, 15461, 15740, 15749, 16000, 16540, 16620, 16623, 16665, 16774, 16835, 16867, 17040, 17505, 17711, 18123, 18124, 18125, 18296, 18363, 18368, 18434, 18532, 18550, 19151, 19222, 20029, 20421, 21400, 22334, 22336, 22466, 26861, 28786-28788, 30496, 31366, 31371, 32533, 33565, 34207, 34221, 34222, 34259, 34435-34440, 34483, 34567, 34800-34802, 34817, 35364, 35373, 35512, 35909, 36214, 37142, 38005, 38006, 38257, 38260, 38263, 38264, 38433, 38436, 38439, 38442, 38443, 38445, 38447, 38449, 38534, 38535, 38955, 39372, 39379, 39665, 39666, 40048, 40441, 41433, 41435, 41518, 41519, 42016, 42021, 42059, 42299, 43689-43727, 43834, 43891, 43908, 43918, 43949, 44207, 44718, 43892, 44750, 44835, 44836, 45011, 45088, 45302, 45733, 45736, 45788, 45835, 45972, 46765, 46848, 46851, 47060, 48362, 51223, 51480, 52222, 52390, 52391, 52518, 52559, 52560, 52561, 54124, 54125\}.$$

The two conics $\mu(\mathcal{L}_{647})$ and $\mu^{-1}(\mathcal{L}_{647})$ are both passing through the circumcenter X_3 and the orthocenter X_4. Further, $\mu^{-1}(\mathcal{L}_{647})$ is a circumconic of Δ_a and contains the de Longchamp point X_{20} of Δ. Since X_{20} is at the same time the orthocenter of Δ_a, we can summarize and state:

Theorem 5 *The μ-image and the μ-pre-image of the Euler line are equilateral hyperbolae with the same ideal points (and hence, parallel asymptotes). The first is centered at X_{125}, the second is centered at X_{110}.*

3.1.3 Brocard axis

The Brocard axis $\mathcal{L}_{523} = [X_3, X_6]$ with trilinear coordinates $bc(b^2-c^2)$ :: is sent to the conic with the equation

$$\mu^{-1}(\mathcal{L}_{523}) : \sum_{\text{cyclic}} a^2(b^2-c^2)\xi^2 = 0$$

via the inverse of the Steiner-Miquel transformation. This conic is centered at X_{99} (Steiner point) and contains the triangle centers X_i with Kimberling indices

$$i \in \{1, 2, 20, 63, 147, 194, 487, 488, 616, 617, 627, 628, 1670, 1671, 1764, 2128, 2582, 2583, 2896, \mathbf{3413}, \mathbf{3414}, 6194, 6462, 6463, 7616, 8591, 8782, 9742, 10336, 11148, 13174, 13678, 13798, 16552, 16563, 17147, 18301, 18596, 20371, 21378, 30562, 30564, 30579, 33404, 33405, 33608, 33609, 33610, 33611, 33612, 33613, 36857, 41914, 41923, 41930, 44010, 45029, 46625, 46717, 46944, 51860, 51952, 51953, 52025, 52676, 53856\},$$

where X_{3413} and X_{3414} are real points on the line at infinity. Hence, $\mu^{-1}(\mathcal{L}_{523})$ is a hyperbola.
On the other hand, μ sends the Brocard axis to the central conic

$$\mu(\mathcal{L}_{523}) : \sum_{\text{cyclic}} c(a^2-b^2) \cdot \left(a^2(b^2+c^2) + c^2(b^2-c^2)\right) \xi\eta = 0$$

centered at the yet unnamed triangle center with the trilinear center function

$$a(b^2-c^2)^2(a^4-a^2b^2-a^2c^2-b^2c^2)\cdot \\ \cdot\big(a^6-2a^4(b^2+c^2)+a^2(b^4-b^2c^2+c^4)-b^2c^2(b^2+c^2)\big).$$

Finally, we shall note that the triangle centers X_i with Kimberling numbers

$$i\in\{54,98,251,1078,1179,1342,1343,1629,3453, \\ 5012,5481,10312,11816,38826,39396,42346\}$$

are located on the conic $\mu(\mathcal{L}_{523})$.

3.2 Images of conics

Again, the huge variety of conics makes it necessary to pick out some special representatives. It is clear that conics only map to conics if they are circumscribed to the triangle of base points, *i.e.*, the anticomplementary triangle Δ_a. The Miquel-Steiner transforms of circumconics of the initial triangle Δ are quartic curves in general.

3.2.1 Steiner circumellipse

Degeneracies of the image curves can only be expected if the circumconics of Δ touch the anticomplementary triangle. This happens escpecially in the following case:

Theorem 6 *The Miquel-Steiner pre-image of the Steiner circumellipse is the central line* $\mathcal{L}_{3051}=[X_{316},X_{512}]$.

Proof. We insert (2) into the equation

$$s:\ bc\eta\zeta+ca\zeta\xi+ab\xi\eta=0$$

of the Steiner ellipse and find

$$\mu^{-1}(s):\ \sum_{\text{cyclic}}a^3(b^2+c^2)\xi=0.$$

Now, it is an elementary task to verify that $\mu^{-1}(s)$ is spanned by X_{316} (Droussent pivot) and $X_{512}\in\omega$. The canonical identification of the trilinear coordinates of $\mu^{-1}(s)$ with the coordinates results in a center with the trilinear center function $a^3(b^2+c^2)$ which is that of X_{3051} (cf. [8, 9]). □

Furthermore, the following triangle centers X_i with Kimberling indices

$$i\in\{316,850,3766,3978,11450,14957,14962,17995, \\ 20022,20295,20352,20556,21282,21301,21302, \\ 21303,33873,44445,47128,52618,53331,53365,54263\}$$

are located on $\mu^{-1}(s)$.

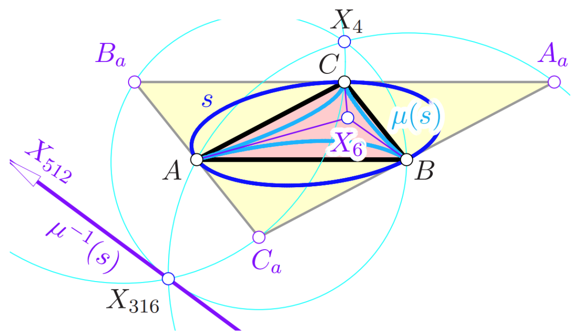

Figure 8: *Steiner-Miquel image and pre-image of the Steiner circumellipse.*

The μ-image of s is a quartic with three cusps at the vertices of Δ passing through the centers X_i with

$$i\in\{249,1016,1252,1262,2226,6185,10630,23586, \\ 23592,23964,23984,34536,34537,34538,34539,40384\}.$$

The tangents at the cusps concur in the Symmedian point $X_6=a:b:c$. Figure 8 shows the Steiner-Miquel image and pre-image of the Steiner circumellipse s of Δ.

3.2.2 Circumcircle

The μ-pre-image of the circumcircle

$$u:\ a\eta\zeta+b\zeta\xi+c\xi\eta=0$$

is the ideal line

$$\omega:\ a\xi+b\eta+c\zeta=0.$$

The circumcircle is mapped under the Miquel-Steiner transformation to the quartic curve

$$\mu(u):\ \sum_{\text{cyclic}}a^2(-a^2+b^2+c^2)\eta^2\zeta^2= \\ =2abc\,\xi\eta\zeta(a\xi+b\eta+c\zeta) \tag{4}$$

housing the triangle centers X_i with

$$i\in\{59,249,250,2065,10419,15378-15388, \\ 15395-15397,15401-15407,15460, \\ 15461,41511,44174\}.$$

The vertices of Δ are ordinary double points of $\mu(u)$. The tangents at the double points are the Cevians through the circumcenter X_3 and the Symmedian point X_6, cf. Figure 9. This can easily be verified by extracting the coefficients of ξ^2, η^2, and ζ^2 from (4) and showing that the resulting quadratic forms factor and split into two linear factors which (if set equal to zero) yield the equations of the tangents at the double points. For example, the coefficient of ξ^2 equals

$$(b\zeta-c\eta)\big(b(a^2-b^2+c^2)\zeta-c(a^2+b^2-c^2)\eta\big).$$

The first factor describes the Cevian through X_6, the second that through X_3.

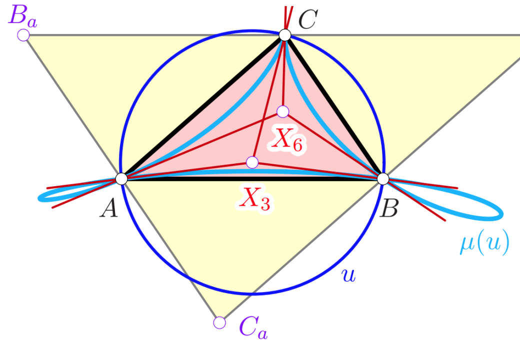

Figure 9: *The Miquel-Steiner transform of the circumcircle u is a quartic with three ordinary double points at the vertices of Δ. The tangents at the double points are the joins with the circumcenter X_3 and the Symmedian point X_6.*

By virtue of (4), it is clear that $\mu(u)$ degenerates if Δ is a right triangle. Let (for example) the right angle be at C. Then, $a^2+b^2=c^2$, the term $\xi^2\eta^2$ vanishes, and the right-hand side becomes

$$2a^2b^2\zeta^2(\xi^2+\eta^2).$$

Thus, the side $[A,B]$ (opposite to the vertex C) splits off from $\mu(u)$.

For an equilateral triangle Δ, *i.e.*, $a=b=c\neq 0$, the curve $\mu(u)$ becomes a Steiner hypocycloid.

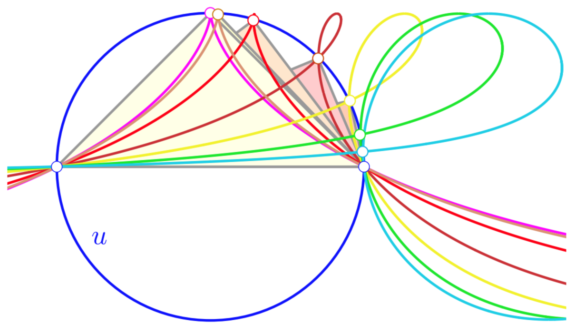

Figure 10: *A sequence of right triangles with ratios of cathetus's lengths 1:1, 20:21, 3:4, 5:12, 9:40, 19:180, 41:840 and the corresponding cubic curves as μ-images of the circumcircle u.*

3.2.3 Incircle

The μ-pre-image of the incircle

$$i:\sum_{\text{cyclic}} a^2(a-b-c)^2\xi^2=\sum_{\text{cyclic}} 2ab(a-b+c)(-a+b+c)\,\xi\eta$$

is the quartic curve

$$\begin{gathered}
\mu^{-1}(i):\sum_{\text{cyclic}} a^9bc(a+b+c)(a-b-c)^2\xi^4\\
-2a^5\big(b(b-c)a^6-(b^3-2b^2c-bc^2+c^3)a^5\\
-(2b^4-b^3c-2bc^3-c^4)a^4\\
+(2b^5-3b^4c-b^3c^2-7b^2c^3-bc^4+2c^5)a^3\\
+(b^6+2b^4c^2+2b^3c^3+3b^2c^4-2bc^5-2c^6)a^2\\
-(b-c)(b^6+2b^4c^2+b^3c^3+2b^2c^4-bc^5-c^6)a\\
c^3(b-c)^2(b+c)^3\big)\xi^3(b\eta+c\zeta)\\
-a^2b^2\big(b(4b-c)a^8-(b-c)(4b^2-bc-2c^2)a^7\\
-(8b^4-b^3c+6b^2c^2-3bc^3-2c^4)a^6\\
+(8b^5-9b^4c+7b^3c^2-5b^2c^3-bc^4+4c^5)a^5\\
+(4b^6-b^5c+10b^4c^2+2b^3c^3+8b^2c^4-5bc^5-4c^6)a^4\\
-(4b^7-5b^6c+15b^5c^2-6b^4c^3-5b^2c^5-bc^6+2c^7)a^3\\
c(b^5+2b^3c^2+10b^2c^3+7bc^4+2c^5)(b-c)^2a^2\\
-bc(b-c)^2(b-c)(b^4-2b^3c-2b^2c^2+c^4)a\\
+2b^3c^2(b+c)^2(b-c)^3\big)\xi^2\eta^2\\
-2a^2bc\big(b(3b-2c)a^8-(3b^3-5b^2c-2bc^2+3c^3)a^7\\
-(6b^4-2b^3c+2b^2c^2-5bc^3-3c^4)a^6\\
+(6b^5-8b^4c+2b^3c^2-18b^2c^3-2bc^4+6c^5)a^5\\
+(3b^6-b^5c+8b^4c^2+4b^3c^3+9b^2c^4-7bc^5-6c^6)a^4\\
-(3b^7-4b^6c+13b^5c^2-3b^4c^3-b^3c^4-6b^2c^5-bc^6-3c^7)a^3\\
c(b-c)^2(b^5+3b^3c^2+13b^2c^3+10bc^4+3c^5)a^2\\
-bc(b+c)(b-c)^2(b^4-2b^3c-2b^2c^2+c^4)a\\
+2b^3c^2(b+c)^2(b-c)^3\big)\xi^2\eta\zeta=0.
\end{gathered}$$

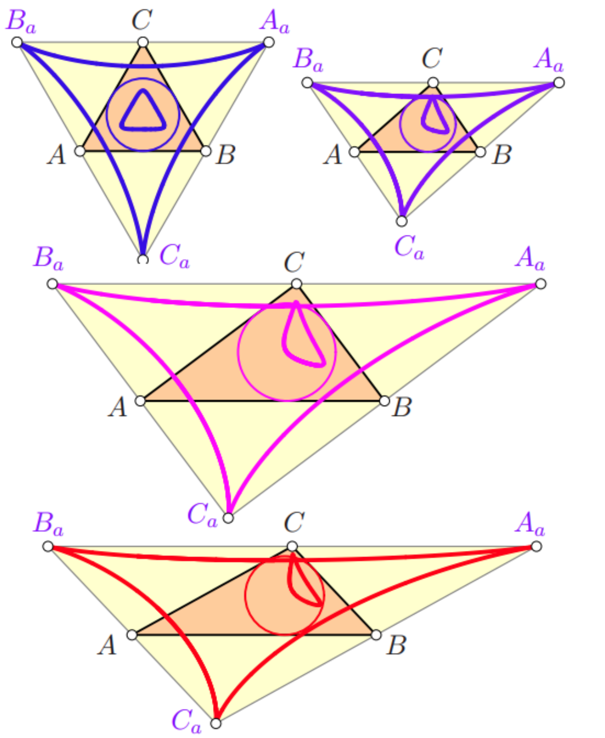

Figure 11: *Miquel-Steiner transforms and the (cusped) inverses of the incircle for an equilateral, an acute, a right, and an obtuse triangle.*

This quartic curve has three cusps at the vertices of the anticomplementary triangle Δ_a of Δ. Therefore, they map to

a conic that touches the three sides lines of the exceptional triangle of the mapping μ^{-1} (which is Δ). In the case of an equilateral triangle Δ (and thus also Δ_a), the curve $\mu^{-1}(i)$ is a Steiner hypocycloid (cf. Figure 11).
The μ-image of the incircle is the quartic

$$\begin{aligned}\mu(i):\ \sum_{\text{cyclic}} c^2\big(&(2a^6-4a^5(b-c)-3a^4(2b^2+bc-2c^2)\\&+a^3(8b^3-b^2c-bc^2-8c^3)\\&+a^2(6b^4-9b^3c+2b^2c^2+7bc^3+6c^4)\\&-a(4b^5-b^4c+b^3c^2+b^2c^3+7bc^4-4c^5)\\&-2(b^2+c^2)(b^2-c^2)^2\big)\xi^2\eta^2\\&+2b^2c\big(2a^5+a^4(2b-c)-a^3(b+c)(4b-7c)\\&-a^2(4b^3-7b^2c-2bc^2+c^3)\\&+a(b+c)(2b^3-b^2c-8bc^2+3c^3)\\&+2(b+c)^2(b-c)^3\big)\xi^2\eta\zeta=0.\end{aligned}$$

The vertices of Δ are isolated double points on the μ-images of i since the incircle of Δ always lies completely in the interior of the anticomplementary triangle Δ_a. Figure 11 shows the Miquel-Steiner image and pre-image of the incircle for four triangles (obtuse, right, acute, equilateral).

3.2.4 Nine-Point Circle

The nine-point circle n can be described by the homogeneous trilinear equation

$$n:\ \sum_{\text{cyclic}} a^2(-a^2+b^2+c^2)\xi^2=2abc(a\eta\zeta+b\zeta\xi+c\xi\eta).$$

The nine-point-circle is mapped under μ^{-1} to the quartic curve

$$\begin{aligned}\mu^{-1}(n):\ \sum_{\text{cyclic}} & a^8(a^2-b^2-c^2)\xi^4+\\&2a^5b\big(a^4-a^2(b^2+c^2)+2b^2c^2\big)\xi^3\eta\\&-2ab^5\big(a^2(b^2-2c^2)-b^2(b^2-c^2)\big)\xi\eta^3\\&+a^2b^2\big(a^6-a^4(b^2+c^2)-a^2(b^4-8b^2c^2+c^4)\\&+(b^2+c^2)(b^2-c^2)^2\big)\xi^2\eta^2=\\&=-2abc\xi\eta\zeta\sum_{\text{cyclic}} a(2a^6-2a^4(b^2+c^2)\\&-a^2(b^2+c^2)(b^2-c^2)^2)\xi.\end{aligned}$$

On it we can find the centers X_{35258}, X_{47785}, and X_{54280}. The μ-image of n is also a quartic curve with the trilinear equation

$$\begin{aligned}\mu(n):\ &\sum_{\text{cyclic}} c^2(c^2-3a^2-3b^2)\xi^2\eta^2=\\&=2\xi\eta\zeta\sum_{\text{cyclic}} bc(-5a^2+b^2+c^2)\xi.\end{aligned}$$

Surprisingly, there are only two labelled triangle centers on $\mu(n)$: X_{18771} (the Miquel-Steiner image of the Feuerbach point X_{11}) and X_{46426}. Depending on the shape of the triangle Δ, the curve $\mu(n)$ may have three cusps (equilateral triangle) or two double points and one cusp (isosceles triangle). For a right triangle Δ, $\mu(n)$ splits into a cubic and a straight line. If the right angle is at the vertex C, the linear component is given by $a\xi+b\eta=0$ and the cusp lies in the vertex C_a of the anticomplementary triangle Δ_a, *i.e.*, Δ_a's vertex opposite to C.

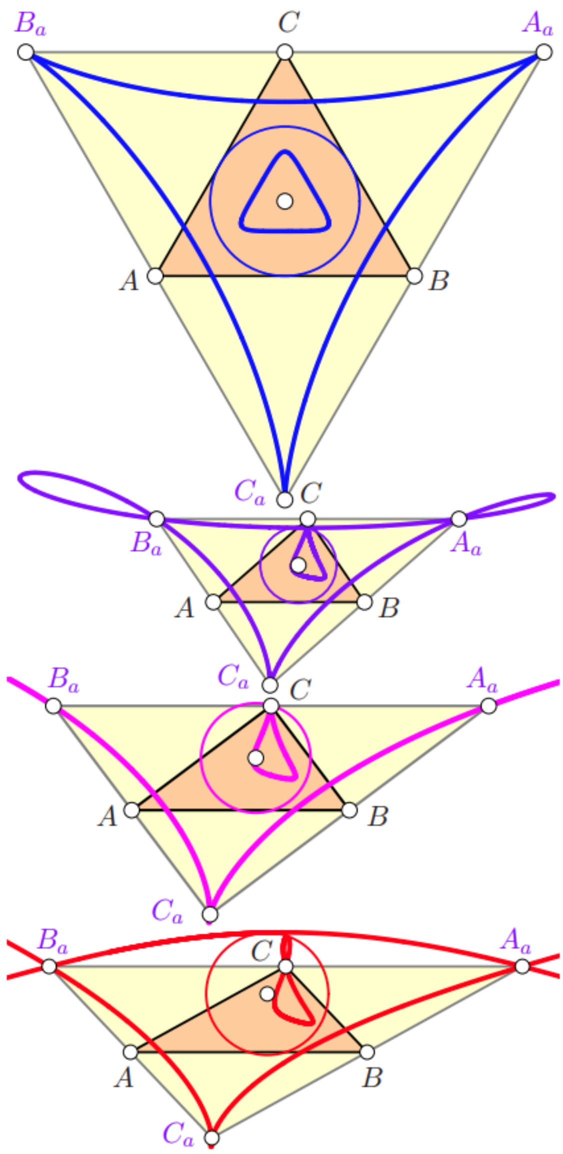

Figure 12: *Images and pre-images of the nine-point circle of an acute, an obtuse, a right, and an equilateral triangle.*

3.3 Triangle cubics

It is clear that the 6-parameter family of triangle cubics

$$
\begin{aligned}
\mathcal{C}^6: &\sum_{\text{cyclic}} \tfrac{a^2}{c^2} q_{102}\,\xi^3 - \sum_{\text{cyclic}} q_{210}\,\xi^2\eta - q_{111} \sum_{\text{cyclic}} \tfrac{a^2}{bc}\,\xi^3 \\
&+ \tfrac{1}{a^2b^2c^2}\left(a^4c^2 q_{120}\,\xi^3 + b^4a^2 q_{012}\,\eta^3 + c^4b^2 q_{201}\,\zeta^3\right) \\
&- (q_{120}\,\xi\eta^2 + q_{012}\,\eta\zeta^2 + q_{201}\,\zeta\xi^2) + q_{111}\,\xi\eta\zeta = 0
\end{aligned} \tag{5}
$$

that pass through the vertices of Δ_a are mapped to cubics under μ (since the side lines of Δ_a split off from the image curve). According to Thms. 2 and 3, the orthocenter X_4 of Δ is fixed under μ and μ^{-1}. If a triangle cubic $\mathcal{C}$ contains X_4, then $X_4 \in \mu(\mathcal{C})$ and $X_4 \in \mu^{-1}(\mathcal{C})$.
Among the triangle cubics listed in B. GIBERT's *Catalogue of Triangle Cubics* (see [6]), we find the following cubics $\mathcal{K}_i$ with indices

$$
\begin{aligned}
i \in \{&7, 8, 45, 80, 92, 133, 141, 142, 144, 146, 154, \\
&170, 211, 240, 242, 254, 279, 311, 347, 355, 371, \\
&380, 449, 455, 548, 605, 611, 617, 659, 753, 860, \\
&985, 1000, 1002, 1004, 1053a, b, 1078, 1131\}
\end{aligned}
$$

which are also contained in the 6-parameter family (5).
For some of the cubics in B. GIBERT's list, their μ-images are also contained in the catalogue of cubics, see Tab. 1.

$\mathcal{K}_i$	7	8	80	141	170
$\mathcal{K}_j$	2	273	361	644	233
$\mathcal{K}_i$	254	311	355	449	611
$\mathcal{K}_j$	379	454	380	447	1172
$\mathcal{K}_i$	617	753	1000	1002	1037
$\mathcal{K}_j$	28	73	354	135	1013
$\mathcal{K}_i$		1053a,b		1131	
$\mathcal{K}_j$		1145a,b		1134	

Table 1: *Triangle cubics $\mathcal{K}_i$ with μ-images $\mathcal{K}_j$ both contained in* B. GIBERT*'s catalogue* [6].

$\mathcal{K}_i$	$X_j \in \mu(\mathcal{K}_i)$
45	2, 4, 6, 54, 275, 1993, 8882, 34756
240	6, 69, 316, 512, 3448, 14360, 53365
242	6, 69, 316, 3448, 14360, 53365
279	2, 4, 6, 30, 323, 2986, 5504, 10419, 15262
380	4, 6, 251, 1976, 2065
455	1, 6, 35, 37, 1126, 1171, 1255, 21353, 33635
605	6, 58, 63, 81, 284, 2287, 7123, 40403
659	6, 32, 83, 251, 51951
860	6, 15, 16, 74, 40384
985	6, 58, 81, 291, 1922, 2311, 7132, 24479, 38810, 38813
1078	1, 6, 56, 57, 266, 289, 1743

Table 2: *Triangle cubics $\mathcal{K}_i$ (from* GIBERT*'s) catalogue whose images are defined by triangle centers X_j (from* KIMBERLING*'s encyclopedia).*

The images of some other cubics are not contained in GIBERT's catalogue, but nevertheless, well defined solely by the triangle centers contained in them, see Tab. 2.
As can be seen in Tab. 1, the Lucas cubic $\mathcal{K}_{007}$ is mapped to the Thomson cubic $\mathcal{K}_{002}$. The image of the Droussent cubic $\mathcal{K}_{008}$ is the pivotal isocubic $\mathcal{K}_{273}$. Figure 13 shows the cubic $\mathcal{K}_{254}$ with some triangle centers on it. The μ-image $\mathcal{K}_{379}$ as well as the μ^{-1}-image of $\mathcal{K}_{254}$ is shown.

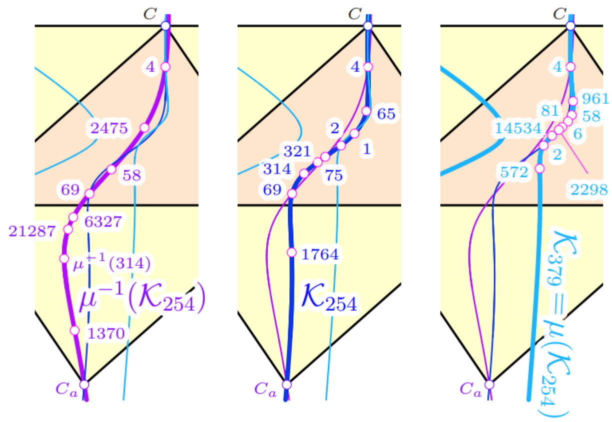

Figure 13: *The cubic $\mathcal{K}_{254}$, its μ-image $\mathcal{K}_{379}$, and its μ^{-1} image together with the centers on it.*

4 Final remarks

As mentioned earlier (and also in [12]), there exists a perspector R for the triangles Δ_M and Δ_D. In terms of trilinear coordinates and depending on $Z = \xi:\eta:\zeta$, the perspector R reads

$$
\begin{aligned}
R = &\left(a(a^2-b^2-c^2)\xi^2 + b(a^2-b^2)\xi\eta + c(a^2-c^2)\zeta\xi + abc\eta\zeta\right) \\
&\left(a(b\eta + c\zeta)\eta\zeta - bc\xi(\eta^2+\zeta^2) + (2a^2-b^2-c^2)\xi\eta\zeta\right) :: .
\end{aligned}
$$

The mapping $Z \mapsto R$ is quintic and by no means involutive. The Miquel-Steiner transformation is not involutive. We can give some chains of triangles centers, where each triangle center in the chain is the Miquel-Steiner transformation of its predecessor (see Tab. 3.).
It is possible to define some more algebraic transformations based on Miquel's theorem (the triangle related theorem illustrated in Figure 1). For example, the assumption that the three points A', B', C' be collinear yields a quartic transformation that sends lines to to points. Unfortunately, this transformation is not invertible. If the points A', B', C' are the vertices of the Cevian triangle of a point P, then the mapping that sends P to the respective Miquel point (as illustrated in Figure 1) is sextic. In this case it has to be clarified under which circumstances this mapping is invertible.

μ^{-3}	μ^{-2}	μ^{-1}	μ^{0}	μ^{1}	μ^{2}
	3436	8	**1**	58	3453
	1370	69	**2**	6	251
	6225	20	**3**	54	1166
			4		
		2888	**5**	1173	
			6 $\uparrow$ 2		
		3434	**7**	57	3451
			8 $\uparrow$ 1		
		329	**9**	1174	
		1330	**10**	1126	
		17035	**51**		
			52	1179	
			54 $\uparrow$ 3		
		144	**55**	3449	
		42020	**56**	3450	
			57 $\uparrow$ 7		
			58 $\uparrow$ 1		
149	513	100	**59**		
		2975	**60**		
		146	**30**	74	10419
		146	**66**	18018	40404
		6327	**75**	81	1169
	147	511	**98**	2065	
	148	512	**99**	249	
			100 $\uparrow$ 59		
	150	514	**101**	15378	
	151	515	**102**	15379	
	152	516	**103**	15380	
	153	517	**104**	15381	
	20344	518	**105**	15382	
	21290	519	**106**	15383	
	34186	520	**107**	15384	
	34188	521	**108**	15385	
	33650	522	**109**	15386	
	3448	523	**110**	250	
	14360	524	**111**	15387	
	13219	525	**112**	15388	

Table 3: *Some centers and the repeated μ-images.* **6** $\uparrow$ 2 *indicates that the center with Kimberling index* **6** *already shows up in the chain defined by center with Kimberling index* **2**.

References

[1] BENZ, W., *Vorlesungen über Geometrie der Algebren,* Springer-Verlag, Berlin-Heidelberg-New York, 1973, https://doi.org/10.1007/978-3-642-88670-6

[2] CAPITÁN, G., JAVIER, F., Locus of centroids of similar inscribed triangles, *Forum Geom.* **16** (2016), 257–267.

[3] CASEY, J., *A Sequel to the First Six Books of the Elements of Euclid, Containing an Easy Introduction to Modern Geometry with Numerous Examples,* 5th ed., rev. enl., Hodges, Figgis, & Co., Dublin, 1888.

[4] FLADT, K., Die Umkehrung der ebenen quadratischen Cremonatransformationen, *J. reine ang. Math.* **170** (1934), 64–68.

[5] FORDER, H.G., *Geometry*, Hutchinson University Library, London, 1960.

[6] GIBERT, B., *Catalogue of Triangle Cubics,* Available at: http://bernard-gibert.fr/index.html

[7] GLAESER, G., STACHEL, H., ODEHNAL, B., *The Universe of Conics.* From the ancient Greeks to 21st century developments, Springer-Spektrum, Springer-Verlag, Heidelberg, 2016, https://doi.org/10.1007/978-3-662-45450-3

[8] KIMBERLING, C., *Encyclopedia of Triangle Centers,*
Available at: http://faculty.evansville.edu/ck6/encyclopedia/etc.html. Last accessed: 5/2023.

[9] KIMBERLING, C., *Triangle Centers and Central Triangles,* (Congressus Numerantium Vol. 129) Utilitas Mathematica Publishing, Winnipeg, 1998.

[10] MIQUEL, A., Mémoire de Géométrie, *Journal de Mathématiques Pures et Appliquées* **1** (1838), 485–487.

[11] MÜLLER, E., KRAMES, J., *Vorlesungen über Darstellende Geometrie II: Die Zyklographie,* Deuticke, Wien-Leipzig, 1929.

[12] ODEHNAL, B., A rarity in geometry: a septic curve, *KoG* **25** (2021), 25–39, https://doi.org/10.31896/k.25.3

[13] ROLÍNEK, M., DUNG, L.A., The Miquel points, Pseudocircumcenter, and Euler-Poncelet-Point of a Complete Quadrilatera, *Forum Geom.* **14** (2014), 145–153.

Boris Odehnal
orcid.org/0000-0002-7265-5132
e-mail: boris.odehnal@uni-ak.ac.at
University of Applied Arts Vienna
Oskar-Kokoschka-Platz 2, A-1010 Vienna, Austria

https://doi.org/10.31896/k.27.3
Original scientific paper
Accepted 3. 11. 2023.

Walther Jank
Georg Glaeser
Boris Odehnal

On the Geometry of Spherical Trochoids

On the Geometry of Spherical Trochoids

ABSTRACT

We provide a synthetic study of the top-views of spherical trochoids. These projections turn out to be higher trochoids, *i.e.*, curves generated by the superposition of more than two rotations. Special shapes of these trochoids show up for special choices of the spherical radii of the rolling circles. A relation to closed algebraic curves of constant width is shown. These curves allow for a kinematic generation.

Key words: spherical trochoid, rolling, evolute, involute, curve of constant width

MSC2020: 53A17, 51N05, 14H45

O geometriji sfernih trohoida

SAŽETAK

U ovom radu se proučavaju tlocrti sfernih trohoida pomoću sintetičke metode. Pokazuje se da su te projekcije više trohoide, tj. krivulje nastale istovremenim djelovanjem više od dvije rotacije. Posebni oblici ovih trohoida pojavljuju se u slučajevima posebnih odabira sfernih polumjera kružnica koje se kotrljaju. Prikazana je veza sa zatvorenim algebarskim krivuljama konstantne širine. Ove krivulje dopuštaju kinematičko izvođenje.

Ključne riječi: sferna trohoida, kotrljanje, evoluta, involuta, krivulja konstantne širine

1 Introduction

1.1 Motivation, prior work, and contributions of the present paper

This paper is devoted to the memory of Walther Jank (1939–2016). An unpublished and hand written manuscript of a talk given by W. Jank at the *Geometrietagung* in Vorau (Austria) in June 2004 was the basis of this article. It deals with the *geometric* deduction of results on the shapes of the top-views of spherical trochoids. Since W. Jank was a dedicated follower of Walter Wunderlich's work of merit on kinematics (cf. [19]) and especially on trochoids and higher trochoids (see [20]), he applied some of these results to spherical trochoids which have gained a little less attention than their planar counterparts.

There exist only a few notable publications on spherical trochoidal curves related to W. Jank's manuscript. In [6], we find historical remarks and a collection of known results. Maybe, it was Rudolf Bereis who first described the images of spherical trochoids under various parallel projections in [1].

This article shall first follow W. Jank's manuscript, *i.e.*, we lay down his results and his reasoning. This includes a detailed description of spherical trochoids based on a constructive approach. The kinematic generation of the top-views of spherical trochoids leads to the finding that some of these top-views are curves of constant width.

Moreover, a synthetic proof of Enneper's theorem on the shape of the top-views of curves of constant slope on ellipsoids of revolution (with their axis in lead direction, *i.e.*, in the direction of the projection) can be found along the way.

At the end of the manuscript, the author raised the question whether it is possible to describe planar algebraic and closed curves of constant width, *i.e.*, planar curves whose projection onto a line (within their plane) is a segment of fixed length independent of the direction of the projection, see [17]. Such curves, comparable to the example given in Fig. 14, were derived in [14]. The results therein were veryfied and improved by [12] and the related Zindler curves were described in [15]. The approaches towards curves of constant width in these references are analytic and algebraic in nature, and by no means, constructive or geometric. We shall close this gap.

The present paper is organized as follows: The remainder of this section describes the constructive treatment of spherical trochoids and discusses the kinematic generation. Special cases occur for special assumptions on the spherical radii of the rolling circles which causes special shapes of the curves and their top-views. We try to follow W. JANK's diction by trying to translate his manuscript as direct as possible. This does not necessarily include the original notation and symbols. In Sec. 2, a special spherical trochoid and its top-view are the starting point for the investigation of algebraic curves of constant width and their kinematic generation.

1.2 Generation of spherical trochoids

In the three-dimensional Euclidean space $\mathbb{R}^3$ of our perception, we distinguish a certain direction L (lead direction) and a fixed sphere Σ centered at O. Further, we assume that the equator e lies in the horizontal plane through Σ's center O (*i.e.*, in the plane orthogonal to the lead L and through O). On a fixed circle $p_0 \subset \Sigma$ (fixed polhode) with its axis parallel to L, spherical center M_0, and spherical radius $\widehat{r_0}$, we roll another circle $p \subset \Sigma$ (moving polhode) with spherical center M and spherical radius $\widehat{r}$.

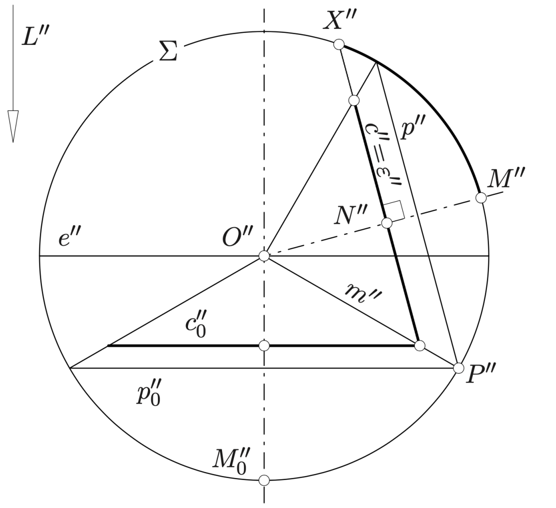

Figure 1: *Front-view of the initial configuration of the rolling cones and circles.*

The path $l \subset \Sigma$ of an arbitrary point $X \in \Sigma$ firmly attached to p is called a *spherical trochoid* of *order 2*. Note that any point rigidly attached to p and not necessarily on Σ traces a spherical trochoid on a sphere concentric with Σ.

The spherical trochoid motion can also be considered as the glide-free rolling of the cone of revolution $\Gamma = p \vee O$ along the cone (of revolution) $\Gamma_0 = p_0 \vee P$ (sharing the vertex O) during the entire motion. The point P is the point of contact of c and c_0 and is also referred to as the spherical instantaneous pole (see Fig. 1). Γ is rolling on Γ_0 without gliding. These cones play the role of the axodes and the instantaneous axis equals the common generator $m = [O,P]$ of these two cones along which they share the tangent plane (cf. [5, 16]).

For the constructive treatment of spherical trochoids, we intersect Σ with the plane ε which is orthogonal to the axis $[O,M]$ of p and passes through X. Then, we consider the rolling of the parallel circle $c = \varepsilon \cap \Sigma$ (center $N = \varepsilon \cap [O,M]$) together with the point X on the fixed cone's parallel circle c_0 (in the plane ε_0, with the spherical radius $\widehat{r_0}$, and axis $[O,M_0]$).

We shall make explicit that each spherical (or planetary) trochoidal motion is equivalent to the (glide-free) rolling of a sphere S on two coaxial circles c_1 and c_2, see Fig. 3.

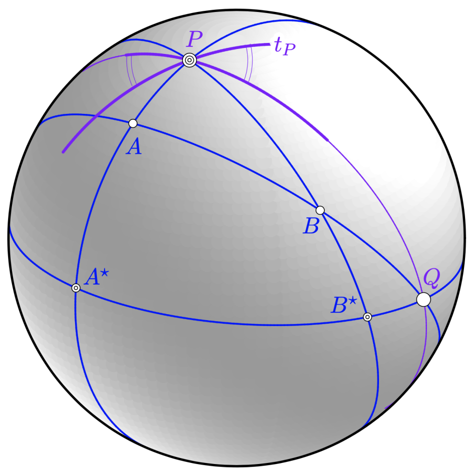

Figure 2: *Construction of osculating circles of the spherical trochoid l at X according to* BOBILLIER.

The tangent of l at X is orthogonal to the (spherical) instantaneous pole P.

Spherical kinematics mirrors another well-known result from planar kinematics. In the Euclidean plane, the theorem by S. ARONHOLD and A.B.W. KENNEDY (cf. [19]) states that *the instantaneous poles P_{01}, P_{02}, P_{12} of the relative motions of three moving systems Σ_0, Σ_1, Σ_2 (concentric with and congruent to Σ) are collinear*. Further the relative angular velocities ω_{01}, ω_{02} and the distances between the poles are related by

$$\overline{P_{01}P_{12}} : \overline{P_{02}P_{12}} = \omega_{02} : \omega_{01}.$$

The center of the osculating circle of l at X can be constructed with the help of É. BOBILLIER's construction (cf. [19]) which is also valid on the sphere. This result holds also in spherical kinematics, see [5, 10, 16].

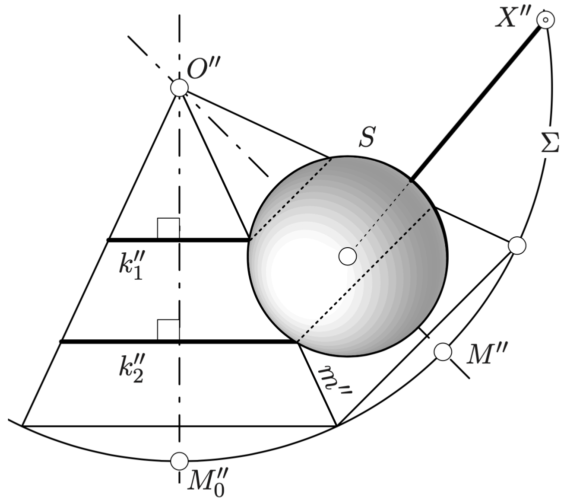

Figure 3: *Alternative generation of a spherical trochoid: A sphere S is rolling on two coaxial circles k_1 and k_2.*

1.2.1 Top-views, trochoids of higher order

The following results on the top-views (orthogonal projections in the direction of the lead L) of spherical trochoids were deduced by W. STRÖHER in an analytic way (see [16]). Here, these results shall be proved by means of synthetical reasoning. In the beginning, we recall a theorem by H. POTTMANN (cf. [13] and see Fig. 4):

Theorem 1 *Let $\overline{k}'$ be an ellipse with center N', semi-major axis length a, and the moving point $X' \in \overline{k}'$. Assume further that the angular velocities of the rods $N'S$ and SX' in the crank slider mechanism $N'SX'$ (derived from the paper strip construction of $\overline{k}'$) are equal to $-\beta$ and β (with regard to $\overline{k}'$) and let $\overline{k}_0'$ be the ellipse's circumcircle (which is an affine image of $\overline{k}'$). Then, any two out of the following three statements are equivalent:*

- $\beta = \text{const.}$
- *$N'X_0'$ rotates with constant angular velocity, and therefore, also constant area velocity (with regard to $\overline{k}_0'$).*
- *$N'X'$ rotates with constant area velocity with respect to $\overline{k}'$.*

The top-view of the situation shown in the front-view in Fig. 1 is displayed in Fig. 5. From the latter we can deduce some results on the top-views of spherical trochoids:

Theorem 2 *The top-view l' of a spherical trochoid l is (in general) a trochoid of order 3 (cf.* [19, 20]*).*

Proof. We see that $\overline{k}'$ rotates with angular velocity α about O'. Provided that α is constant, NX rotates with constant angular and area velocity (with respect to $\overline{k}$) according to Thm. 1. Thus, $N'X'$ rotates with constant area velocity with respect to $\overline{k}'$. Because of the existence of the affine mapping between the ellipse and its circumcircle, $N'X'$ rotates with constant area velocity $-\beta$ with respect to $\overline{k}'$. Hence, $N'X'$ moves with constant and absolute angular velocity $\alpha - \beta(\alpha+\beta)$. $\square$

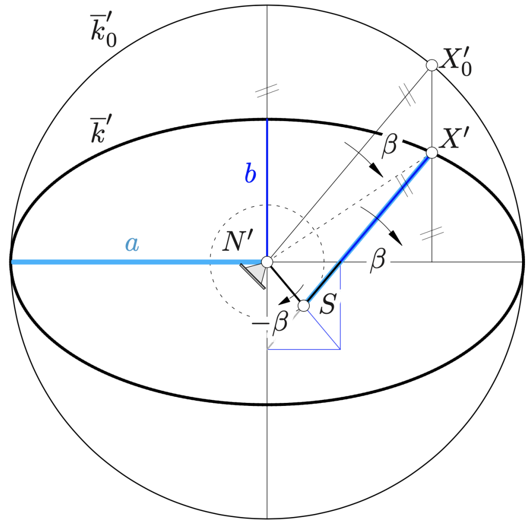

Figure 4: *The crank slider mechanism and the equivalencies around an ellipse.*

In [1], it is already mentioned that the top-view (orthogonal projection in the direction of the axis of the fixed cone) is a trochoid of order 3. Moreover, R. BEREIS has shown that the generic orthogonal projection of a spherical trochoid of order 2 is a planar trochoid of order 5, and a generic (oblique) parallel projection results in a planar trochoid of order 8 (see also [1]). This means that the latter curves are path curves of points under planar motions which are the superpositions of 5 or 8 planar rotations (cf. [20]).
More precisely, we can infer:

Theorem 3 *The top-view l' of a spherical trochoid l is, in general, a trochoid of order 3, and its characteristic equals*

$$\alpha : (\alpha-\beta) : (\alpha+\beta),$$

cf. [19, p. 164] *and* [20]*. It can be generated by the open-loop three-bar mechanism $O'N'SX'$.*

In the special case $\widehat{b} = \widehat{MX} = \frac{\pi}{2}$ and $N = O$, l' has the characteristic

$$(\alpha-\beta) : (\alpha+\beta). \tag{1}$$

In this case, a great circle $\overline{k}$ is rolling, taking the point $X \in \overline{k}$ with it. Hence, l a *spherical involute* of a (spherical) circle, and also, a spherical curve of constant slope. Naturally, l'

is a curve with cusps gathering on a circle which is concentric with the equator's top view e'. (It is the top view of that parallel circle of Σ along which Σ's tangent planes have the same slope as l.) The vertices of l' lie on e'. By virtue of (1), l' is an epicycloid.

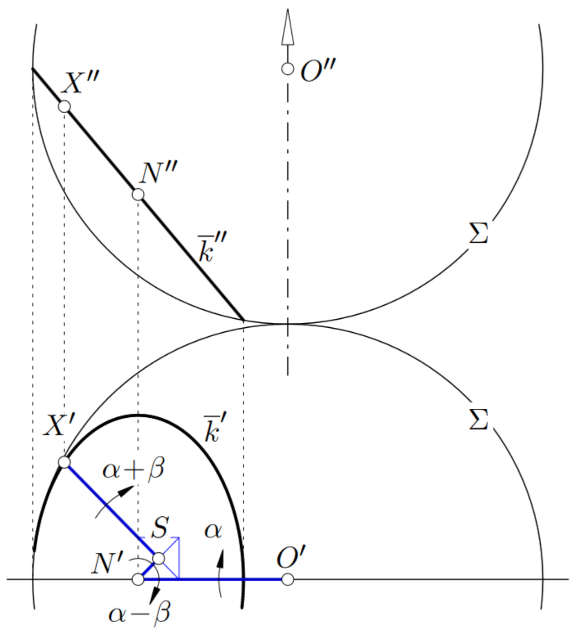

Figure 5: *The top view of a spherical trochoid is a planar trochoid of order three. It can be generated by an open three-bar mechanism.*

Referring to the very special case of spherical trochoids l as curves of constant slope on Σ, we shall point out the following: It is possible to transform the sphere Σ into ellipsoids of revolution by applying orthogonal affine mappings with the equator plane as a fixed plane (corresponding points are joined by lines orthogonal to the equator plane). Although such an orthogonal affine mapping changes the value of the slope of l, the slope remains constant. Some examples of curves of constant slope are shown in Fig. 6. Hence, we have verified that part of ENNEPER's theorem (see [7, p. 138] and [11, p.462]) describing the shape of curves of constant slope on ellipsoids of revolution (see Fig. 7): *The top-view (orthogonal projection in the direction of the lead L) of a curve of constant slope on an ellipsoid of revolution is an epicycloid, provided that the axis of revolution is parallel to L.*

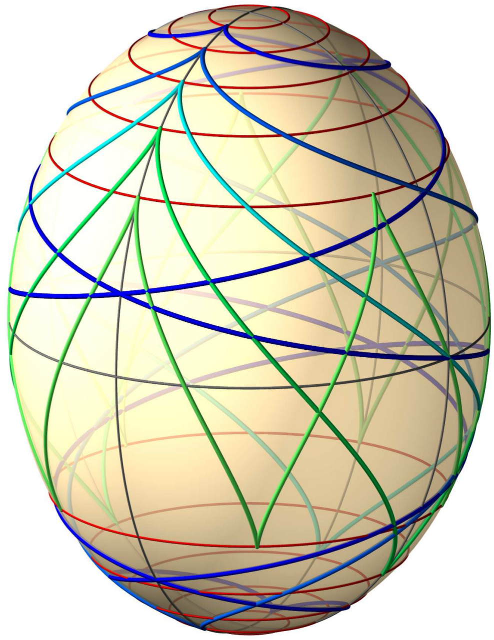

Figure 6: *Some curves of constant slope on an ellipsoid of revolution with vertical axis.*

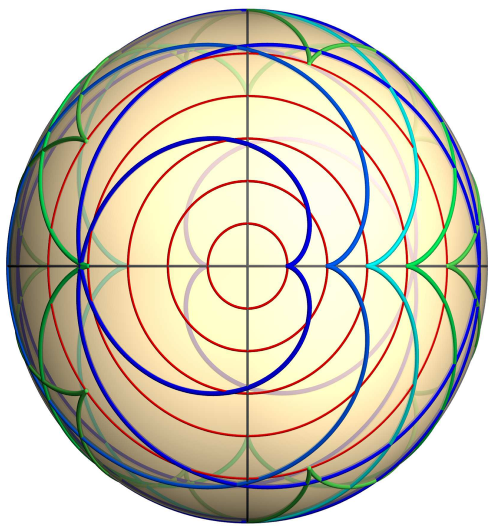

Figure 7: *The top-view of the curves of constant slope on an ellipsoid shows some epicycloids.*

In Fig. 8, the top-view of the case of congruent polhodes k_0 and k_1 is illustrated. In the top-view, we can see a so-called *symmetric rolling* if we flip the moving circle k_1[1] into the horizontal plane of the fixed circle k_0. So, we see that the locus $l^{\circ\prime}$ of all points $X_i^{\circ\prime\prime}$ (*i.e.*, the orbit of $X_1^{\circ\prime}$ or $X_2^{\circ\prime}$) equals a Pascal limaçon. Further, we can deduce that the top-view l' of the spherical trochoid is also a limaçon which is a similar and smaller copy of $l^{\circ\prime}$. The mapping

[1]Here, the indices 1, 2, ... assigned to the moving circle refer to different (time) instances.

$\zeta:\ l^{\circ\prime} \to l'$ is a central similarity with center Z (cf. Fig. 8) and similarity factor

$$0 < \mu = \frac{1}{2}(1+\cos\nu) < 1, \tag{2}$$

where ν is the angle enclosed by the planes of the moving circles (on Σ) and the horizontal planes.

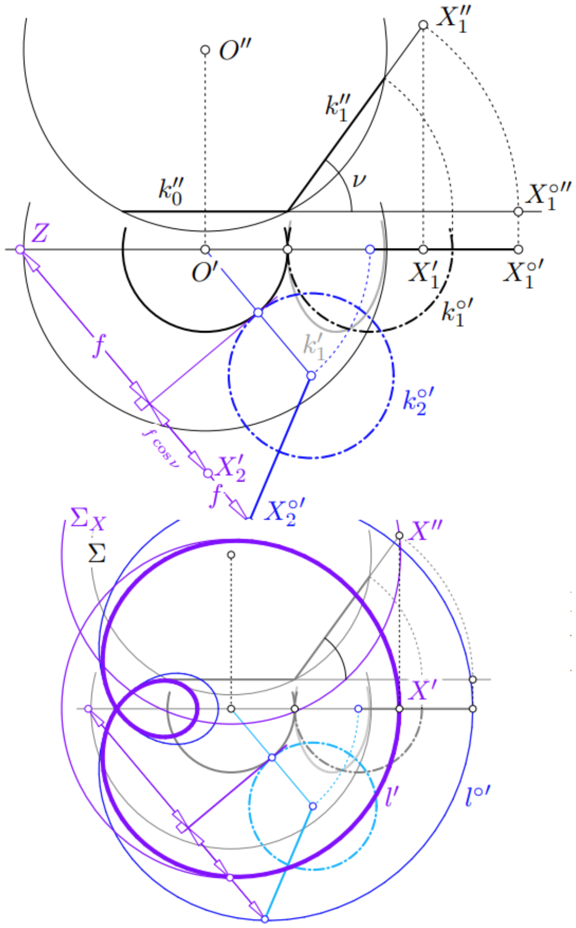

Figure 8: *Top: The similarity factor between l' and $l^{\circ\prime}$ depends on the inclination of the rolling circle's plane. Bottom: The fixed and moving polhodes are congruent and the top-view shows a symmetric rolling. Therefore, l' is a Pascal limaçon, as is $l^{\circ\prime}$.*

In Fig. 9, another special case is illustrated: A great circle $\overline{k} \subset \Sigma$ is rotating about Σ's vertical axis while its radius OX rotates with the same absolute angular velocity. By rotating the initial position ε_1 (which is projecting in the front-view) into a generic position ε_2, we find that the interior angle bisector of $[O', X_1']$ and $[O', X_2^{\circ\prime}]$ equals the trace of ε_2 in the equator plane. Therefore, l' is the image of e' under a central similarity ζ with center X_1' and the similarity factor (2). Hence, l' is a circle.

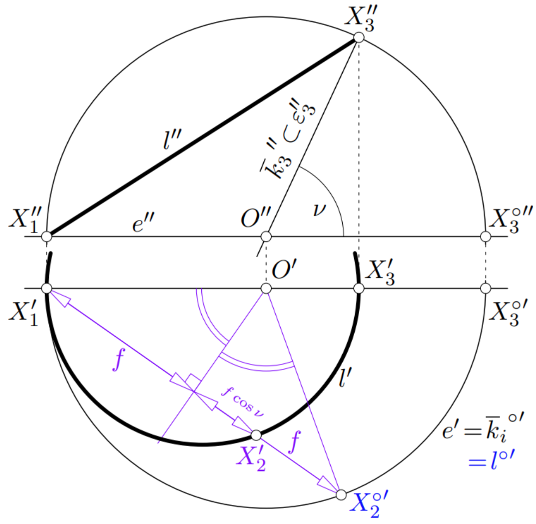

Figure 9: *A very simple form of a spherical trochoid which is still a similar copy of an undistorted image: a circle.*

In the much more special case $\nu = \frac{\pi}{2}$, we have $\mu = \frac{1}{2}$, and it is rather obvious that the latitude and the longitude of each point $X \in l$ are equal, provided that Σ is considered as the Earth and the contour for the top-view is assumed to be the zero meridian. In this case, l is Viviani's curve (see Fig. 10, the orange curve l).

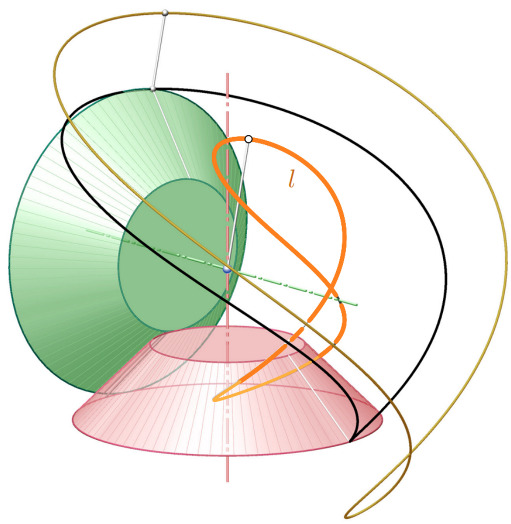

Figure 10: *Viviani's curve (orange) can also be found among the spherical trochoids.*

In Fig. 11, we recall again the constructive approach and flip the plane ε (including k, N, and X) to both sides, *i.e.*, to the interior and exterior of the sphere. For the inner version, this yields the circle k° with the center N° and radius r_1. The moving point shall be denoted by X°. The outer circle $k_{\circ}$ has the center $N_{\circ}$, the radius r_2, and the moving point shall be labelled with $X_{\circ}$.

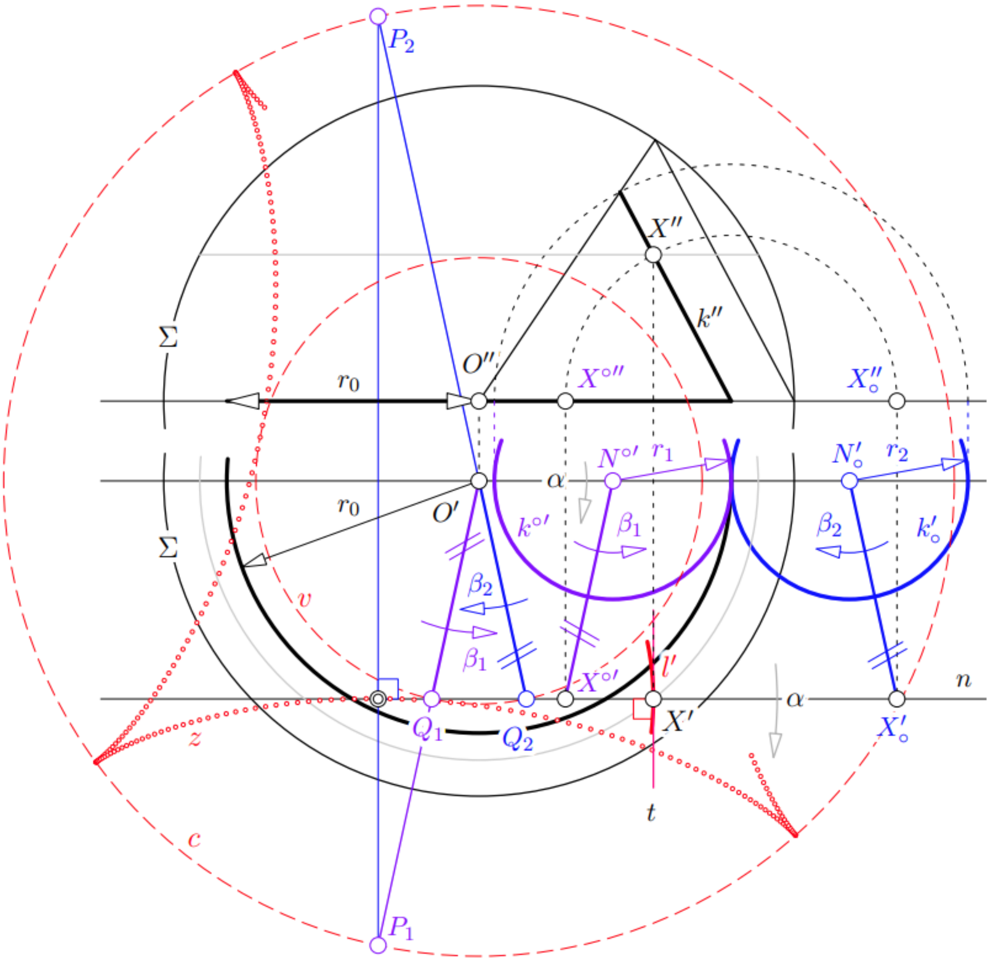

Figure 11: *The top-view l' of a spherical trochoid is the involute of a hypocycloid z. The two different flips of k''s plane are displayed in different colors (blue = to the outside, violet = to the inside).*

Then, we complete the parallelograms

$$O'N^{\circ\prime}X^{\circ\prime}Q_1 \text{ and } O'N'_\circ X'_\circ Q_2.$$

Now, we have $0 < r_0$, $0 < r_1 < r_0$, $r_1 = -r_2$, and $\alpha = r_2 =$ const., see Fig. 11. If now $O'N^{\circ\prime}N'_\circ$ rotates with the angular velocity α, then $O'Q_i$ rotates with angular velocity β_i ($i \in \{1,2\}$), where

$$0 < \beta_1 = r_0 + r_2 \text{ and } 0 > \beta_2 = -r_0 + r_2$$

holds. According to [19, p. 151], we can see the twofold generation of a hypocycloid z as the envelope of $n = [Q_1, Q_2, X^{\circ\prime}, X', X'_\circ]$ with the characteristic $\beta_1 : \beta_2 < 0$ (cf. [19, p. 156]). From the top-view $O'N^{\circ\prime}N'_\circ$ of the instantaneous axis, we can infer that n is orthogonal to l' at X'. Therefore, l' is the involute of z or an offset curve (parallel curve) of its similar involute. For the two instantaneous poles P_i ($i \in \{1,2\}$) corresponding to the i-th Euler generation (cf. [19, p. 151]) of the path (or i-th generation as the envelope of a straight line) of z, we have: $\overline{OP_i} = \overline{OQ_i} \cdot \frac{r_0}{r_i}$. Further, the circle c centered at O' with radius $\overline{O'P_i}$ carries the cusps of z and the concentric circle v with radius $\overline{O'Q_i}$ carries the vertices of z

Special values of some spherical distances result in special shapes of the spherical trochoid and simplify their top-views:

Theorem 4 *For the following values of spherical distances $\widehat{r_0}$, $\widehat{r}$, $\widehat{a} = \widehat{M_0M}$, $\widehat{b} = \widehat{MX}$, the top-views of spherical trochoids are ordinary trochoids (of order 2):*

- *If $\widehat{r} = \widehat{b} = \frac{\pi}{2}$, l' is an epicycloid.*
- *If $\widehat{r_0} = \widehat{r}$, l' is a Pascal limaçon.*
- *In the special case $\widehat{r_0} = \widehat{r}$, $b = \frac{\pi}{2}$, l is a hippopede of Eudoxus with a circle l' for its top-view.*
- *If $\widehat{r_0} = \widehat{r}$ and $\widehat{a} = \widehat{b} = \frac{\pi}{2}$, l is Viviani's curve.*

- *If $\widehat{r_0} = \frac{\pi}{2}$, l' is the envelope of a straight line undergoing an ordinary trochoid (planetary) motion or the offset of a cycloid (cf.* [19]*).*

1.3 Algebraic spherical trochoids

The spherical trochoids are algebraic if the ratio $r_0 : r_1 : r_2$ is rational. With a proper scaling, we can achieve that each r_i ($j \in \{0,1,2\}$) is an integer.
Then, the rotation number w and the algebraic degree d of the top-view are

$$w = \frac{\beta_1 - \beta_2}{|\gcd(\beta_1,\beta_2)|} \quad \text{and} \quad d = 2\left|\frac{\beta_2}{\gcd(\beta_1,\beta_2)}\right|.$$

Since the spherical curve can be considered as the intersection of the projection cylinder and the sphere Σ, the algebraic degree of the spherical trochoid equals

$$2d = 4\left|\frac{\beta_2}{\gcd(\beta_1,\beta_2)}\right|.$$

We shall have a look at the following example, see Fig. 12. Here, a circle k is rolling on Σ's equator e and the radius of the rolling circle k is half that of e. That means $r_0 = 2$ and $r_1 = 1$, and thus, $\beta_1 = 1$, $\beta_2 = -3$, and $\alpha = -1$. Since $w = 4$ and $d = 6$, z is an astroid. Since a point on the boundary of k is moving, l' is an involute of z with two cusps X_1' and X_3' of the third kind[2].
The initial position of the rolling circle shall be labelled with k_1.

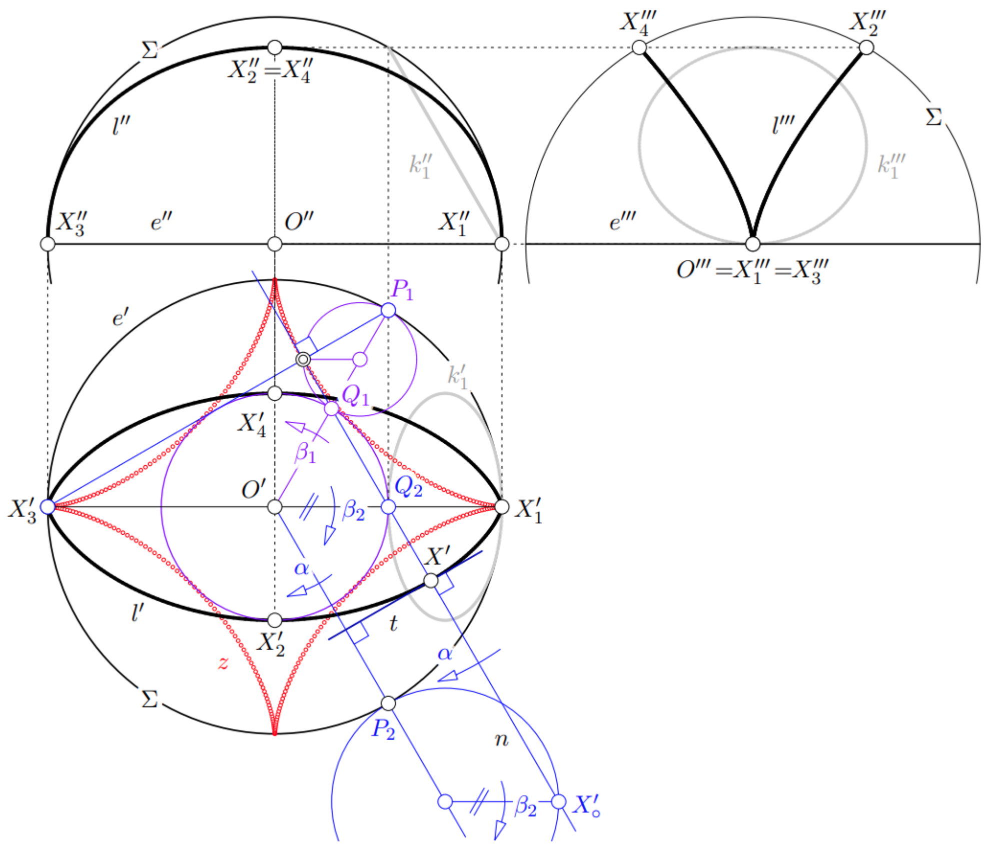

Figure 12: *The spherical trochoid with $r_0 = 2$, $r_1 = 1$, and thus, with $\beta_1 = 1$, $\beta_2 = -3$, and $\alpha = -1$ is mapped to a sextic curve l' in the top-view with two cusps of the third kind at X_1' and X_3', to the upper half l'' of a doubly covered cubic (with an ordinary node) in the front-view, and to a part l''' of Neil's parabola in the left-side view.*

[2] Cusps of the first and second are characterized by the initial terms of their local expansions (t^2,t^3) and (t^2,t^4), respectively. The expansion at a cusp of the third kind starts with (t^3,t^4). In German such a point is called *Spitzpunkt*.

2 Some algebraic curves of constant width

A further example shall be illustrated in Fig. 14. Here, we have chosen $r_0 = 3$ and $r_1 = 1$. Therefore, $\beta_1 = 2$, $\beta_2 = -4$, and $\alpha = -1$. This yields $w = 3$ and $d = 4$ which makes z a Steiner hypocycloid. In this case, l' is a closed algebraic curve of constant width. This raises the question, if spherical trochoids can be generated such that their top-views are curves of constant width.

As mentioned earlier, the top-view l' of the spherical trochoid is the involute of a cycloid. It is well-known (see [4, 8, 9, 18]) that the involute of a cycloid is a trochoid, and moreover, it is also the envelope of a straight line under a trochoidal motion. Therefore, it is nearby to look for curves of constant width among trochoidal, and eventually, among higher order trochoidal curves.

Up to scale and w.r.t. a properly chosen Cartesian coordinate system, the curve z in Fig. 14 can be parametrized as

$$z(t) = 2\mathrm{e}^{2\mathrm{i}t} + \mathrm{e}^{-4\mathrm{i}t}, \quad t \in [0, \pi[$$

and l' allows the representation

$$l'(t) = \frac{2}{3}\mathrm{e}^{2\mathrm{i}t} - \frac{1}{3}\mathrm{e}^{-4\mathrm{i}t} - d\mathrm{e}^{-\mathrm{i}t}. \tag{3}$$

The curve l' is an involute of z and the choice of real constant d determines the starting point of the involute. We shall use the support function $h:\ \mathrm{S}^2 \to \mathbb{R}$ which assigns to each point on the unit circle the oriented distance of the curve's tangent from the origin of the coordinate system. From the parametrization of z, we obtain the unit normal vector field $\mathbf{n} = (\sin t, \cos t)$. Now, the support function h equals the canonical scalar product of the position vector $\mathbf{l}' = (\mathrm{Re}\, l', \mathrm{Im}\, l')$ of the points of l' (from (3)) with the corresponding unit normal. This yields $h = \langle \mathbf{n}, \mathbf{l}' \rangle = d - \frac{1}{3}\cos 3t$ which agrees, up to a scaling, with the support function used in [14] to compute a closed algebraic curve of constant width. It is necessary and sufficient that h fulfills

$$\begin{aligned} &h(t) + h(t+\pi) = \text{const.}, && \text{const. width}\\ &\dot{h}(t) + \dot{h}(t+\pi) = 0, &&\\ &h(t) - h(t+2\pi) = 0, && \text{closedness} \end{aligned} \tag{4}$$

besides some conditions on continuity and differentiability (which are always fulfilled in the case of trochoidal curves). The dot indicates differentiation w.r.t. the parameter t.

It is a matter of fact that functions that fulfill (4) can be expanded in Fourier series

$$\begin{aligned} h(t) &= a_0 + \sum_{k=1}^{n} (a_k \cos kt + b_k \sin kt) = \\ &= \tfrac{1}{2}\sum_{k=0}^{\infty} (a_k - \mathrm{i}b_k)\mathrm{e}^{\mathrm{i}kt} + (a_k + \mathrm{i}b_k)\mathrm{e}^{-\mathrm{i}kt}, \end{aligned} \tag{5}$$

where $n \in \mathbb{N}^{\times}$ and $a_k, b_k \in \mathbb{R}$ (not all zero at the same time). Fourier series are to be preferred for they naturally fulfill the third condition in (4). An alternatively, Chebyshev polynomials were used in [15].

Closed algebraic curves of constant width whose support functions can be given as a finite Fourier series are always rational and their representations can always be converted into an equivalent series of complex exponential functions

$$l'(t) = h(t)\mathrm{e}^{\mathrm{i}t} + \dot{h}(t)\mathrm{e}^{-\mathrm{i}t} \tag{6}$$

with h from (5). Hence, these curves are higher trochoids of order n and first and intensively studied in [20]. They allow for a generation as the superposition of n independent rollings in $n!$ ways which includes the two-fold generation of ordinary trochoids (were $n = 2$). Further, they can be generated by closed n-bar linkages.

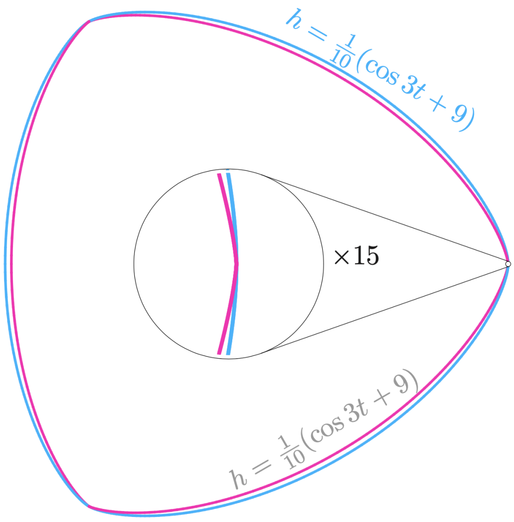

Figure 13: *Two curves of constant width (similar to those mentioned in the text and scaled to equally sized circumcircles. The vicinity of the right vertex is enlarged by the factor 15 in order to display the differences between the two curves.*

The example of a closed algebraic curve of constant width given in [14] can be described by the support function

$$h = 9 + \cos 3t$$

and is an algebraic curve of degree 8. It admits a rational parametrization, and thus, it has to have the maximum number of singularities two of which are the absolute points of Euclidean geometry (pair of complex conjugate ideal points, ordinary double points with self-osculation) and three of which are real isolated ordinary double points on the curves' lines of symmetry. In [12], the authors modified the support function to

$$\widetilde{h} = 8 + \cos 3t$$

in order to remove the isolated double points. This particular choice of the support function pushes the isolated double points to points on the curve, and thus, they become cusps of the third kind (see [2, 3, 4, 18]).

The choice of a support function of the form (3) (such that it fulfills (4)) leads in any case to a curve of constant width which allows for a kinematic generation by means of sufficiently many rotations. These curves can always be interpreted as the top-view of spherical curves. Depending on whether $\sqrt{1-l'(t)\overline{l'}(t)}$ can be written as a finite sum of exponential functions (or trigonometric functions) or not, the curve l allows for a kinematic generation by means of superposed rollings on a sphere. The *order* of the spherical trochoid l will, in general, be higher than 2.

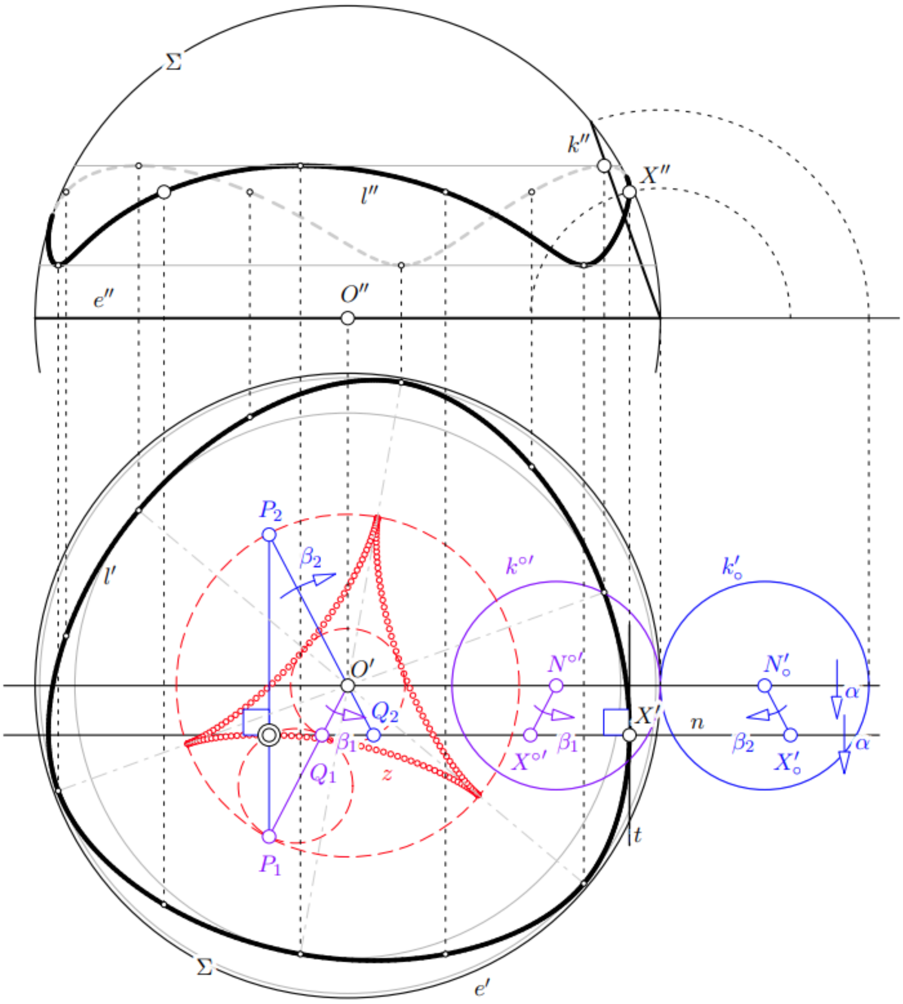

Figure 14: *The top-view l' of a spherical trochoid may even be a closed and algebraic curve of constant width.*

References

[1] Bereis, R., Über sphärische Radlinien, *Wiss. Z. Techn. Hochschule Dresden* **7** (1957/58), 841–844.

[2] Brieskorn, E., Knörrer, H., *Ebene algebraische Kurven*, Birkhäuser, Basel-Boston-Stuttgart, 1981.

[3] Coolidge, J.L., *A treatise on algebraic plane curves*, Dover Publications, New York, 1959.

[4] Fladt, K., *Analytische Geometrie spezieller ebener Kurven*, Akademische Verlagsgesellschaft, Frankfurt am Main, 1962.

[5] Husty, M., Karger, A., Sachs, H., Steinhilper, W., *Kinematik und Robotik*, Springer-Verlag, Berlin, 1997, https://doi.org/10.1007/978-3-642-59029-0

[6] Jeffery, H.M., On spherical cycloidal and tro-

choidal curves, *Quart. J. Pure Applied Math.* **XIX** (1883), 44–66.

[7] KRUPPA, E., *Analytische und konstruktive Differentialgeometrie*, Springer, Wien, 1957, `https://doi.org/10.1007/978-3-7091-7867-6`

[8] LAWRENCE, J.D., *A catalog to plane algebraic curves*, Birkhäuser, Boston, 2000.

[9] LORIA, G., *Spezielle algebraische und transzendente ebene Kurven*, B.G. Teubner, Leipzig-Berlin, 1911.

[10] ODEHNAL, B., Conchoids on the sphere, *KoG* **17** (2014), 43–52.

[11] ODEHNAL, B., STACHEL, H., GLAESER, G., *The universe of quadrics*, Springer, Wien, 2020, `https://doi.org/10.1007/978-3-662-61053-4`

[12] PANRAKSA, C., WASHINGTON, L.C., Real algebraic curves of constant width, *Period. Math. Hung.* **74** (2017), 235–244., `https://doi.org/10.1007/s10998-016-0149-9`

[13] POTTMANN, H., Zum Satz von Holditch in der euklidischen Ebene, *Elem. Math.* **41**(1) (1986), 1–6.

[14] RABINOWITZ, S., A polynomial curve of constant width, *Missouri J. Math. Sci.* **9**(1) (1997), 23–27, `https://doi.org/10.35834/1997/0901023`

[15] ROCHERA, D., Algebraic equations for constant width curves and Zindler curves, *J. Symbolic Comp.* **113** (2022), 139–147, `https://doi.org/10.1016/j.jsc.2022.03.001`

[16] STRÖHER, W., *Raumkinematik*, Unpublished manuscript, TU Wien, 1973.

[17] TENNISON, R.L., Smooth Curves of Constant Width, *Math. Gazette* **60**(114) (1976), 270–272, `https://doi.org/10.2307/3615436`

[18] WIELEITNER, H., *Spezielle ebene Kurven*, Sammlung Schubert LVI, Göschen'sche Verlagshandlung, Leipzig, 1908.

[19] WUNDERLICH, W., *Ebene Kinematik*, Bibliographisches Institut, Mannheim, 1970.

[20] WUNDERLICH, W., Höhere Radlinien, *Österr. Ingen. Archiv* **1** (1947), 277–296.

Walther Jank

TU Wien
Wiedner Hauptstraße 8–10, 1040 Vienna, Austria

Georg Glaeser
e-mail: georg.glaeser@uni-ak.ac.at

University of Applied Arts Vienna
Oskar-Kokoschka-Platz 2, 1010 Vienna, Austria

Boris Odehnal
orcid.org/0000-0002-7265-5132
e-mail: boris.odehnal@uni-ak.ac.at

University of Applied Arts Vienna
Oskar-Kokoschka-Platz 2, 1010 Vienna, Austria

https://doi.org/10.31896/k.27.4
Original scientific paper
Accepted 5. 12. 2023.

Iva Kodrnja
Helena Koncul

Locus Curves in Triangle Families

Locus Curves in Triangle Families

ABSTRACT

In this article, we observe a one-parameter triangle family, where two vertices are fixed and the third vertex lies on a given line. For this family of triangles, we observe the loci of centroids, orthocenters, circumcenters, incenters, excenters and some triangle elements associated to these triangle points.

Key words: family of triangles, centroid, orthocenter, circumcenter, incenter, excenter

MSC2010: 51M04, 51N20, 51M15

Lokus krivulje u familijama trokuta

SAŽETAK

U ovom članku proučava se jednaparametarska familija trokuta kojemu su dva vrha fiksna, a treći vrh leži na zadanom pravcu. Za takvu familiju trokuta promatraju se geometrijska mjesta težišta, ortocentara, središta opisanih kružnica, središta upisanih i pripisanih kružnica te nekih elemenata vezanih za te karakteristične točke trokuta.

Ključne riječi: familija trokuta, težište, ortocentar, središte opisane kružnice, središte upisane kružnice, središte pripisane kružnice

1 Introduction

The evergrowing field of triangle geometry can be systematically researched in [8] where we can find numerous points, lines, circles, curves, objects etc. associated to a triangle. If we observe a set of triangles somehow connected, i.e., a one-parameter family of triangles or a pencil of triangles, then the locus of a certain triangle center of those triangles lies on a curve. In the same way, we can observe what will be the locus of a certain line, or other object associated to triangles in a triangle family. Some results in this area, especially for the Euclidean plane can be found in [1, 2, 4, 9, 10, 12], while [5, 6, 7] deal with the situation in the isotropic plane. This paper contains a family of triangles whose basic elements are dual to the family of triangles in [4] but the resulting locus curves are different.

We will define the triangle family τ as it follows:
Let A and B be two different fixed points and let p be a fixed line. We study one-parameter family τ of triangles $\triangle ABC_i$ such that the point C_i lies on the line p.

$$\tau = \{\triangle ABC_i : C_i \in p\}, \quad i \in \mathbb{R} \cup \{\infty\}.$$

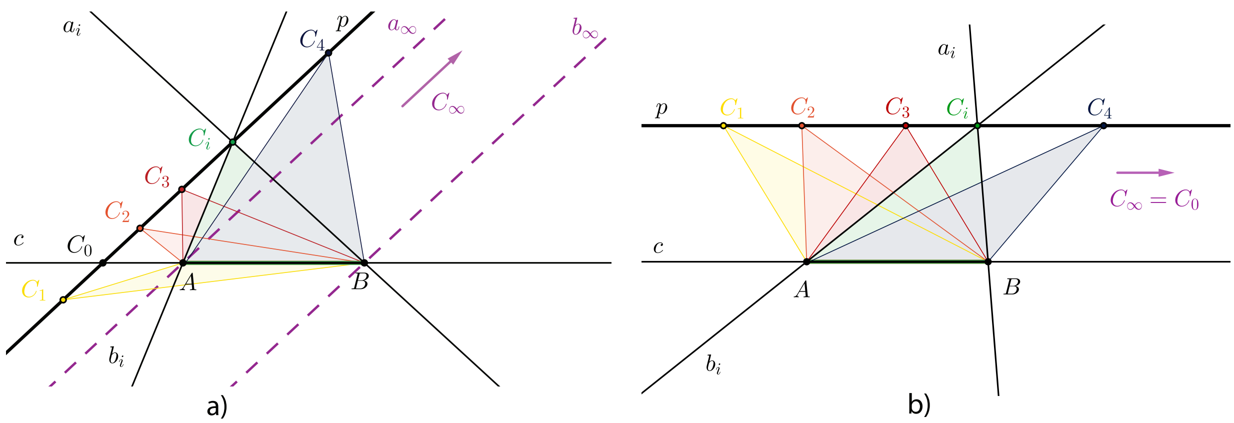

Figure 1: *The family of triangles $\triangle ABC_i$ where $C_i \in p$: a) p in general position, b) $p \parallel c$.*

We will use the following notation

$$\begin{aligned} a_i &= BC_i, \quad b_i = AC_i, i \in \mathbb{R}\cup\{\infty\}, \\ c &= AB, \quad C_0 = p\cap c, \end{aligned} \tag{1}$$

and the ideal point on the line p will be denoted with C_∞ (see Fig. 1).

From the view point of projective geometry, in this structure we view a line p as a range of points (C_i), $i\in\mathbb{R}\cup\{\infty\}$, the points A and B as vertices of pencils of lines a_i and b_i, $i\in\mathbb{R}\cup\{\infty\}$, which contain the triangle sides $\overline{BC_i}$ and $\overline{AC_i}$ of the triangles $\triangle ABC_i$ in the family τ. The pencils will be denoted with (A) and (B).

Fig. 1 shows two different families of triangles:

- (case a) when the line p is in an arbitrary position to the line c,
- (case b) when the line p and c are parallel.

In every family, we have two special triangles that are degenerate which occur when $i = \{0,\infty\}$:

- (case 0) $\triangle ABC_0, C_0 = p\cap c$, i.e., when vertices of the triangle are collinear and the triangle degenerates to a line segment,
- (case ∞) $\triangle ABC_\infty$, where C_∞ is the ideal point of the line p, i.e., when a triangle has a vertex at infinity.

If the line p is parallel to the line c (case b) then the degenerate triangles coincide, i.e., $C_0 = C_\infty$ (see Fig. 1b).

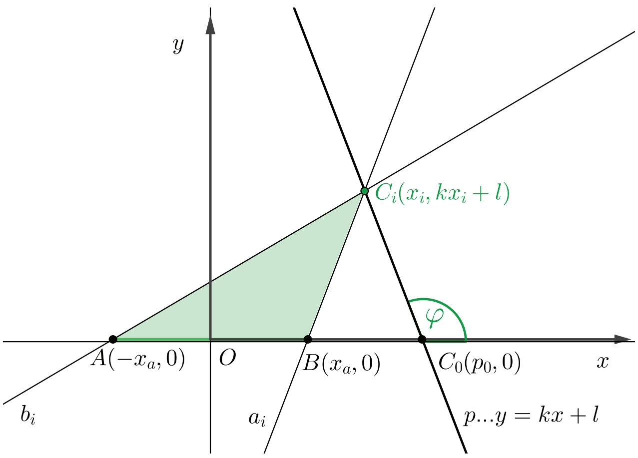

Figure 2: *The family of triangles τ positioned in the coordinate system.*

For all analytic treatment, we will put the coordinate system such that the x-axis is the line c and the points A and B are symmetric regarding to the origin of the coordinate system (see Fig. 2), i.e., we will put the family of triangles τ in the coordinate system as follows:

$$\begin{aligned} &A = (-x_a,0), \quad B = (x_a,0), \\ &c\ldots y=0, \quad p\ldots y = kx+l, \\ &C_i = (x_i, kx_i+l), \quad C_0 = (p_0,0), \quad p_0 = -\frac{l}{k} \\ &a_i\ldots y = \frac{kx_i+l}{x_i-x_a}(x-x_a), \quad b_i\ldots y=\frac{kx_i+l}{x_i+x_a}(x+x_a). \end{aligned} \tag{2}$$

2 The locus of centroids

Lemma 1 *The midpoints M_{a_i} and M_{b_i} of the corresponding triangle sides $\overline{BC_i}$ and $\overline{AC_i}$ of the triangle family τ lie on lines parallel to the line p.*

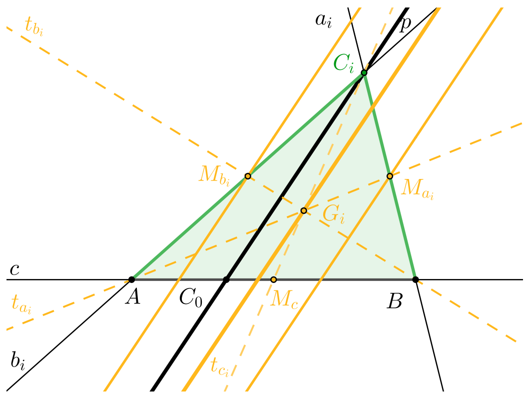

Figure 3: *The locus of midpoints and centroids are parallel lines.*

Lemma 1 is an immediate consequence of the Intercept Theorem.

From the view point of projective geometry, the range of points C_i is in perspectivity with ranges of points M_{a_i} and M_{b_i} where the centers of perspectivity are the points A and B

$$(C_i)\,\overline{\overline{\wedge}}\,(M_{a_i}), \quad (C_i)\,\overline{\overline{\wedge}}\,(M_{b_i}).$$

Theorem 1 *The triangle centroids G_i of the triangle family τ lie on a line parallel to the line p.*

Proof. The points A and B are fixed, hence the midpoint M_c of the triangle side $\overline{AB}$ is fixed. Since the centroid divides the segment $\overline{M_cC_i}$ in ratio 1:2, the locus of all points G_i is a line parallel to the line p. □

From (2) the equations of the triangle medians are

$$\begin{aligned} t_{a_i}\ldots y &= \frac{kx_i+l}{x_i+3x_a}(x+x_a), \\ t_{b_i}\ldots y &= \frac{kx_i+l}{x_i-3x_a}(x-x_a), \\ t_{c_i}\ldots y &= \frac{kx_i+l}{x_i}(x-x_i). \end{aligned} \tag{3}$$

Hence, the coordinates of the centroids G_i are

$$G_i = \left(\frac{x_i}{3}, \frac{kx_i + l}{3}\right), \tag{4}$$

and satisfy the following equation of a line

$$\mathcal{G}_i \ldots y = kx + \frac{l}{3} \tag{5}$$

From the view point of projective geometry, the correspondence between the pencils (A) and (B) is established so that for every triangle $\triangle ABC_i$ of the family τ the median t_{a_i} corresponds to the median t_{b_i}. This is a 1-1 correspondence, but in the degenerate triangle $\triangle ABC_0$ the medians coincide and the centroid G_0 can be interpreted as line c. Therefore, we have a projectivity between the pencils (A) and (B) for which the product degenerates to two lines, the one with the locus of all centroids of the triangle family τ and the line c of the degenerate case 0.

3 The locus of orthocenters

Theorem 2 *The orthocenters H_i of the triangle family τ lie on a conic, which is a hyperbola or parabola or degenerates to two lines.*

Proof. From (2) we can calculate the equations of the triangle altitudes

$$\begin{aligned} v_{a_i} \ldots y &= \frac{x_a - x_i}{kx_i + l}(x + x_a), \\ v_{b_i} \ldots y &= -\frac{x_a + x_i}{kx_i + l}(x - x_a), \\ v_{c_i} \ldots x &= x_i, \end{aligned} \tag{6}$$

and they are lines of the pencils (A), (B) and a pencil of parallel lines orthogonal to the line c, respectively. The coordinates of the orthocenters H_i are

$$H_i = \left(x_i, \frac{x_a^2 - x_i^2}{kx_i + l}\right), \tag{7}$$

and satisfy the following equation

$$\mathcal{H}_i \ldots x^2 + kxy + ly - x_a^2 = 0 \tag{8}$$

which is an equation of a conic. A conic is degenerate if the coefficient matrix $(c_{ij}), i, j \in \{0,1,2\}$ of its homogeneous equation is singular, i.e, the determinant of (c_{ij}) equals zero.
In our case, this yields

$$\begin{vmatrix} 1 & \frac{k}{2} & 0 \\ \frac{k}{2} & 0 & \frac{l}{2} \\ 0 & \frac{l}{2} & -x_a^2 \end{vmatrix} = -\frac{l^2}{4} + \frac{k^2}{4}x_a^2 = 0, \tag{9}$$

$$p_0 = -\frac{l}{k} \implies x_a = \pm p_0.$$

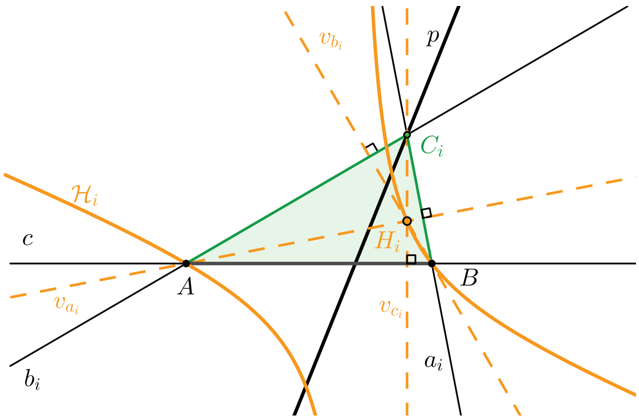

Figure 4: *The locus of orthocenters is a hyperbola when p is in general position.*

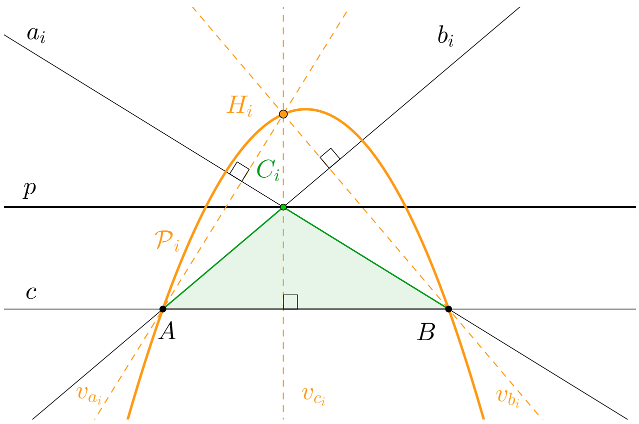

Figure 5: *The locus of orthocenters is a parabola when $p \parallel c$.*

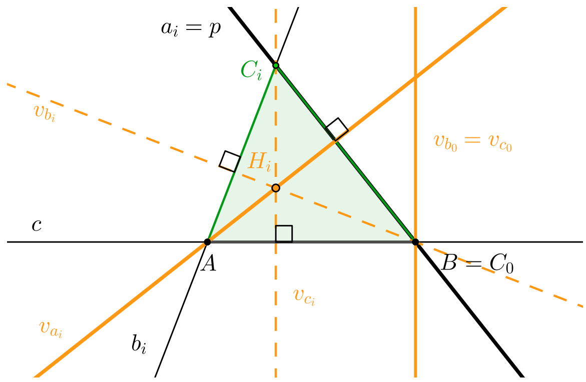

Figure 6: *The locus of orthocenters are two lines when $C_0 = A$.*

From this and (2) follows that the conic degenerates to two lines if the line p intersects c at point A or B, i.e., $C_0 = A$ or $C_0 = B$ (see Fig. 6).

The matrix H associated to the quadratic form of the conic (8) is

$$H = \begin{pmatrix} 1 & \frac{k}{2} \\ \frac{k}{2} & 0 \end{pmatrix} \tag{10}$$

and its determinant is

$$\det H = -\frac{k^2}{4}, \tag{11}$$

wherefrom we can read off the affine type of the conic $\mathcal{H}_i$ ([3], p.20).

The determinant of the conic can never be positive, so $\mathcal{H}_i$ cannot be an ellipse. For $k = 0$, we have $\det H = 0$ and the line p is parallel to the line c and the conic is a parabola (see Fig. 5). From (8), we can derive that the equation of the parabola is

$$\mathcal{P}_i \ldots y = \frac{-x^2 + x_a^2}{l}.$$

For $k \neq 0$, the determinant is always negative, and therefore, $\mathcal{H}_i$ is a hyperbola. □

From the view point of projective geometry, for every line in the pencil (A) there is a unique triangle $\triangle ABC_i$ where that line is the altitude v_{a_i} which corresponds to one line from the pencil (B) which is the altitude v_{b_i}. This is an 1-1 correspondence between these two projective pencils, hence the locus of orthocenters is a conic. For the degenerate triangle $\triangle ABC_0$, the altitudes are orthogonal to the line c, hence they are parallel and the orthocenter H_0 is at infinity. For the degenerate triangle $\triangle ABC_\infty$ the altitudes are orthogonal to the line p, thus the orthocenter H_∞ is also an ideal point. Therefore the conic has two different real points at infinity, hence is a hyperbola where from the degenerate triangles, we can conclude the directions of the asymptotes.

In the case $p \parallel c$, $C_0 = C_\infty$ and $H_0 = H_\infty$, the conic is a parabola. In this case, we can also conclude, that the infinite point of the conic is the infinite point of the line orthogonal to the line AB so that the axis of the parabola will also be orthogonal to the line AB.

In the case $p \cap c = \{A, B\}$, the altitudes v_{a_i} (or v_{b_i}) coincide if $i \neq 0$. For $i = 0$, the altitudes of the degenerate triangle $\triangle ABC_0$ are parallel lines orthogonal to the line c whereby altitudes v_{a_0} and v_{c_0} (or v_{b_0} and v_{c_0}) coincide.

Lemma 2 *The intersection N_{a_i} and N_{b_i} of the triangle altitudes v_{a_i} and v_{b_i} with the triangle sides $\overline{BC_i}$ and $\overline{AC_i}$, respectively, of the triangle family τ lie on a circle whose diameter is the line segment $\overline{AB}$.*

The Lemma 2 is an immediate consequence of the Thales's theorem.

The equation of the circle k is

$$k \ldots x^2 + y^2 = x_a^2$$

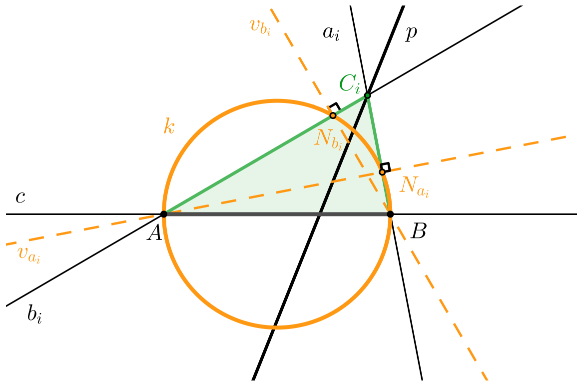

Figure 7: *The locus of $v_{a_i} \cap \overline{AC_i}$ and $v_{b_i} \cap \overline{BC_i}$ is a circle.*

4 The locus of circumcenters

Theorem 3 *The circumcenters O_i for the triangle family τ lie on a line.*

Proof. The circumcenter of a triangle is the intersection of the bisectors of the triangle sides and since all the triangles $\triangle ABC_i$ of the triangle family τ share the same side $\overline{AB}$ the bisector of that side for every triangle is always the same line s_c. Therefore the circumcenters O_i for the triangle family τ lie on it. □

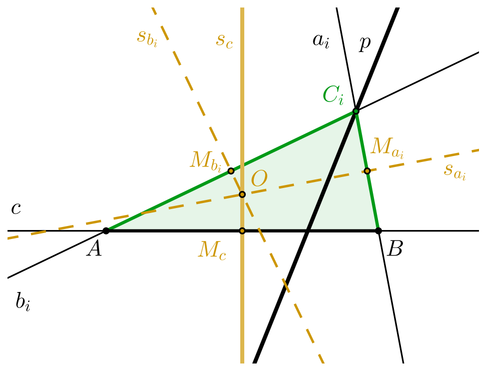

Figure 8: *The locus of circumcenters is the bisector of s_c.*

Theorem 4 *The bisectors s_{a_i} and s_{b_i} of the triangle sides $\overline{BC_i}$ and $\overline{AC_i}$, respectively, in the triangle family τ envelope parabolas. The line p is the common directrix of the parabolas and the points B and A are the foci of the parabolas, respectively.*

Proof. Let P_i be the intersection point of the bisector s_{a_i} and the line p, and S_{a_i} the intersection point of the orthogonal line from the points C_i to the line p and the bisector s_{a_i} (see Fig. 9). It follows that

$$\triangle P_i S_{a_i} C_i \cong \triangle P_i S_{a_i} B$$

because two sides of triangles and the angle between them are congruent. This is valid for every triangle $\triangle ABC_i$ in the triangle family τ, thus from

$$|\overline{C_iS_{a_i}}| = |\overline{BS_{a_i}}|, \quad \angle C_iS_{a_i}P_i = \angle P_iS_{a_i}B$$

we can conclude that the bisector s_{a_i} will be the tangent line with the contact point S_{a_i} of a parabola whose focus is the point B and directrix p. We can argue, analogously, for the other envelope corresponding to the point A. $\square$

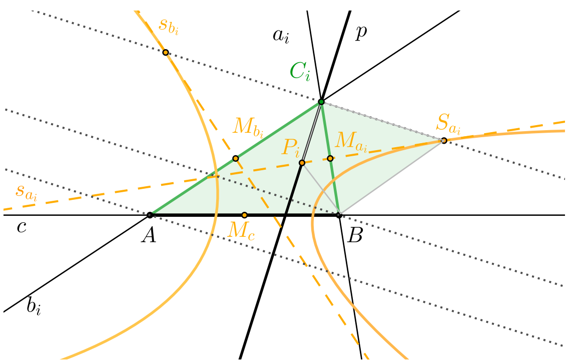

Figure 9: *The locus of bisectors of s_{a_i} and s_{b_i} envelop parabolas.*

From here, we can conclude that the axis of parabolas will be orthogonal to the line p and passing through vertices A or B, respectively. This property of a tangent to a parabola can be found in ([3], p. 31-32), from where we can also conclude that the locus of midpoints M_{a_i} and M_{b_i} of the triangle sides of the family τ from Lemma 1 are the tangent lines to parabolas at the vertex of the parabola.

Since the bisectors of a triangle side do not depend on the opposite vertex, we can choose the line p to be vertical

$$p \dots x = l.$$

Then the equations of the parabolas are

$$y^2 = 2(l \pm x_a)x.$$

5 The locus of incenters and excenters

Theorem 5 *The incenters I_i and excenters I_{a_i}, I_{b_i}, I_{c_i} of the triangle family τ lie on a cubic or degenerate cubic which can be the union of a hyperbola and a straight line, or even the union of three lines.*

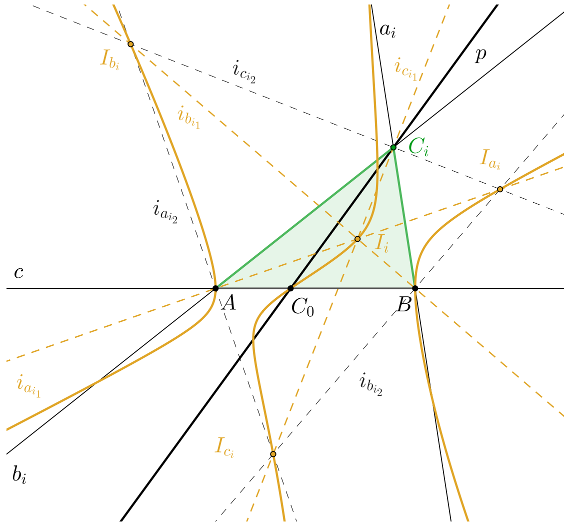

Figure 10: *The locus of incenters and excenters when p intersects $\overline{AB}$ in an interior point.*

For the triangle $\triangle ABC_i$, the angle bisectors at the vertex A will be denoted with $i_{a_{i_1}}$ (interior bisector) and $i_{a_{i_2}}$ (exterior bisector). Analogously, we denote the angle bisectors $i_{b_{i_1}}$, $i_{b_{i_2}}$ at vertex B and angle bisectors $i_{c_{i_1}}$, $i_{c_{i_2}}$ at vertex C_i (see Fig. 10).

Proof. From the view point of projective geometry, every line of the pencil (A) corresponds to two lines of the pencil (B), i.e., to every line of the pencil (A) which is an angle bisector at vertex A correspond two angle bisectors (interior and exterior) at vertex B, and vice versa. Three out of these four points of intersection are different points, i.e., one of them is counted twice, therefore the result of these two projective pencils is a curve of degree three.

We can also view it in this way: for every triangle $\triangle ABC_i$, the angle bisectors $i_{a_{i_1}}$, $i_{a_{i_2}}$, $i_{b_{i_1}}$, $i_{b_{i_2}}$ determine a quadrilateral whose vertices and two diagonal points are points A, B, I_i, I_{a_i}, I_{b_i}, and I_{c_i}. Diagonals of the quadrilateral are the line c and the angle bisectors $i_{c_{i_1}}$, $i_{c_{i_2}}$.

If the line p is the bisector s_c of the line segment $\overline{AB}$, then the family τ is a family of isosceles triangles (see Fig. 11). The intersection of bisectors $i_{a_{i_1}}$, $i_{b_{i_1}}$ and $i_{a_{i_2}}$, $i_{b_{i_2}}$, i.e., the incenters I_i and the excenters I_{c_i} lie on the bisector s_c. To any line from the (A) which is an interior angle bisector $i_{a_{i_1}}$ there exists a corresponding line from the pencil (B) which is an exterior angle bisector $i_{b_{i_2}}$, and vice versa. The intersection points are excenters I_{a_i} and I_{b_i}. Hence, from the latter we have a 1-1 correspondence and the set of intersection points is a conic. For the degenerate triangle $\triangle ABC_\infty$, the angle bisector $i_{a_{\infty_1}}$ is parallel to the angle bisector $i_{b_{\infty_2}}$, and vice versa, hence the conic is a hyperbola. Note that these two points of the locus curve of incenters and excenters are at infinity. This is also true in the case of an arbitrary line p (see Fig. 13). The third diagonal point of the aforementioned quadrilateral is the point $C_0 = M_c$.

If the line p is incident with the point A (or B), then the sides $\overline{AC_i}$ (or $\overline{BC_i}$) of triangles in the family τ lie on the line p. Therefore, for every triangle $\triangle ABC_i$ the angle bisectors at the vertex A (or B) are always the same two lines i_{a_1} and i_{a_2} (or i_{b_1}, i_{b_2}) which is the part of the degenerate cubic. The third line of the degenerate cubic is the exterior angle bisector $i_{b_{0_2}}$ at the vertex B for the degenerate triangle ABC_0, respectively $i_{a_{0_2}}$ if the line p is incident with the point B (see Fig. 12). □

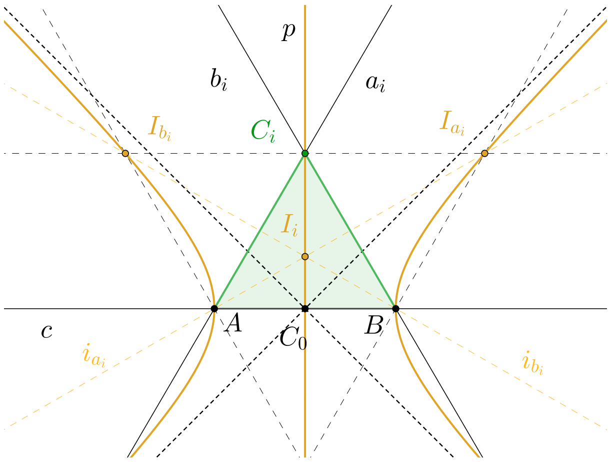

Figure 11: *The locus of incenters and excenters if $p = s_c$.*

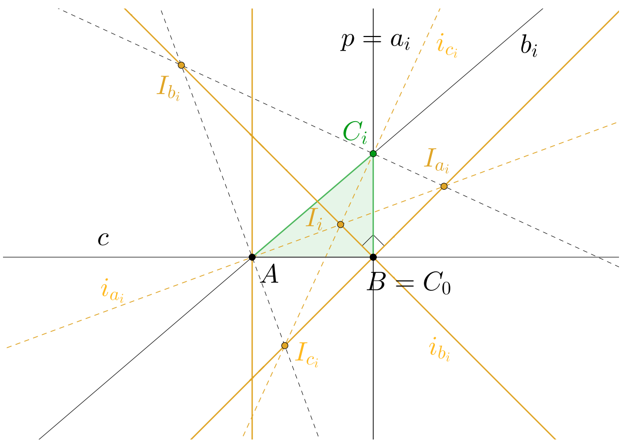

Figure 12: *The locus of incenters and excenters consists of three lines if $C_0 = B$.*

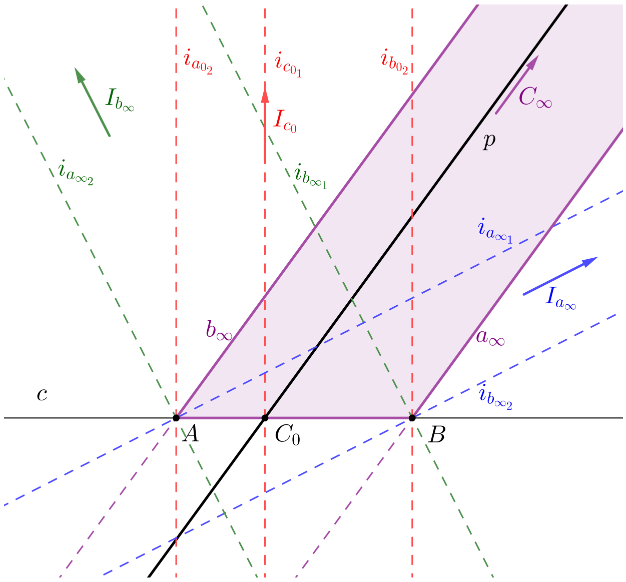

Figure 13: *The directions of the asymptotes of the cubic.*

We can distinguish these cases for the initial elements:

- (case a) The line p is in general position relative to the line AB when the intersection point $C_0 = p \cap AB$ lies between the points A and B.
- (case b) The line p is in general position to the line AB when the intersection point $C_0 = p \cap AB$ lies outside the segment $\overline{AB}$.
- (case c) The line p is parallel to AB.
- (case d) The line p is the bisector of segment $\overline{AB}$.
- (case e) The line p passes through either A or B.

For the first three cases, the locus curve is a cubic. For the last two, according to Theorem 5, the curve degenerates. In (case a), for the degenerate triangle $\triangle ABC_0$, the bisectors $i_{a_{0_2}}$, $i_{b_{0_2}}$, and $i_{c_{0_1}}$ are parallel lines which are orthogonal to the line AB. Therefore one asymptote of the locus curve of the incenters and the excenters is orthogonal to the line AB. The other two directions of the asymptotes we can deduce from the triangle $\triangle ABC_\infty$ where two of the triangle excenters are at infinity whereas the angle bisectors are parallel as stated in the proof of Theorem 5 (see Fig. 12). In (case b), for the degenerate triangle $\triangle ABC_0$, the bisectors $i_{a_{0_2}}$, $i_{b_{0_1}}$, and $i_{c_{0_2}}$ are parallel but the way to find the direction of the asymptotes is the same as in (case a).
We will now derive the equation of the curve.
The general equation of a cubic is

$$
\begin{aligned}
P(x,y) = & Ax^3 + Bx^2y + Cxy^2 + Dy^3 \\
& + Ex^2 + Fxy + Gy^2 + Hx + Ky + L = 0 \qquad (12)
\end{aligned}
$$

where we will denote the cubic homogeneous part as

$$P_3(x,y) = Ax^3 + Bx^2y + Cxy^2 + Dy^3 \tag{13}$$

and the quadratic part as

$$P_2(x,y) = Ex^2 + Fxy + Gy^2. \tag{14}$$

Let $k_1, -\frac{1}{k_1}$ be the slopes of the angle bisectors between the lines p and c, $k_1 = \tan\frac{\varphi}{2}$, and $p_0 = -\frac{l}{k}$ (see Fig. 2) hence the asymptotes of the cubic are

$$x = p_0,\ y = k_1x + l_1,\ y = -\frac{1}{k_1}x + l_2. \tag{15}$$

Now one can use results from [11] and [13] regarding asymptotes of algebraic curves and their relations to the equation of the curve. In [11] we find relations between linear factors of the highest degree homogeneous part of the equation and equations of asymptotes as follows in our case of degree 3 polynomial P:

- a linear factor $(ax+by)$ is a simple factor of $P_3(x,y)$ if $P_3(x,y) = (ax+by)Q_3(x,y)$ where $Q_3(b,-a) \neq 0$, with
$$P_3(x,y) = (ax+by)Q_3(x,y)$$
and to this simple factor is associated the single asymptote to $P(x,y) = 0$ given by
$$(ax+by)Q_3(b,-a) + P_2(b,-a) = 0. \tag{16}$$

From (15) we know the three linear factors of P_3 to be as follows, with respect to (18):

$$\begin{aligned} P_3(x,y) &= \frac{1}{k_1}x(y-k_1x)(k_1y+x) \\ &= -x^3 + \left(\frac{1}{k_1} - k_1\right)yx^2 + xy^2 \end{aligned}$$

and it follows that

$$A = -1, \quad B = \left(\frac{1}{k_1} - k_1\right), \quad C = 1, \quad D = 0. \tag{17}$$

If we include in consideration the three intersections of the curve with the x-axis, which tells us that the equation (12) contains the expression $(x-p_0)(x^2-x_a^2)$ we can deduce that

$$A = -1, \quad E = p_0, \quad H = x_a^2, \quad L = -p_0x_a^2. \tag{18}$$

This leaves us to determine the remaining three coefficients F, G, K. We used a particular curve and solved the system of equations from the condition of the incenter and excenter being on the curve and calculated the following values:

$$F = 0, \quad G = p_0, \quad K = -\left(\frac{1}{k_1} - k_1\right)x_a^2. \tag{19}$$

Hence, the equation of the cubic, in (case a) and (case b), can be written as

$$\left(\frac{1}{k_1} - k_1\right)y(x^2 - x_a^2) + y^2(x+p_0) = (x-p_0)(x^2-x_a^2).$$

If the line p intersects outside the segment $\overline{AB}$ (case b) the curve has three open branches and an oval (see Fig. 14). If the line p intersects the segment $\overline{AB}$ inside (case a), then an open branch is stretched along the vertical asymptote which the cubic intersects and converges to the asymptote from different directions and different sides.

In (case c), if $p \parallel c$ then $C_0 = C_\infty$, i.e., there is only one degenerate triangle from which we can conclude that one asymptote of the cubic is parallel to the line c and the line at infinity is a tangent of the cubic with the tangent point at the ideal point of the axis y. The cubic has a parabolic asymptote. The equation of the cubic is

$$-\frac{l}{2}y^2 + (x^2 - x_a^2)\left(y - \frac{l}{2}\right) = 0$$

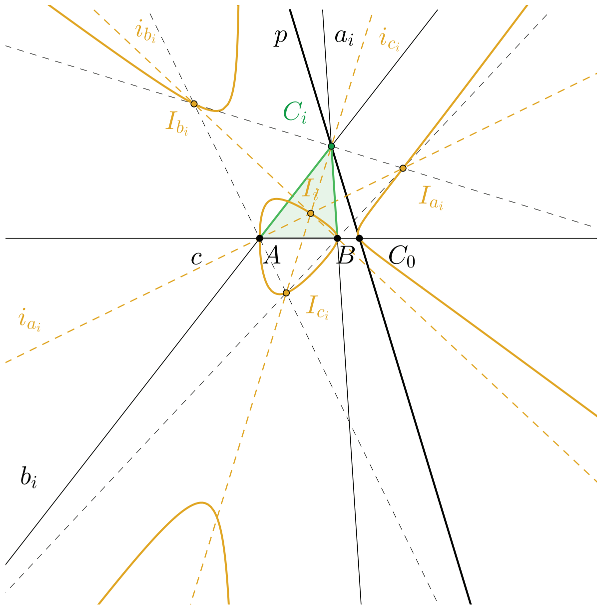

Figure 14: *The locus of incenters and excenters when p intersects $\overline{AB}$ outside.*

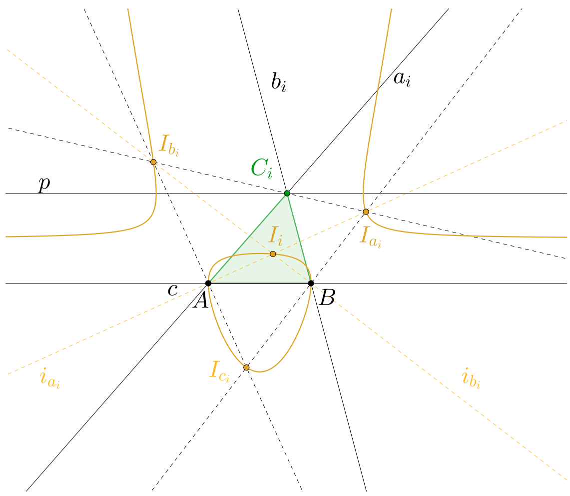

Figure 15: *The locus of incenters and excenters when $p \parallel c$.*

References

[1] GARCIA, R.A., ODEHNAL, B., REZNIK, D., Loci of Poncelet Triangles in the General Closure Case, *J. Geom.* **113**(17) (2022), `https://doi.org/10.1007/s00022-022-00629-3`

[2] GARCIA, R.A., ODEHNAL, B., REZNIK, D., Poncelet porisms in hyperbolic pencils of circles, *J. Geom. Graph.* **25**(2) (2021), 205–225.

[3] GLAESER, G., STACHEL, H., ODEHNAL, B., *The Universe of conics*, Springer-Verlag Berlin Heidelberg, 2016, `https://doi.org/10.1007/978-3-662-45450-3`

[4] SLIEPČEVIĆ, A., HALAS, H., Family of triangles and related curves, *Rad Hrvat. Akad. Znan. Umjet. Mat. Znan.* **17**(515) (2013), 203–210.

[5] JURKIN, E., Curves of Brocard Points in Triangle Pencils in Isotropic Plane, *KoG* **22** (2018), 20–23, `https://doi.org/10.31896/k.22.3`

[6] JURKIN, E., Loci of centers in pencil of triangles in the isotropic plane, *Rad Hrvat. Akad. Znan. Umjet. Mat. Znan.* **26**(551) (2022), 155–169, `https://doi.org/10.21857/94kl4cl6wm`

[7] KATIĆ ŽLEPALO, M., JURKIN, E., Curves of centroids, Gergonne points and symmedian centers in triangle pencils in isotropic plane, *Rad Hrvat. Akad. Znan. Umjet. Mat. Znan.* **22**(534) (2018), 119–127.

[8] KIMBERLING, C., Encyclopedia of Triangle Centers, `http://faculty.evansville.edu/ck6/encyclopedia/ETC.html`

[9] KODRNJA, I., KONCUL, H., The Loci of Vertices of Nedian Triangles, *KoG* **21** (2017), 19–25, `https://doi.org/10.31896/k.21.5`

[10] KOVAČEVIĆ, N., SLIEPČEVIĆ, A., On the Certain Families of Triangles, *KoG* **16** (2012), 21–26.

[11] NUNEMACHER, J., Asymptotes, Cubic Curves, and Projective Plane, *Math. Mag.* **3** (1999), 183–192.

[12] ODEHNAL, B., Poristic loci of triangle centers, *J. Geom. Graph.* **15**(1) (2011), 45–67.

[13] SAVELOV, A.A., *Ravninske krivulje*, Školska knjiga, Zagreb, 1979.

Iva Kodrnja
orcid.org/0000-0003-3976-4166
e-mail: iva.kodrnja@geof.unizg.hr

University of Zagreb Faculty of Geodesy
10 000 Zagreb, Kačićeva 26, Croatia

Helena Koncul
orcid.org/0000-0002-6890-7835
e-mail: helena.koncul@grad.unizg.hr

University of Zagreb Faculty of Civil Engineering
10 000 Zagreb, Kačićeva 26, Croatia

https://doi.org// 10.31896/k.27.5
Stručni rad
Prihvaćeno 18. 10. 2023.

Monika Đuzel
Ivana Filipan
Ljiljana Primorac Gajčić

Krivulje u 3-dimenzionalnom Minkowskijevom prostoru

Curves in 3-dimensional Minkowski Space

ABSTRACT

In this paper curves in threedimensional Minkowski space were analyzed and the main differences in local theory of curves in Euclidean and Minkowski space were emphasized. Special attention is paid to curves with no Euclidean counterpart. There are numerous examples of studied curves whose graphic representations were made by *Mathematica* software.

Key words: Minkowski space, spacelike curve, timelike curve, lightlike curve

MSC2010: 53A35, 53B30

Krivulje u trodimenzionalnom Minkowskijevom prostoru

SAŽETAK

U radu su promatrane krivulje u trodimenzionalnom Minkowskijevom prostoru, te su istaknute razlike u lokalnoj teoriji krivulja u odnosu na euklidski prostor. Posebna pažnja posvećena je krivuljama koje nemaju svoj analogon u euklidskom prostoru. Navedeni su i brojni primjeri krivulja, za čiju vizualizaciju je korišten program *Mathematica*.

Ključne riječi: Minkowskijev prostor, prostorna krivulja, vremenska krivulja, svjetlosna krivulja

1 Uvod

Iako je francuski matematičar i teorijski fizičar Henri Poincaré (1854.-1912.) predviđao da će euklidska geometrija zauvijek ostati najprikladnija za proučavanje fizike, danas je, zahvaljujući njemačkom matematičaru i fizičaru Hermannu Minkowskom (1864.-1909.), poznato da je to zapravo 4-dimenzionalna ne-euklidska mnogostrukost.

U jesen 1907. Minkowski je uvidio značaj Einsteinove teorije relativnosti za cjelokupnu fiziku te je održao predavanje Matematičkom društvu Göttingena pod naslovom "O principu relativnosti u elektroidnamici: novi oblik jednadžbi elektrodinamike". Tom prilikom je Minkowski predstavio svoju reformulaciju zakona fizike u terminima 4-dimenzionalnog prostora, koja se temeljila na Lorentzovoj invarijantnosti kvadratne forme $x^2+y^2+z^2-c^2t^2$, gdje su x,y,z pravokutne prostorne koordinate, t je vrijeme, a c brzina svjetlosti u vakuumu. Svjetlosni signal iz točke O se širi u obliku kružnice zadane jednadžbom $(ct)^2 = x^2+y^2+z^2$ i ona predstavlja doseg širenja informacija brzinama ispod brzine svjetlosti. Svaki događaj T u 4-dimenzionalnom prostoru zadan s koordinatama (t,x,y,z) koji zadovoljava gornju jednadžbu pripada svjetlosnom konusu. Takav konus možemo pridružiti svakom događaju T, pri čemu događaji s $t>0$ predstavljaju događaje koje je moguće posjetiti iz događaja T brzinom gibanja manjom ili jednakom brzini svjetlosti. Potaknut time, Minkowski definira metriku zadanu s $ds^2 = (ct)^2-dx^2-dy^2-dz^2$ koja očito nije definitna, odnosno postoje događaji čija je udaljenost od fiksnog događaja jednaka nuli. Takvi događaji su događaji koji se odvijaju istovremeno. Četiridimenzionalni prostor s ovako definiranom (pseudo)-metrikom naziva se Minkowskijev prostor i to je najprikladniji prostor za izučavanje moderne fizike. Definiranu (pseudo)-metriku možemo analogno definirati i na trodimenzionalnom prostoru, te izučavati krivulje i plohe unutar takvog prostora, što možemo lako vizualno predočiti. Dakle, Minkowskijev 3-dimenzionalni (ili čak n-dimenzionalni) prostor je vrlo privlačan za izučavanje objekata diferencijalne geometrije, budući da se u njemu javljaju razlike u odnosu na teoriju euklidskog prostora. U ovom radu bavit ćemo se krivuljama u Minkowskijevom trodimenzionalnom prostoru, s posebnim naglaskom na krivulje kakvih nema u euklidskom prostoru, te ćemo isticati bitne razlike u teoriji krivulja u odnosu na euklidski slučaj. Dijelovi ovog članka temelje se na diplomskom radu [3] kojeg je pod voditeljstvom doc.dr.sc.Ljiljane Primorac Gajčić izradila studentica Odjela za matematiku, Sveučilišta u Osijeku, Monika Đuzel.

2 Trodimenzionalni Minkowskijev prostor

Minkowskijev trodimenzionalni prostor, koji se zbog važnosti Lorentzovih transformacija pri njegovom definiranju naziva još i Lorentz-Minkowskijev, a katkad i samo Lorentzov prostor predstavlja uređeni par realnog trodimenzionalnog vektorskog prostora i odgovarajuće pseudometrike.

Definicija 1 *Minkowskijev prostor je metrički prostor* $\mathbb{R}^3_1 = (\mathbb{R}^3, \langle , \rangle)$, *gdje je metrika (pseudo-skalarni produkt indeksa 1) definirana s*

$$\langle x,y\rangle = x_1y_1 + x_2y_2 - x_3y_3,$$
$$x = (x_1,x_2,x_3), \quad y = (y_1,y_2,y_3).$$

Neki autori ([7]), definiraju metriku s minusom na prvoj koordinati ($\langle x,y\rangle = -x_1y_1 + x_2y_2 + x_3y_3$), dok ćemo se mi u radu služiti definicijom 1.

Definirana metrika je pseudo-metrika budući da ne zadovoljava svojstvo pozitivne definitnosti. S obzirom na definiranu pseudo-metriku u Minkowskijevom prostoru razlikujemo tri vrste vektora koje definiramo kao slijedi:

Definicija 2 *Za vektor* $x \in \mathbb{R}^3_1$ *kažemo da je prostorni ako je* $\langle x,x\rangle > 0$ *ili* $x = 0$, *vremenski ako je* $\langle x,x\rangle < 0$ *i svjetlosni (nul, izotropni) ako je* $\langle x,x\rangle = 0$ *i* $x \neq 0$.

Svojstvo vektora iz prethodne definicije nazivamo kauzalnim karakterom vektora. Promotrimo li sad klasifikaciju vektora s obzirom na skalarni kvadrat vektora, možemo uočiti da prostorni vektori pripadaju jednoplošnom hiperboloidu zadanom jednadžbom $x^2 + y^2 - z^2 = r^2$, $r > 0$, vremenski vektori pripadaju dvoplošnom hiperboloidu zadanom jednadžbom $x^2 + y^2 - z^2 = -r^2$, $r > 0$, dok svjetlosni vektori pripadaju stošcu zadanom jednadžbom $x^2 + y^2 - z^2 = 0$. Spomenute plohe su i primjeri kvadrika u Minkowskijevom prostoru [12], te ih redom nazivamo, vremenska ili pseudo-sfera, prostorna sfera ili hiperbolična ravnina te svjetlosni stožac, slika 1.

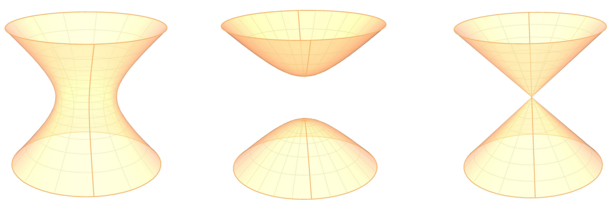

Slika 1: *Pseudo-sfera, hiperbolična ravnina i svjetlosni stožac*

Primjer 1 *Vektor* $x_1 = (3,2,1)$ *je prostorni jer je* $\langle x_1,x_1\rangle = 12 > 0$. *Vektor* $x_2 = (1,2,3)$ *je vremenski jer je* $\langle x_2,x_2\rangle = -4 < 0$ *i vektor* $x_3 = (2,0,2)$ *je svjetlosni jer je* $\langle x_3,x_3\rangle = 0$.

Okomitost vektora u $\mathbb{R}^3_1$ definira se isto kao i u euklidskom prostoru.

Definicija 3 *Za vektore* $x, y \in \mathbb{R}^3_1$ *kažemo da su okomiti (ortogonalni) ako je* $\langle x,y\rangle = 0$.

Istaknimo da za razliku od euklidskog prostora, gdje za kolinearne vektore $x, y \in \mathbb{R}^3 \setminus \{(0,0,0)\}$ nikako ne vrijedi da je $\langle x,y\rangle = 0$ jer bi to značilo da su vektori istovremeno kolinearni i okomiti, u Minkowskijevom prostoru to nije tako. Štoviše, za svaka dva kolinearna svjetlosna vektora $x, y \in \mathbb{R}^3_1$ vrijedi $\langle x,y\rangle = 0$, Odnosno, svjetlosni ortogonalni vektori su kolinearni vektori.

Primjer 2 *Neka su* $x = (1,0,1)$ *i* $y = (\lambda,0,\lambda)$, $\lambda \in \mathbb{R}$ *dva svjetlosna vektora. Očito su x i y kolinearni jer vrijedi* $y = \lambda x$, *no za njih također vrijedi* $\langle x,y\rangle = 0$ *što znači da su okomiti.*

Za vremenske vektore vrijedi druga osobitost. Naime, može se pokazati da takva dva vektora nisu nikada okomita, tj. ako su $x, y \in \mathbb{R}^3_1$ vremenski vektori onda vrijedi $\langle x,y\rangle \neq 0$. Nadalje, vrijede sjedeća svojstva za dva ortogonalna v i w vektora u $\mathbb{R}^3_1$.

1. Ako je v vremenski vektor, onda je w prostorni vektor.
2. Ako je v prostorni vektor, onda je w ili prostorni ili vremenski ili svjetlosni vektor.
3. Ako je v svjetlosni vektor, onda je w prostorni ili svjetlosni vektor.

Definicija 4 *Pseudo-norma vektora* $x \in \mathbb{R}^3_1$ *definirana je s* $\|x\| = \sqrt{|\langle x,x\rangle|}$.

Napomena 1 *Za vektor* $x \in \mathbb{R}^3_1$ *kažemo da je jedinični (normiran) ako je* $\|x\| = 1$. *Za razliku od euklidskog prostora gdje se svaki vektor različit od* $\vec{0}$ *može normirati, u Minkowskijevom prostoru to nije tako. Svaki prostorni vektor različit od* $\vec{0}$ *i svaki vremenski vektor može se normirati, dok svjetlosni vektori se ne mogu normirati jer je njihova norma* 0.

Euklidski i Minkowskijev prostor razlikuju se i u Cauchy-Schwarzovoj nejednakosti. Ako su $x,y \in \mathbb{R}^3$ tada vrijedi $|\langle x,y\rangle| \leq \|x\|\|y\|$, dok u Minkowskijevom prostoru za vremenske vektore $x,y \in \mathbb{R}^3_1$ vrijedi $|\langle x,y\rangle| \geq \|x\|\|y\|$. Jednakost vrijedi ako i samo ako su vektori x,y kolinearni.

Definicija vektorskog produkta je analogna definiciji vektorskog produkta u $\mathbb{R}^3$.

Definicija 5 *Vektorski produkt $v \times_L w$ vektora v i w u $\mathbb{R}^3_1$ dan je s $v \times_L w = J(v \times w)$, gdje $\times$ označava euklidski vektorski produkt, a matrica J je dana s*

$$J = \begin{pmatrix} 1 & 0 & 0 \\ 0 & 1 & 0 \\ 0 & 0 & -1 \end{pmatrix}.$$

Dalje u radu ispuštamo indeks L u oznaci $\times_L$, te će oznaka $\times$ predstavljati vektorski produkt u Minkowskijevom prostoru, osim ako nije istaknuto drugačije.

Promotrimo sad kut između dva vektora u Minkowskijevom prostoru. S obzirom na vezu između skalarnog produkta dva vektora i kuta koji zatvaraju, prirodno je za očekivati da će postojati razlike pri definiciji kuta između dva vektora u Minkowskijevom prostoru. Za dva vektora $x, y \in \mathbb{R}^3$ u euklidskom prostoru koji zatvaraju kut θ, vrijedi $\langle x, y \rangle = \|x\|\|y\| \cos\theta$. U Minkowskijevom prostoru vrijedi slična jednakost pomoću koje se definira kut između vektora pri čemu definicija kuta ovisi o kauzalnom karakteru vektora koji ga zatvaraju ([13]). Pri definiranju kuta treba voditi računa i o vremenskoj orijentaciji vektora koja se definira na sljedeći način:

Definicija 6 *Neka je $e_1 = (1,0,0)$. Za dani vektor $x \in \mathbb{R}^3_1$ kažemo da je orijentiran u budućnost (odnosno prošlost) ako vrijedi $\langle x, e_1 \rangle < 0$ (odnosno $\langle x, e_1 \rangle > 0$).*

Definicija 7 *Neka su x i y vremenski vektori iste orijentacije u $\mathbb{R}^3_1$. Tada postoji jedinstveni realni broj $\theta \geq 0$ takav da*

$$\langle x, y \rangle = -\|x\|\|y\| \cosh\theta.$$

Broj θ se naziva hiperbolički kut između vektora x i y.

Definicija 8 *Neka su x i y prostorni vektori u $\mathbb{R}^3_1$ koji razapinju vremenski (prostorni) potprostor. Tada postoji jedinstveni realni broj $\theta \geq 0$ takav da*

$$\langle x, y \rangle = \|x\|\|y\| \cosh\theta, \quad (\langle x, y \rangle = \|x\|\|y\| \cos\theta).$$

Broj θ se naziva središnji kut između vektora x i y.

Definicija 9 *Neka je x prostorni, a y vremenski vektor u $\mathbb{R}^3_1$. Tada postoji jedinstveni realni broj $\theta \geq 0$ takav da*

$$\langle x, y \rangle = \|x\|\|y\| \sinh\theta.$$

Broj θ se naziva Lorentzov vremenski kut između vektora x i y.

Za razliku od euklidskog prostora gdje možemo definirati kut između bilo koja dva ne-nul vektora, u Minkowskijevom prostoru kut između dva vektora od kojih je jedan svjetlosnog karaktera se ne definira.

Definicija i svojstva baze za Minkowskijev prostor analogni su onima u euklidskom prostoru tako da ćemo ih izostaviti. Navest ćemo samo definiciju svjetlosne baze i propoziciju koja nema euklidski analogon.

Definicija 10 *Uređenu trojku (A, B, C) koja se sastoji od dva svjetlosna i jednog prostornog vektora za koje vrijedi:*

$$\langle A, A \rangle = \langle B, B \rangle = 0, \quad \langle C, C \rangle = 1$$

$$\langle A, B \rangle = 1, \quad \langle A, C \rangle = 0, \quad \langle B, C \rangle = 0$$

nazivamo svjetlosni (nul) trobrid ili svjetlosna baza.

Propozicija 1 *Svaka ortonormirana baza $\{a_1, a_2, a_3\}$ za $\mathbb{R}^3_1$ ($a_i \perp a_j$ za sve $i \neq j$ i $\|a_i\| = 1$ za $i \in \{1,2,3\}$) sastoji se od točno dva prostorna i jednog vremenskog vektora.*

Potprostore Minkowskijevog prostora također možemo razlikovati po kauzalnom karakteru, što je određeno sljedećom definicijom.

Definicija 11 *Za potprostor $W \leq \mathbb{R}^3_1$ kažemo da je:*

1. *prostorni ako je svaki vektor $x \in W$ prostorni,*
2. *vremenski ako sadrži neki vremenski vektor,*
3. *svjetlosni ako sadrži neki svjetlosni vektor, ali ne sadrži vremenski vektor.*

Definicija 12 *Neka je $W \leq \mathbb{R}^3_1$ potprostor. Za pseudo-skalarni produkt u $\mathbb{R}^3_1$ kažemo da je degeneriran na W ako postoji vektor $v \in W$, $v \neq 0$ takav da je $v \perp x$ za svaki $x \in W$. U suprotnom kažemo da je pseudo-skalarni produkt nedegeneriran na W.*

Pseudo-skalarni produkt na potprostoru $W \leq \mathbb{R}^3_1$ je degeneriran ako i samo ako je W svjetlosni potprostor.

Propozicija 2 *Ako je $W \leq \mathbb{R}^3_1$ potprostor.*

1. *W je prostorni ako i samo ako je $W^\perp$ vremenski.*
2. *W je vremenski ako i samo ako je $W^\perp$ prostorni.*
3. *W je svjetlosni ako i samo ako je $W^\perp$ svjetlosni.*

U prva dva slučaja je $W \cap W^\perp = \{0\}$, dok je u trećem $W \cap W^\perp \neq \{0\}$, odnosno u trećem slučaju vrijedi $\dim(W \cap W^\perp) = 1$.

3 Lokalna teorija krivulja u $\mathbb{R}^3_1$

Krivulje u Minkowskijevom prostoru definiramo kao i u euklidskom. Njihova lokalna teorija je u mnogočemu analogna lokalnoj teoriji krivulja u euklidskom prostoru. No ipak postoje neke razlike uzrokovane indefinitnošću pseudo-metrike o kojima će više riječi biti u nastavku.

Kauzalni karakter krivulje u Minkowskijevom prostoru određen je kauzalnim karakterom njezinog tangencijalnog vektora.

Definicija 13 *Krivulja $c\colon I\subset\mathbb{R}\to\mathbb{R}^3_1$ je prostorna (odnosno vremenska, svjetlosna (nul)) u točki $s_0\in I$ ako je vektor $c'(s_0)$ prostorni (odnosno vremenski, svjetlosni).*

Krivulja $c\colon I\subset\mathbb{R}\to\mathbb{R}^3_1$ je prostorna (odnosno vremenska, svjetlosna (nul)) ako je prostorna (odnosno vremenska, svjetlosna) u svakoj točki $s\in I$.

Primjer 3 *Krivulja $\alpha\colon\mathbb{R}\to\mathbb{R}^3_1$, $\alpha(s)=(\cosh s,\frac{s^2}{2},\sinh s)$ nema jedinstveni kauzalni karakter. Budući da je $\langle\alpha'(s),\alpha'(s)\rangle=s^2-1$, onda je α prostorna krivulja na intervalu $(-\infty,-1)\cup(1,\infty)$, vremenska na intervalu $(-1,1)$ i svjetlosna u točkama $s=\pm1$. Vidi sliku 2.*

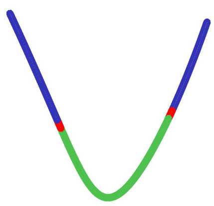

Slika 2: Plavi dio krivulje α je prostorni, zeleni dio je vremenski, a crveni svjetlosni.

Definicija 14 *Za prostornu (vremensku) krivulju $c\colon I\to\mathbb{R}^3_1$ kažemo da je jedinične brzine ili da je parametrizirana duljinom luka ako je $\|c'(s)\|=1,\ s\in I$.*

Napomena 2 *Svjetlosnu krivulju c ne možemo parametrizirati parametrom duljine luka jer vrijedi $\|c'(s)\|=0$, ali je možemo parametrizirati tzv. parametrom duljine pseudo-luka. Kasnije ćemo opisati tu reparametrizaciju.*

Budući da se teorija prostornih i vremenskih krivulja u $\mathbb{R}^3_1$ razlikuje od teorije svjetlosnih krivulja, najprije ćemo navesti rezultate vezane za prostorne i vremenske krivulje, a zatim za svjetlosne krivulje. Prostorne krivulje razlikujemo s obzirom na kauzalni karakter normale, koji može biti prostorni, vremenski ili svjetlosni. Vremenske krivulje i prostorne krivulje s prostornom ili vremenskom normalom nazivamo Frenetove krivulje.

Za svaku Frenetovu krivulju c u $\mathbb{R}^3_1$, analogno kao u euklidskom prostoru, definiramo ortonormirani trobrid (reper), tj. ortonormiranu bazu vektorskog prostora $\mathbb{R}^3_{1,c(s)}$ u svakoj točki krivulje $c(s)$. Neka je $c:I\to\mathbb{R}^3_1$ Frenetova krivulja parametrizirana duljinom luka pri čemu c' i c'' nisu kolinearni vektori. Polje $T(s)=c'(s)$ je jedinično tangencijalno polje od c. Polje vektora glavnih normala dano je s $N(s)=\frac{c''(s)}{\|c''(s)\|}$, $c''(s)\neq0$, a polje binormala s $B(s)=T(s)\times N(s)$. Tada je $\{T(s),N(s),B(s)\}$ ortonormirana baza od $\mathbb{R}^3_{1,c(s)}$ i nazivamo je Frenetovim (Frenet-Serretovim) trobridom (reperom, okvirom) krivulje c ([9]).

Definiramo sada za krivulju parametriziranu duljinom luka i sljedeće funkcije:

Definicija 15 *Neka je $c\colon I\to\mathbb{R}^3_1$ Frenetova krivulja parametrizirana duljinom luka.*

1. *Funkciju $\kappa\colon I\to\mathbb{R}$, $\kappa(s)=\|c''(s)\|$ nazivamo zakrivljenošću (fleksijom) krivulje c u točki $c(s)$.*
2. *Funkciju $\tau\colon I\to\mathbb{R}$, $\tau(s)=\langle N(s),B'(s)\rangle$ nazivamo torzijom (sukanjem) krivulje c u točki $c(s)$.*

U $\mathbb{R}^3_1$ također vrijede Frenetove formule analogne onima u euklidskom prostoru,

$$\begin{pmatrix}T'\\N'\\B'\end{pmatrix}=\begin{pmatrix}0&\kappa&0\\-\varepsilon\eta\kappa&0&\tau\\0&\varepsilon\tau&0\end{pmatrix}\begin{pmatrix}T\\N\\B\end{pmatrix}$$

pri čemu je $\varepsilon=\langle T,T\rangle=\pm1$, $\eta=\langle N,N\rangle=\pm1$.

U primjeru 4 dane su parametarske jednadžbe ravninskih krivulja s pripadnim trobridima.

Primjer 4

(1) Krivulja $\alpha(s)=r\big(\cos\big(\frac{s}{r}\big),\sin\big(\frac{s}{r}\big),0\big)$ je prostorna krivulja s prostornom normalom. Leži u prostornoj ravnini s jednadžbom $z=0$. Njezin Frenetov trobrid je

$$T(s)=\big(-\sin\big(\tfrac{s}{r}\big),\cos\big(\tfrac{s}{r}\big),0\big),$$
$$N(s)=\big(-\cos\big(\tfrac{s}{r}\big),-\sin\big(\tfrac{s}{r}\big),0\big),$$
$$B(s)=(0,0,-1)$$

i zakrivljenosti su $\kappa=\frac{1}{r}$ i $\tau=0$. Budući da je α ravninska krivulja s konstantnom zakrivljenošću, ona je kružnica u Minkowskijevom prostoru, kao i u euklidskom. Vidi sliku 4 lijevo.

(2) *Krivulja* $\alpha(s) = r\left(0, \sinh\left(\frac{s}{r}\right), \cosh\left(\frac{s}{r}\right)\right)$ *je prostorna krivulja s vremenskom normalom. Leži u vremenskoj ravnini s jednadžbom* $x = 0$*. Njezin Frenetov trobrid je*

$$T(s) = \left(0, \cosh\left(\frac{s}{r}\right), \sinh\left(\frac{s}{r}\right)\right),$$
$$N(s) = \left(0, \sinh\left(\frac{s}{r}\right), \cosh\left(\frac{s}{r}\right)\right),$$
$$B(s) = (1, 0, 0)$$

i zakrivljenosti su $\kappa = \frac{1}{r}$ *i* $\tau = 0$*. Budući da je* α *ravninska krivulja s konstantnom zakrivljenošću, ona je kružnica u Minkowskijevom prostoru. Euklidskim očima gledano ona je jednakostrana hiperbola. Vidi sliku 4 sredina (žuta).*

(3) *Krivulja* $\alpha(s) = r\left(0, \cosh\left(\frac{s}{r}\right), \sinh\left(\frac{s}{r}\right)\right)$ *je vremenska krivulja koja leži u vremenskoj ravnini s jednadžbom* $x = 0$*. Njezin Frenetov trobrid je*

$$T(s) = \left(0, \sinh\left(\frac{s}{r}\right), \cosh\left(\frac{s}{r}\right)\right),$$
$$N(s) = \left(0, \cosh\left(\frac{s}{r}\right), \sinh\left(\frac{s}{r}\right)\right),$$
$$B(s) = (-1, 0, 0)$$

i zakrivljenosti su $\kappa = \frac{1}{r}$ *i* $\tau = 0$*. Budući da je* α *ravninska krivulja s konstantnom zakrivljenošću, ona je kružnica u Minkowskijevom prostoru. Euklidskim očima gledano ona je jednakostrana hiperbola. Vidi sliku 4 sredina (zelena).*

Sada ćemo navesti neke primjere prostornih krivulja u $\mathbb{R}^3_1$.

Primjer 5

(1) *Obična cilindrična spirala* $\alpha(s) = (r\cos s, r\sin s, hs)$, $h \neq 0, r > 0$ *je prostorna (vremenska, svjetlosna) krivulja ako je* $r^2 > h^2$, $(r^2 < h^2, r^2 = h^2)$.

(2) *Obična cilindrična hiperbolična spirala* $\alpha(s) = (hs, r\sinh s, r\cosh s)$, $h \neq 0, r > 0$ *je prostorna krivulja (slika 3 lijevo).*

(3) *Obična cilindrična spirala* $\alpha(s) = (hs, r\cosh s, r\sinh s)$, $h \neq 0, r > 0$ *je prostorna (vremenska, svjetlosna) krivulja ako je* $h^2 > r^2$, $(h^2 < r^2, r^2 = h^2)$.

(4) *Krivulja* $\left(2s - \frac{4}{c}\arctan(cs), -\frac{1}{c}\left(3 + 2\ln\left(1 + c^2 s^2\right)\right), 2s\right)$, $c \in \mathbb{R}$ *je nul krivulja (slika 3 desno).*

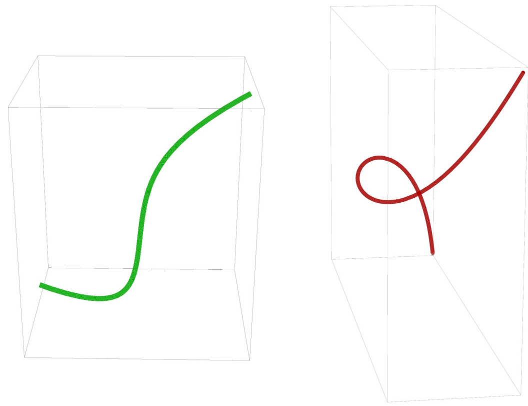

Slika 3: Prostorna krivulja $(20s, 2\sinh s, 2\cosh s)$ *i svjetlosna krivulja* $\left(2s - 2\arctan(2s), -\frac{1}{2}(3 + 2\ln(1 + 4s^2)), 2s\right)$*, u prostoru.*

Za razliku od euklidskog prostora, u Minkowskijevom prostoru postoje tzv. pseudo-nul krivulje ([14]). To su prostorne krivulje sa svjetlosnom normalom. Njihove Frenetove formule su

$$\begin{pmatrix} T' \\ N' \\ B' \end{pmatrix} = \begin{pmatrix} 0 & \kappa & 0 \\ 0 & \tau & 0 \\ -\kappa & 0 & -\tau \end{pmatrix} \begin{pmatrix} T \\ N \\ B \end{pmatrix}$$

gdje zakrivljenost κ poprima samo dvije vrijednosti, 0 ili 1. Ako je $\kappa = 0$, onda je $c(u)$ pravac. Vrijedi i obrat. Ako je $c(u)$ pravac, onda je $c''(u) = 0 = T'(u)$, što znači da je $\kappa = 0$. Ako $c(u)$ nije pravac, onda postoji interval na kojem je $c''(u) \neq 0$. $N(u)$ je definiran kao $N(u) = c''(u) = T'(u)$, prema tome $\kappa = 1$. Polje binormala $B(u)$ je svjetlosni vektor okomit na $T(u)$ u svakoj točki krivulje $c(u)$ takav da vrijedi $\langle N, B\rangle = 1$. (T, N, B) je svjetlosna baza (vidi definiciju 10). Torzija krivulje $c(u)$ je definirana s $\tau = \langle N', B\rangle$ i autor u ([9]) je naziva pseudo-torzija. Poznato je da su sve pseudo-nul krivulje ravninske krivulje koje leže u svjetlosnoj ravnini ([1, 2]).

Primjer 6 *Krivulja* $\alpha(s) = r\left(\frac{s}{r}, \left(\frac{s}{r}\right)^2, \left(\frac{s}{r}\right)^2\right)$ *je pseudo-nul krivulja koja leži u svjetlosnoj ravnini s jednadžbom* $y - z = 0$*. Njena svjetlosna baza je*

$$T(s) = \left(1, \frac{2s}{r}, \frac{2s}{r}\right),\ N(s) = \left(0, \frac{2}{r}, \frac{2}{r}\right),\ B(s) = \left(0, \frac{r}{4}, -\frac{r}{4}\right)$$

i zakrivljenosti su $\kappa = 1$ *i* $\tau = 0$*. Budući da je* α *ravninska krivulja s konstantnom zakrivljenošću, ona je kružnica u Minkowskijevom prostoru. Euklidskim očima gledano, ona je parabola čija je os paralelna sa svjetlosnim smjerom. Vidi sliku 4 desno.*

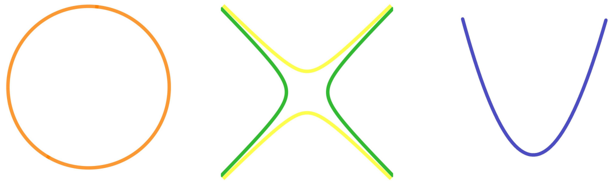

Slika 4: *Kružnice u Minkowskijevom prostoru.*

Euklidska elipsa je također Minkowskijeva kružnica, što je pokazano u [11]. Promatran je presjek svjetlosnog stošca

$$LC(p) = \{q \in \mathbb{R}^3_1 \setminus \{p\} : \langle q-p, q-p\rangle = 0\},$$

prostornom, vremenskom i svjetlosnom ravninom. U presjeku se dobiju Minkowsijeve kružnice koje su euklidske elipsa, jednakostrana hiperbola i parabola, slika 5.

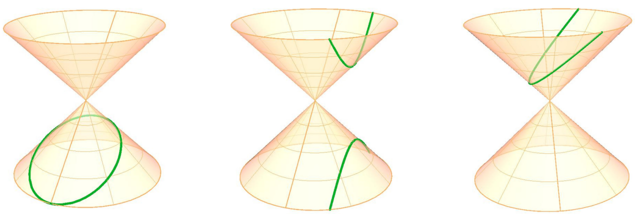

Slika 5: *Kružnice u Minkowskijevom prostoru kao presjeci svjetlosnog stošca i ravnine.*

Poznato je da u euklidskom prostoru vrijedi tvrdanja: Neka je $c\colon I \to \mathbb{R}^3$ regularna krivulja pri čemu c' i c'' nisu kolinearni. Krivulja c je ravninska ako i samo ako je $\tau = 0$. U Minkowskijevom prostoru za pseudo-nul krivulje ta tvrdnja ne vrijedi. Sljedeća dva primjera pokazuju da su pseudo-nul krivulje ravninske, iako je $\tau \neq 0$.

Primjer 7 *Dana je pseudo-nul krivulja*

$$\alpha(s) = \frac{1}{\tau}(\cosh(\tau s) + \sinh(\tau s), \tau^2 s, \cosh(\tau s) + \sinh(\tau s)).$$

To je ravninska krivulja koja leži u svjetlosnoj ravnini $x - z = 0$. Svjetlosni trobrid $(T(s), N(s), B(s))$ krivulje $\alpha(s)$ je

$$T(s) = \Big(\frac{\cosh(\tau s) + \sinh(\tau s)}{\tau}, 1, \frac{\cosh(\tau s) + \sinh(\tau s)}{\tau}\Big),$$

$$N(s) = \Big(\cosh(\tau s) + \sinh(\tau s), 0, \cosh(\tau s) + \sinh(\tau s)\Big),$$

$$B(s) = \Big(\frac{-(1+\tau^2)\cosh(\tau s) + (-1+\tau^2)\sinh \tau s)}{2\tau^2}, -\frac{1}{\tau}, \frac{(-1+\tau^2)\cosh(\tau s) - (1+\tau^2\sinh(\tau s)}{2\tau^2}\Big).$$

To je jedina pseudo-nul prostorna krivulja s pseudo-torzijom $\tau = const. \neq 0$, [14]. Vidi sliku 6 lijevo.

Primjer 8 *Neka je $\alpha(s)$ pseudo-nul prostorna krivulja*

$$\alpha(s) = \Big(\frac{s^3 - 12s}{12\sqrt{2}}, \frac{s^3 + 12s}{12\sqrt{2}}, \frac{s^3}{12}\Big)$$

s pseudo-torzijom $\tau = \frac{1}{s}$. Ona leži u svjetlosnoj ravnini $x + y = \sqrt{2}z$ i njezin svjetlosni trobrid je

$$T = \Big(\frac{-4+s^2}{4\sqrt{2}}, \frac{4+s^2}{4\sqrt{2}}, \frac{s^2}{4}\Big), \quad N = \Big(\frac{s}{2\sqrt{2}}, \frac{s}{2\sqrt{2}}, \frac{s}{2}\Big),$$

$$B = \Big(\frac{16+8s^2-s^4}{16\sqrt{2}s}, \frac{16-8s^2-s^4}{16\sqrt{2}s}, -\frac{16+s^4}{16s}\Big).$$

Vidi sliku 6 desno.

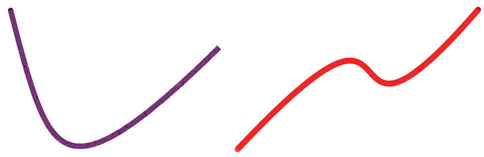

Slika 6: *Pseudo-nul krivulja s parametrizacijom* $\alpha(s) = (\cosh s + \sinh s, s, \cosh s + \sinh s)$, *(lijevo), odnosno* $\alpha(s) = \big(\frac{s^3-12s}{12\sqrt{2}}, \frac{s^3+12s}{12\sqrt{2}}, \frac{s^3}{12}\big)$ *(desno).*

Sada ćemo definirati funkcije zakrivljenosti svjetlosne krivulje i njenu reparametrizaciju pseudo-lukom.

Teorem 1 (Osnovni teorem za svjetlosne krivulje, [7]) *Ako su zadani početni podatci (p, k_0, k_1, k_2, k_3), gdje je p fiksna točka i k_0, k_1, k_2, k_3 funkcije klase C^1, tada postoji jedinstvena svjetlosna Frenetova krivulja $(c(t), (A(t), B(t), C(t)))$ takva da $c(0) = p$, $\dot{c}(t) = k_0(t)A(t)$ i vrijede Frenet-Serretove formule:*

$$\begin{pmatrix} A' \\ B' \\ C' \end{pmatrix} = \begin{pmatrix} k_1 & 0 & k_2 \\ 0 & -k_1 & k_3 \\ -k_3 & -k_2 & 0 \end{pmatrix} \begin{pmatrix} A \\ B \\ C \end{pmatrix}.$$

Funkcije $\kappa_i, i = 1,2,3$ se nazivaju zakrivljenosti funkcije $c(t)$ s obzirom na svjetlosni trobrid $(A(t), B(t), C(t))$. Svjetlosni trobrid nije jedinstven, stoga je potrebno uz svjetlosnu krivulju navesti njezin trobrid. Svjetlosna krivulja u $\mathbb{R}^3_1$ je pravac ako i samo ako je $\kappa_2 = 0$ ([2, 10]).

U sljedeća dva primjera dani su primjeri svjetlosnih pravaca kojima su pridruženi različiti svjetlosni trobridi i pripadne zakrivljenosti.

Primjer 9 *Nul pravac* $c(s) = \Big(as - \frac{s^2}{2}, -a, as - \frac{s^2}{2}\Big)$, *$a \in \mathbb{R}$ sa svjetlosnim trobridom*

$$A = (1,0,1), \quad B = \frac{1}{2}(1,0,-1), \quad C = (0,-1,0),$$

ima zakrivljenosti $\kappa_0(s) = a - s$, $\kappa_1 = \kappa_2 = \kappa_3 = 0$.
Ako krivulji $c(s)$ *pridružimo svjetlosni trobrid*

$$A = (a-s)(1,0,1), \quad B = \frac{1}{s-a}\Big(\frac{s^2-1}{2}, -s, \frac{s^2+1}{2}\Big),$$

$$C = (s,-1,s),$$

tada krivulja $c(s)$ *ima zakrivljenosti* $\kappa_0 = 1$, $\kappa_1(s) = \kappa_3(s) = \dfrac{1}{(s-a)}$, $\kappa_2 = 0$.

Primjer 10 *Nul pravac*

$$c(s) = \Big(\frac{2s^3 - 3a\left(s^2-4\right)}{12\sqrt{2}}, \frac{2s^3-3a\left(4+s^2\right)}{12\sqrt{2}}, \frac{(2s-3a)s^2}{12}\Big),$$

$a \in \mathbb{R}$ *sa svjetlosnim trobridom o*

$$A = \left(\frac{1}{2\sqrt{2}}, \frac{1}{2\sqrt{2}}, \frac{1}{2}\right), \quad B = (\sqrt{2}, -\sqrt{2}, -2),$$

$$C = (0, -\sqrt{2}, -1),$$

ima zakrivljenosti $\kappa_0 = s(s-a)$, $\kappa_1 = \kappa_2 = \kappa_3 = 0$, *dok sa svjetlosnim trobridom*

$$A = \left(\frac{1}{2\sqrt{2}}, \frac{1}{2\sqrt{2}}, \frac{1}{2}\right)$$
$$B = \Big(-\sqrt{2}m^2 + m\kappa_3 s - \frac{\kappa_3^2 s^2 - 8}{4\sqrt{2}},$$
$$-\sqrt{2}m^2 + m(\kappa_3 s - 4) + \frac{\kappa_3 s(8-\kappa_3 s) - 8}{4\sqrt{2}},$$
$$-2 - 2m^2 - \frac{1}{4}\kappa_3 s(\kappa_3 s - 4) + \sqrt{2}m(\kappa_3 s - 2)\Big)$$
$$C = \Big(\frac{1}{4}\big(\sqrt{2}\kappa_3 s - 4m\big), \frac{1}{4}\big(\sqrt{2}(\kappa_3 s - 4) - 4m\big),$$
$$-\big(1 + \sqrt{2}m - \frac{\kappa_3 s}{2}\big)\Big), \quad m = const.,$$

ima zakrivljenosti $\kappa_0(s) = s(s-a), \kappa_1 = \kappa_2 = 0$ *i* $\kappa_3 = const$.

Svjetlosnu krivulju $c(t)$ možemo reparametrizirati $t = t(u)$ tako da je $k_1 = 0$. Duggal i Bejancu ([4]) zovu parametar u *istaknuti parametar* od c i krivulju $c(u)$ svjetlosna Frenetova krivulja.

Nadalje, svjetlosnu Frenetovu krivulju $c(u)$ za koju vrijedi $\langle \frac{d^2c}{du^2}, \frac{d^2c}{du^2}\rangle > 0$ (pa vrijedi i uvjet $k_2 \neq 0$) mažemo reparametrizirati $u = u(s)$ tako da vrijedi $\langle c_{ss}, c_{ss}\rangle = 1$. Stoga, za trobrid (A,B,C) pridružen krivulji $c(s)$ vrijedi

$$A = c_s = \frac{dc}{ds} \quad \text{i} \quad C = c_{ss} = \frac{d^2c}{ds^2}.$$

Parametar s nazivamo *parametar duljine pseudo-luka* ([6, 7]) i trobrid (A,B,C) krivulje $c(s)$ zadovoljava sljedeće Frenetove formule:

$$\begin{pmatrix} A' \\ B' \\ C' \end{pmatrix} = \begin{pmatrix} 0 & 0 & 1 \\ 0 & 0 & k_L \\ -k_L & -1 & 0 \end{pmatrix} \begin{pmatrix} A \\ B \\ C \end{pmatrix}.$$

Funkciju $k_L = \langle B', C\rangle = -\langle C', B\rangle$ zovemo *svjetlosna zakrivljenost* od $c(s)$, B binormalni vektor i C glavna normala krivulje $c(s)$ ([7]). Ako je $k_2 = 0$, tada krivulju ne možemo reparametrizirati na opisani način. Neki autori poput ([9]) koriste drugačije definicije i oznake ((T,N,B) za svjetlosni trobrid i τ za odgovarajuću zakrivljenost koju nazivaju pseudo-torzija).

Primjer 11 *Svjetlosna zavojnica parametrizirana parametrom duljine pseudo-luka,* ([5, 7]), *kongruentna je s jednom od sljedećih krivulja:*

$$c_1(s) = \big(\frac{1}{\sigma^2}\cos(\sigma s), \frac{1}{\sigma^2}\sin(\sigma s), -\frac{s}{\sigma}\big), \qquad k_L = \frac{\sigma^2}{2} > 0$$
$$c_2(s) = \big(-\frac{s}{\sigma}, \frac{1}{\sigma^2}\cosh(\sigma s), \frac{1}{\sigma^2}\sinh(\sigma s)\big), \quad k_L = -\frac{\sigma^2}{2} < 0$$
$$c_3(s) = \big(\frac{s^3}{4} - \frac{s}{3}, \frac{s^2}{2}, \frac{s^3}{4} + \frac{s}{3}\big), \qquad k_L = 0.$$

Krivulju $c_3(s)$ *zovemo svjetlosna kubika (slika 7).*

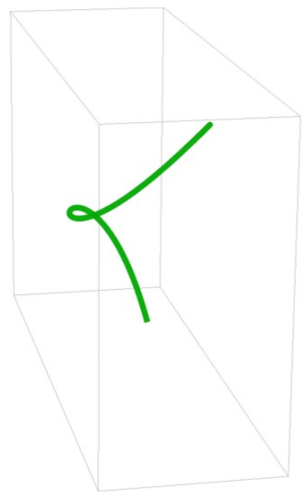

Slika 7: Svjetlosna kubika.

Literatura

[1] Chino, S., Izumiya, S., Lightlike developables in Minkowski 3-space, *Demonstr. Math.* **43**(2) (2010), 387–399, https://doi.org/10.1515/dema-2013-0236

[2] DA SILVA, L.C.B., Moving frames and the characterization of curves that lie on a surface, *J. Geom.* **108** (2017), 1091–1113, https://doi.org/10.1007/s00022-017-0398-7

[3] ĐUZEL, M., *Lokalna teorija krivulja u trodimenzionalnom Minkowskijevom prostoru*, Diplomski rad, Sveučilište Josipa Jurja Strossmayera u Osijeku, Odjel za matematiku, Osijek, 2023.

[4] DUGGAL, K.L., BEJANCU, A., *Lightlike Submanifolds of Semi-Riemannian Manifolds and Applications*, Mathematics and its Applications, Kluwer Academic Publishers, Dordrecht, 1996, https://doi.org/10.1007/978-94-017-2089-2

[5] FERRÁNDEZ, A., GIMÉNEZ, A., LUCAS, P., Null generalized helices in Lorentz-Minkowski spaces, *J. Phys. A: Math. Gen.* **35** (2002), 8243–8251, https://doi.org/10.1088/0305-4470/35/39/308

[6] FERRÁNDEZ, A., GIMÉNEZ, A., LUCAS, P., Null helices in Lorentzian space forms, *Internat. J. Modern Phys. A.* **16** (2001), 4845–4863, https://doi.org/10.1142/S0217751X01005821

[7] INOGUCHI, J., LEE, S., Null curves in Minkowski 3-space, *Int. Electron. J. Geom.* **1** (2008), 40–83.

[8] LIU, H., Curves in the Lightlike Cone, *Beitr. Algebra Geom. [Contributions to Algebra and Geometry]* **45** (2004), 291–303.

[9] LÓPEZ, R., Differential Geometry of Curves and Surfaces in Lorentz-Minkowski space, *Int. Electron. J. Geom.* **7** (2014), 44–107, https://doi.org/10.36890/iejg.594497

[10] LÓPEZ, R., MILIN ŠIPUŠ, Ž., PRIMORAC GAJČIĆ, LJ., PROTRKA, I., Involutes of pseudo-null curves in Lorentz–Minkowski 3-space, *Mathematics* **11**(9) (2021), 41–46, https://doi.org/10.3390/math9111256

[11] MILIN ŠIPUŠ, Ž., PROTRKA, I., PRIMORAC GAJČIĆ, LJ., Generalized Helices on a Lightlike Cone in 3-Dimensional Lorentz-Minkowski Space, *KoG* **24** (2020), 41–46, https://doi.org/10.31896/k.24.4

[12] PROTRKA, I., *Plohe konstantne srednje zakrivljenosti i njima pridružene fokalne krivulje i plohe u Minkowskijevom prostoru*, Disertacija, Sveučilište u Zagrebu, Prirodoslovno-matematički fakultet, Zagreb, 2019.

[13] RATCLIFFE, J.G., *Foundations of Hyperbolic Manifolds*, Springer Science+Business Media, New York, 1994, https://doi.org/10.1007/978-1-4757-4013-4

[14] WALRAVE, J., *Curves and Surfaces in Minkowski Space*, Ph. D. Thesis, K. U. Leuven, Faculteit Der Wetenschappen, 1995.

Monika Đuzel
e-mail: monikadj@outlook.com

Odjel za matematiku, Sveučilište u Osijeku
Trg Ljudevita Gaja 6, HR-31000 Osijek, Hrvatska

Ivana Filipan
orcid.org/0000-0001-6616-3206
e-mail: ivana.filipan@rgn.unizg.hr

Sveučilište u Zagrebu
Rudarsko-geološko-naftni fakultet
Pierottijeva 6, HR-10000 Zagreb, Hrvatska

Ljiljana Primorac Gajčić
orcid.org/0000-0002-8460-3196
e-mail: lprimora@mathos.hr

Fakultet primijenjene matematike i informatike, Sveučilište u Osijeku
Trg Ljudevita Gaja 6, HR-31000 Osijek, Hrvatska

https://doi.org/10.31896/k.27.6
Professional paper
Accepted 29. 11. 2023.

Vladimir Volenec
Ema Jurkin
Marija Šimić Horvath

Circles Related to a Complete Quadrangle

Circles Related to a Complete Quadrangle

ABSTRACT

This paper presents an overview of some properties of a complete quadrangle $ABCD$ in the Euclidean plane. We study the circles with diameters AB, AC, AD, BC, BD, and CD, as well as the pedal triangles and the pedal circles of the points A, B, C, D with respect to the triangles BCD, ACD, ABD and ABC, respectively. The presented results are known in literature, but here we prove them using a single method.

Key words: complete quadrangle, pedal triangles, pedal circles

MSC2020: 51N20

Kružnice pridružene potpunom četverovrhu

SAŽETAK

U radu dajemo pregled nekih svojstava potpunog četverovrha $ABCD$ u euklidskoj ravnini. Proučavamo kružnice s promjerima AB, AC, AD, BC, BD, CD, kao i nožišne trokute i nožišne kružnice točaka A, B, C, D s obzirom na trokute BCD, ACD, ABD, ABC redom navedene. Svi prikazani rezultati su poznati iz literature, ali ih ovdje dokazujemo koristeći istu metodu.

Ključne riječi: potpuni četverovrh, nožišni trokuti, nožišne kružnice

1 Introduction

Studying the geometry of the complete quadrangle in the Euclidean plane, we came across a large number of papers in which the properties of the quadrangle are proven in different ways. Our aim was to prove these claims using one method and, if possible, to prove some original claim. This paper is the third in a series of such works. In [12] we introduced the choice of the suitable coordinate system that enables us to prove all the properties in the same way, while in [13] we focused on the center, anticenter and a diagonal triangle of the quadrangle, as well as on the isogonality with respect to the four triangles formed by the sides of the quadrangle. In this paper we give an overview of some properties of the quadrangle regarding the circles related to it. Let us start by recalling some basic definitions and statements proved in [12] and [13].

The complete quadrangle $ABCD$ is formed by four points A,B,C,D and six lines AB, AC, AD, BC, BD, CD. There we distinguish the opposite sides, ones that have no common vertex. We use rectangular coordinates working with four parameters $a,b,c,d \neq 0$. For such a quadrangle we have proved: each quadrangle with no perpendicular opposite sides has a circumscribed rectangular hyperbola.
Choosing suitable coordinate system we get for the circumscribed hyperbola $\mathcal{H}$

$$xy = 1. \tag{1}$$

The center of this hyperbola is the point O and we will call it the center of the quadrangle $ABCD$. Asymptotes of $\mathcal{H}$ are the axes of the quadrangle $ABCD$.
Vertices of the quadrangle $ABCD$ are

$$A = \left(a, \frac{1}{a}\right), B = \left(b, \frac{1}{b}\right), C = \left(c, \frac{1}{c}\right), D = \left(d, \frac{1}{d}\right), \tag{2}$$

and the sides are

$$\begin{aligned} &AB \ldots x + aby = a + b, \quad AC \ldots x + acy = a + c, \\ &AD \ldots x + ady = a + d, \quad BC \ldots x + bcy = b + c, \\ &BD \ldots x + bdy = b + d, \quad CD \ldots x + cdy = c + d. \end{aligned} \tag{3}$$

Very often we will use elementary symmetric function in four variables a,b,c,d:

$$\begin{aligned} &s = a + b + c + d, \quad q = ab + ac + ad + bc + bd + cd, \\ &r = abc + abd + acd + bcd, \quad p = abcd. \end{aligned} \tag{4}$$

The Euler's circles of the triangles BCD, ACD, ABD, and ABC are given in the next equation on the example of the circle $\mathcal{N}_d$ of the triangle ABC

$$\begin{aligned}\mathcal{N}_d \quad \ldots \quad & 2abc\left(x^2+y^2\right)+[1-abc\,(a+b+c)]\,x \\ & -\left(a^2b^2c^2-ab-ac-bc\right)y=0\end{aligned} \tag{5}$$

with the center

$$N_d=\left(\frac{1}{4}\left(a+b+c-\frac{1}{abc}\right),\frac{1}{4}\left(\frac{1}{a}+\frac{1}{b}+\frac{1}{c}-abc\right)\right). \tag{6}$$

By H_a,H_b,H_c,H_d we denote the orthocenters of the triangles BCD, ACD, ABD, and ABC, respectively. Their forms are

$$\begin{aligned} H_a&=\left(-\frac{1}{bcd},-bcd\right), \qquad H_b=\left(-\frac{1}{acd},-acd\right), \\ H_c&=\left(-\frac{1}{abd},-abd\right), \qquad H_d=\left(-\frac{1}{abc},-abc\right). \end{aligned} \tag{7}$$

The diagonal triangle UVW of the quadrangle $ABCD$ is given by the vertices

$$\begin{aligned} U&=AB\cap CD=\left(\frac{ab(c+d)-cd(a+b)}{ab-cd},\frac{a+b-c-d}{ab-cd}\right), \\ V&=AC\cap BD=\left(\frac{ac(b+d)-bd(a+c)}{ac-bd},\frac{a+c-b-d}{ac-bd}\right), \\ W&=AD\cap BC=\left(\frac{ad(b+c)-bc(a+d)}{ad-bc},\frac{a+d-b-c}{ad-bc}\right), \end{aligned} \tag{8}$$

and the sides are

$$\begin{aligned} &\mathcal{U}=VW\ldots \\ &\quad (a+b-c-d)x+[ab(c+d)-cd(a+b)]y=2(ab-cd), \\ &\mathcal{V}=UW\ldots \\ &\quad (a+c-b-d)x+[ac(b+d)-bd(a+c)]y=2(ac-bd), \\ &\mathcal{W}=UV\ldots \\ &\quad (a+d-b-c)x+[ad(b+c)-bc(a+d)]y=2(ad-bc). \end{aligned} \tag{9}$$

By A',B',C',D' we consider the points isogonal to the points A,B,C,D with respect to the triangles BCD, ACD, ABD, ABC, respectively. E. g.

$$D'=\left(\frac{2d-s}{p-1},\frac{r-2abc}{p-1}\right). \tag{10}$$

And, the following relations are also valid

$$\begin{aligned} AB\cdot CD&=\left|\frac{(a-b)(c-d)}{p}\right|\sqrt{\lambda\lambda'}, \\ AC\cdot BD&=\left|\frac{(a-c)(b-d)}{p}\right|\sqrt{\mu\mu'}, \\ AD\cdot BC&=\left|\frac{(a-d)(b-c)}{p}\right|\sqrt{\nu\nu'}. \end{aligned} \tag{11}$$

where the next notations are used

$$\begin{aligned} &\lambda=a^2b^2+1, \quad \mu=a^2c^2+1, \quad \nu=a^2d^2+1, \\ &\lambda'=c^2d^2+1, \quad \mu'=b^2d^2+1, \quad \nu'=b^2c^2+1. \end{aligned} \tag{12}$$

The circumscribed circles of the triangles BCD, ACD, ABD, ABC are given by

$$\begin{aligned} \mathcal{K}_a \quad \ldots \quad & bcd\left(x^2+y^2\right)-[1+bcd\,(b+c+d)]\,x \\ & -\left(b^2c^2d^2+bc+bd+cd\right)y \\ & +b+c+d+bcd\,(bc+bd+cd)=0, \\ \mathcal{K}_b \quad \ldots \quad & acd\left(x^2+y^2\right)-[1+acd\,(a+c+d)]\,x \\ & -\left(a^2c^2d^2+ac+ad+cd\right)y \\ & +a+c+d+acd\,(ac+ad+cd)=0, \\ \mathcal{K}_c \quad \ldots \quad & abd\left(x^2+y^2\right)-[1+abd\,(a+b+d)]\,x \\ & -\left(a^2b^2d^2+ab+ad+bd\right)y \\ & +a+b+d+abd\,(ab+ad+bd)=0, \\ \mathcal{K}_d \quad \ldots \quad & abc\left(x^2+y^2\right)-[1+abc\,(a+b+c)]\,x \\ & -\left(a^2b^2c^2+ab+ac+bc\right)y \\ & +a+b+c+abc\,(ab+ac+bc)=0 \end{aligned}$$

with the centers

$$\begin{aligned} O_a&=\left(\frac{1}{2}\left(b+c+d+\frac{1}{bcd}\right),\frac{1}{2}\left(\frac{1}{b}+\frac{1}{c}+\frac{1}{d}+bcd\right)\right), \\ O_b&=\left(\frac{1}{2}\left(a+c+d+\frac{1}{acd}\right),\frac{1}{2}\left(\frac{1}{a}+\frac{1}{c}+\frac{1}{d}+acd\right)\right), \\ O_c&=\left(\frac{1}{2}\left(a+b+d+\frac{1}{abd}\right),\frac{1}{2}\left(\frac{1}{a}+\frac{1}{b}+\frac{1}{d}+abd\right)\right), \\ O_d&=\left(\frac{1}{2}\left(a+b+c+\frac{1}{abc}\right),\frac{1}{2}\left(\frac{1}{a}+\frac{1}{b}+\frac{1}{c}+abc\right)\right) \end{aligned}$$

and the radii

$$\begin{aligned} \rho_a&=\frac{1}{2}\left|\frac{a}{p}\right|\sqrt{\lambda'\mu'\nu'}, \quad \rho_b=\frac{1}{2}\left|\frac{b}{p}\right|\sqrt{\lambda'\mu\nu}, \\ \rho_c&=\frac{1}{2}\left|\frac{c}{p}\right|\sqrt{\lambda\mu'\nu}, \quad \rho_d=\frac{1}{2}\left|\frac{d}{p}\right|\sqrt{\lambda\mu\nu'}, \end{aligned} \tag{13}$$

respectively.

It would be important the following formula for two lines $\mathcal{L}$ and $\mathcal{L}'$ with slopes $\frac{m}{n}$ and $\frac{m'}{n'}$ and their oriented angle $\angle(\mathcal{L},\mathcal{L}')$

$$tg\angle(\mathcal{L},\mathcal{L}')=\frac{m'n-mn'}{mm'+nn'}. \tag{14}$$

2 Circles with diameters AB, AC, AD, BC, BD, CD and few more circles

The points $P_1 = (x_1, y_1)$ and $P_2 = (x_2, y_2)$ are incident to the circle with the equation

$$x^2 + y^2 - (x_1 + x_2)x - (y_1 + y_2)y + x_1x_2 + y_1y_2 = 0 \qquad (15)$$

with the center in the midpoint $(\frac{1}{2}(x_1 + x_2), \frac{1}{2}(y_1 + y_2))$ of these points, so (15) is the equation of the circle with the diameter P_1P_2. Using this formula, for the circle with diameter AB we get the equation

$$x^2 + y^2 - (a+b)x - \frac{a+b}{ab}y + ab + \frac{1}{ab} = 0$$

so the power p_{AB} of the point $P = (x, y)$ with respect to that circle is

$$p_{AB} = x^2 + y^2 - (a+b)x - \frac{a+b}{ab}y + ab + \frac{1}{ab}.$$

Analogously, the power p_{CD} of the point P with respect to the circle with the diameter CD equals

$$p_{CD} = x^2 + y^2 - (c+d)x - \frac{c+d}{cd}y + cd + \frac{1}{cd},$$

so it follows

$$p_{AB} + p_{CD} = 2x^2 + 2y^2 - sx - \frac{r}{p}y + ab + cd + \frac{ab+cd}{p}.$$

For the power of the point P with respect to the circles with diameters AC, BD and AD, BC the following equalities are valid

$$p_{AC} + p_{BD} = 2x^2 + 2y^2 - sx - \frac{r}{p}y + ac + bd + \frac{ac+bd}{p},$$
$$p_{AD} + p_{BC} = 2x^2 + 2y^2 - sx - \frac{r}{p}y + ad + bc + \frac{ad+bc}{p}.$$

The midpoints of the sides AB and CD are points $(\frac{a+b}{2}, \frac{a+b}{2ab})$, $(\frac{c+d}{2}, \frac{c+d}{2cd})$, and a power p_u of the point P with respect to the circle whose the diameter is connecting line of these two midpoints, is equal to

$$p_u = x^2 + y^2 - \frac{s}{2}x - \frac{r}{2p}y + \frac{1}{4}(a+b)(c+d) + \frac{1}{4p}(a+b)(c+d).$$

Two more equalities are valid

$$p_v = x^2 + y^2 - \frac{s}{2}x - \frac{r}{2p}y + \frac{1}{4}(a+c)(b+d) + \frac{1}{4p}(a+c)(b+d),$$
$$p_w = x^2 + y^2 - \frac{s}{2}x - \frac{r}{2p}y + \frac{1}{4}(a+d)(b+c) + \frac{1}{4p}(a+d)(b+c)$$

for the powers of the point P with respect to the circles, for which the diameters are connecting lines of the midpoints of the sides AC, BD and AD, BC. Out of these equalities the following statement is valid

Theorem 1 *The powers of the point P with respect to the circles, for which the diameters are connecting lines of the midpoints of the sides AB, CD; AC, BD and AD, BC fulfil*

$$p_{AB} + p_{CD} + p_{AC} + p_{BD} = 4p_w,$$
$$p_{AB} + p_{CD} + p_{AD} + p_{BC} = 4p_v,$$
$$p_{AC} + p_{BD} + p_{AD} + p_{BC} = 4p_u$$

and

$$p_{AB} + p_{CD} + p_{AC} + p_{BD} + p_{AD} + p_{BC} = 2(p_u + p_v + p_w),$$

where p_u, p_v, p_w are powers of the point P with respect to the circle whose the diameter is connecting line of the midpoints of AB, CD; AC, BD and AD, BC.

The first three equalities can be found in [4], and the last equality is in [11].
Let $\mathcal{L}$ be the line with the equation $fx + gy + h = 0$. Its intersection points with lines AB and CD from (3) are points $P_{AB} = (u_1, v_1)$ and $P_{CD} = (u_2, v_2)$, where

$$u_1 = -\frac{ag + bg + abh}{abf - g}, v_1 = \frac{af + bf + h}{abf - g},$$
$$u_2 = -\frac{cg + dg + cdh}{cdf - g}, v_2 = \frac{cf + df + h}{cdf - g}.$$

As $(abf - g)(cdf - g) = pf^2 - (ab+cd)fg + g^2$, and

$$(abf - g)(cdf - g)(u_1 + u_2) =$$
$$= (ab+cd)gh + sg^2 - rfg - 2pfh,$$
$$(abf - g)(cdf - g)(v_1 + v_2) =$$
$$= (ab+cd)fh + rf^2 - sfg - 2gh,$$
$$(abf - g)(cdf - g)(uu' + vv') =$$
$$= ph^2 + rgh + (q - ab - cd)(f^2 + g^2) + sfh + h^2,$$

then the circle $\mathcal{K}_{AB,CD}$ with the diameter $P_{AB}P_{CD}$ has the equation

$$\begin{aligned}&[pf^2 - (ab+cd)fg + g^2](x^2 + y^2)\\ &\quad - [(ab+cd)gh + sg^2 - rfg - 2pfh]x\\ &\quad - [(ab+cd)fh + rf^2 - sfg - 2gh]y + ph^2 + rgh\\ &\quad + (q - ab - cd)(f^2 + g^2) + sfh + h^2 = 0.\end{aligned}$$

Analogously, the circle $\mathcal{K}_{AC,BD}$ with the diameter $P_{AC}P_{BD}$ has the equation

$$\begin{aligned}&[pf^2 - (ac+bd)fg + g^2](x^2 + y^2)\\ &\quad - [(ac+bd)gh + sg^2 - rfg - 2pfh]x\\ &\quad - [(ac+bd)fh + rf^2 - sfg - 2gh]y\\ &\quad + ph^2 + rgh + (q - ac - bd)(f^2 + g^2) + sfh + h^2 = 0.\end{aligned}$$

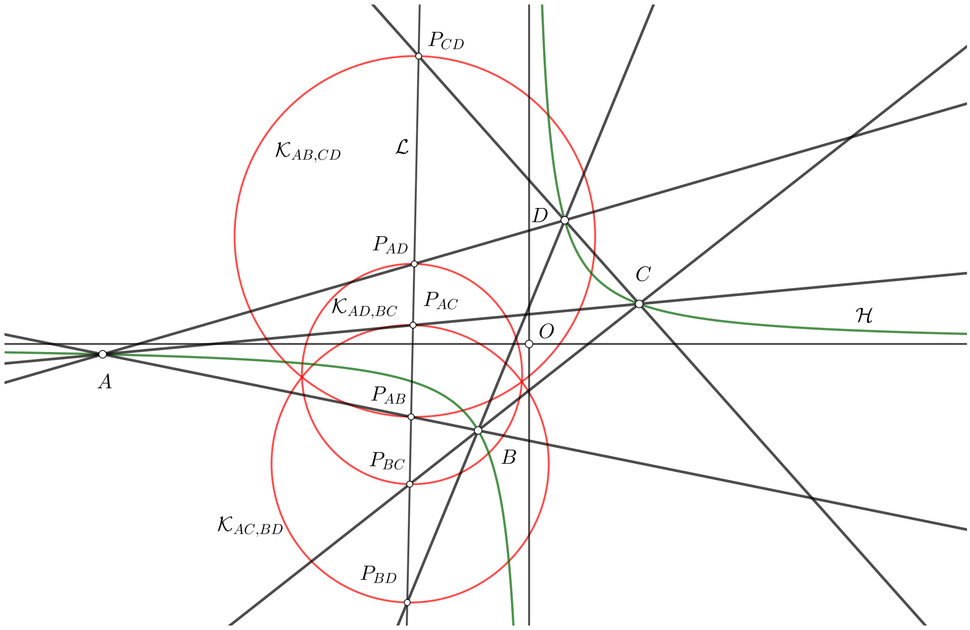

Figure 1: *Visualization of Theorem 2.*

Subtracting these two equations and dividing the obtained result by the common factor $(a-d)(b-c)$ we get the equation of a circle $\mathcal{K}$ in the form

$$fg(x^2+y^2)+ghx+fhy+f^2+g^2=0.$$

Hence, the circles $\mathcal{K}_{AB,CD}$, $\mathcal{K}_{AC,BD}$, $\mathcal{K}$ belong to the same pencil of circles. However, out of symmetry of the circle $\mathcal{K}$ on a,b,c,d we conclude that $\mathcal{K}_{AB,CD}$, $\mathcal{K}_{AD,BC}$, $\mathcal{K}$ belong to one pencil of circles. Hence,

Theorem 2 *Let $\mathcal{L}$ be a line. Three circles with diameters $P_{AB}P_{CD}$, $P_{AC}P_{BD}$, $P_{AD}P_{BC}$ belong to one pencil of circles, where $P_{AB},P_{CD},P_{AC},P_{BD},P_{AD},P_{BC}$ are intersection points of the line $\mathcal{L}$ with lines AB,CD,AC,BD,AD,BC.*

This result can be found in [7], [9] and [10]. See Figure 1.

3 Pedal triangles and pedal circles of the points A,B,C,D with respect to the triangles BCD, ACD, ABD, ABC

A normal from the point $A=(a,\frac{1}{a})$ to the line BC with equation $x+bcy=b+c$ has the equation $bcx-y=abc-\frac{1}{a}$, and these two lines are intersected in the point

$$A_d=\left(\frac{1}{a\nu'}(a^2b^2c^2+ab+ac-bc),\frac{1}{a\nu'}(ab^2c+abc^2-a^2bc+1)\right), \tag{16}$$

and, analogously, the pedal of the normal from A to the line BD is the point

$$A_c=\left(\frac{1}{a\mu'}(a^2b^2d^2+ab+ad-bd),\frac{1}{a\mu'}(ab^2d+abd^2-a^2bd+1)\right). \tag{17}$$

Because of that,

$$a^2\mu'^2\nu'^2 A_cA_d{}^2 =$$
$$=[\mu'(a^2b^2c^2+ab+ac-bc)-\nu'(a^2b^2d^2+ab+ad-bd)]^2$$
$$+[\mu'(ab^2c+abc^2-a^2bc+1)-\nu'(ab^2d+abd^2-a^2bd+1)]^2.$$

It is easy to see

$$(b^2d^2+1)(a^2b^2c^2+ab+ac-bc)$$
$$-(b^2c^2+1)(a^2b^2d^2+ab+ad-bd)]^2=$$
$$=(a-b)(c-d)(ab^2c+ab^2d-b^2cd+1),$$
$$(b^2d^2+1)(ab^2c+abc^2-a^2bc+1)$$
$$-(b^2c^2+1)(ab^2d+abd^2-a^2bd+1)=$$
$$=(a-b)(c-d)(ab^3cd-ab+bc+bd),$$
$$(ab^2c+ab^2d-b^2cd+1)^2+(ab^3cd-ab+bc+bd)^2=$$
$$=(a^2b^2+1)(b^2c^2+1)(b^2d^2+1)=\lambda\mu'\nu',$$

so $a^2\mu'^2\nu'^2A_cA_d{}^2=(a-b)^2(c-d)^2\lambda\mu'\nu'$ or, finally, $a^2\mu'\nu'A_cA_d{}^2=(a-b)^2(c-d)^2\lambda$. We proved the first of three analogous formulae

$$\begin{aligned} A_cA_d &= \left|\frac{(a-b)(c-d)}{a}\right|\sqrt{\frac{\lambda}{\mu'\nu'}}, \\ A_bA_d &= \left|\frac{(a-c)(b-d)}{a}\right|\sqrt{\frac{\mu}{\lambda'\nu'}}, \qquad (18) \\ A_bA_c &= \left|\frac{(a-d)(b-c)}{a}\right|\sqrt{\frac{\nu}{\lambda'\mu'}} \end{aligned}$$

for the lengths of the sides of the pedal triangle $A_bA_cA_d$ of the point A with respect to the triangle BCD. Analogous formulae for the lengths of the pedal triangle $B_aB_cB_d$ of the point B with respect to the triangle ACD are

$$\begin{aligned} B_cB_d &= \left|\frac{(a-b)(c-d)}{b}\right|\sqrt{\frac{\lambda}{\mu\nu}}, \\ B_aB_c &= \left|\frac{(a-c)(b-d)}{b}\right|\sqrt{\frac{\mu'}{\lambda'\nu}}, \\ B_aB_d &= \left|\frac{(a-d)(b-c)}{b}\right|\sqrt{\frac{\nu'}{\lambda'\mu}} \end{aligned}$$

Formulae for the lengths of the sides of the pedal triangles $C_aC_bC_d$ and $D_aD_bD_c$ of the points C and D with respect to the triangles ABD and ABC look similarly. Out of previously mentioned formulae

$$A_cA_d : B_cB_d = A_bA_d : B_aB_c = A_bA_c : B_aB_d = \left|\frac{b}{a}\right|\sqrt{\frac{\mu\nu}{\mu'\nu'}}$$

follow, meaning that triangles $A_bA_cA_d$ and $B_aB_dB_c$ are similar. Due to analogy, the triangles $C_dC_aC_b$ and $D_cD_bD_a$ are also similar to these triangles. So, we proved the result that can be found in [2], [3] and [6].

Theorem 3 *The pedal triangles of the points A,B,C,D with respect to the triangles BCD,ACD,ABD,ABC, respectively, are similar.*

Out of the corresponding equalities (11) and (18) we get the ratios

$$\begin{aligned} &AB\cdot CD : A_cA_d = AC\cdot BD : A_bA_d = AD\cdot BC : A_bA_c = \\ &= \sqrt{\lambda'\mu'\nu'} : |bcd| \end{aligned}$$

i.e.

Theorem 4 *The lengths of sides of the pedal triangles of $A_bA_cA_d$, $B_aB_cB_d$, $C_aC_bC_d$, $D_aD_bD_c$ are related as the products of the lengths of pairs of opposite sides of the quadrangle ABCD.*

The last ratio equals to $2\rho_a$ because of (13). These statements can be found in [6].
The point A_d from (16) is incident to the circle $\mathcal{P}_a$ with the equation

$$a(p-1)(x^2+y^2) - a\,[a(p+1)-s]\,x + (p+1-ar)y = 0$$

i.e.

$$(p-1)(x^2+y^2) - [a\,(p+1)-s]\,x + \left(\frac{p+1}{a} - r\right)y = 0 \qquad (19)$$

because of

$$\begin{aligned} &(p-1)[(a^2b^2c^2+ab+ac-bc)^2+(ab^2c+abc^2-a^2bc+1)^2]- \\ &-a(b^2c^2+1)(a^2b^2c^2+ab+ac-bc)(a(p+1)-s)+ \\ &+(b^2c^2+1)(ab^2c+abc^2-a^2bc+1)(p+1-ar)=0. \end{aligned}$$

Because of symmetry on b,c,d, of the equation (19) the circle $\mathcal{P}_a$ is a pedal circle of A with respect to the triangle BCD. Obviously, it is incident to the center O. Hence,

Theorem 5 *The pedal circles $\mathcal{P}_a,\mathcal{P}_b,\mathcal{P}_c,\mathcal{P}_d$ of the points A, B, C, D with respect to the triangles BCD, ACD, ABD, ABC, respectively are incident to the center O of the quadrangle ABCD.*

This result can be found in [1], [2], [5], [6].
The circle (19) has the center

$$\begin{aligned} P_a = \Big(&\frac{1}{2(p-1)}(a^2bcd-b-c-d), \\ &\frac{1}{2(p-1)}(abc+abd+acd-\frac{1}{a})\Big) \qquad (20) \end{aligned}$$

and the length OP_a is the radius r_a of that circle and easily we get

$$\begin{aligned} r_a &= \frac{1}{2|a(p-1)|}\sqrt{(a^2b^2+1)(a^2c^2+1)(a^2d^2+1)} = \\ &= \frac{1}{2|a(p-1)|}\sqrt{\lambda\mu\nu}, \end{aligned}$$

together with the first equality from (13) it proves the equality $\rho_a r_a = \frac{1}{4|p(p-1)|}\sqrt{\lambda\mu\nu\lambda'\mu'\nu'}$. This equality together with three analogous equalities prove that $\rho_a r_a = \rho_b r_b = \rho_c r_c = \rho_d r_d$, i.e.

Theorem 6 *The radii of the pedal circles $\mathcal{P}_a,\mathcal{P}_b,\mathcal{P}_c,\mathcal{P}_d$ of the points A, B, C, D with respect to the triangles BCD,ACD,ABD,ABC respectively, are inversely proportional to the radii of the circles BCD,ACD,ABD,ABC.*

This result can be reached in [6] and [8].
The point P_a from (20) is the midpoint of the point A and the point A' analogous to the point D' from (10), that is in accordance with the fact that the pedal circle of the point with respect to the triangle has the center in the midpoint of that point and its isogonal point with respect to this triangle. The ratio of the radii $r_a = \frac{1}{2|a(p-1)|}\sqrt{\lambda\mu\nu}$ and $r_b = \frac{1}{2|b(p-1)|}\sqrt{\lambda\mu'\nu'}$ is equal to the coefficient $|\frac{b}{a}|\sqrt{\frac{\mu\nu}{\mu'\nu'}}$ of the similarity of the triangles $A_bA_cA_d$ and $B_aB_dB_c$.

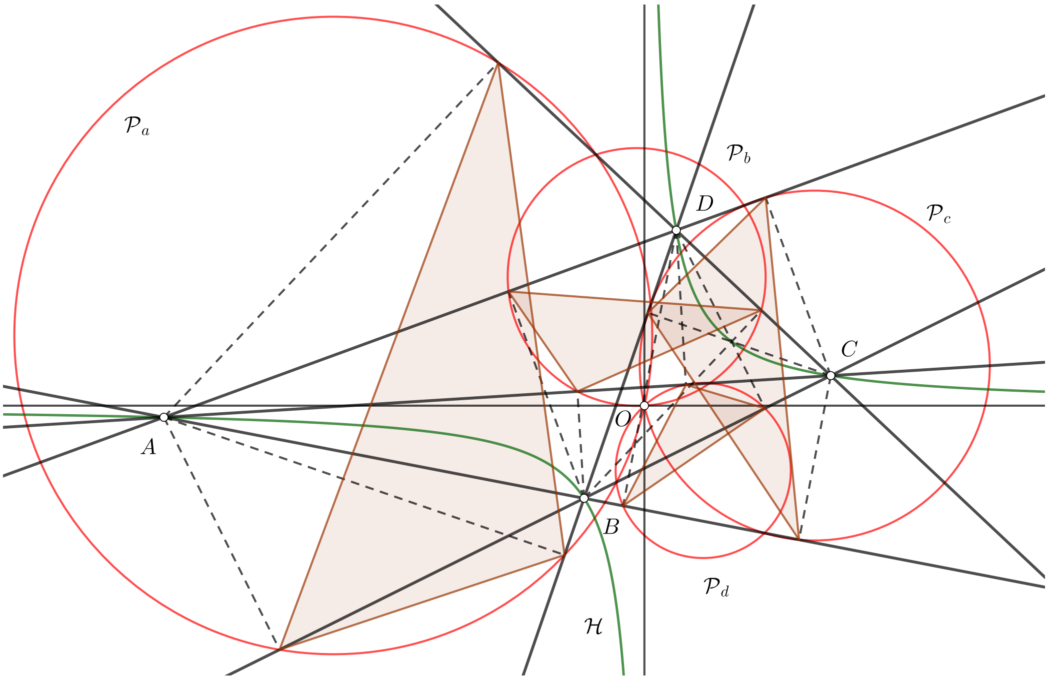

Figure 2: *Visualization of Theorem 5.*

The points A' and B' analogous to D' from (10) have the midpoint

$$M_{ab} = \left(-\frac{c+d}{p-1}, ab\frac{c+d}{p-1}\right), \tag{21}$$

that is incident to the circle $\mathcal{P}_a$ with the equation (19). Taking the analogous results in consideration, we proved

Theorem 7 *The midpoints of the triples of segments $A'B', A'C', A'D'$; $A'B', B'C', B'D'$; $A'C', B'C', C'D'$; $A'D', B'D', C'D'$ are incident to the pedal circles $\mathcal{P}_a, \mathcal{P}_b, \mathcal{P}_c, \mathcal{P}_d$ of points A, B, C, D with respect to the triangles BCD, ACD, ABD, ABC, respectively.*

This result can be reached in [1].

The point A_c from (17) is incident to the line with equation

$$(a^2bd+abd^2-ab^2d+1)x+(a^2b^2d^2+ab+bd-ad)y = \\ = 2b(a^2d^2+1),$$

and the point D_c is also incident to this line because of symmetry of this equation on a and d. We conclude that this is the line A_cD_c. It is incident to the point

$$\Big(-\frac{2b}{(p-1)\lambda}(a^2bc+a^2bd-a^2cd+1), \\ \frac{2b}{(p-1)\lambda}(a^3bcd+ac+ad-ab)\Big) \tag{22}$$

as well. Because the symmetry on c and d in the form of this point, obviously it lies on the line A_dC_d, hence this point is $A_cD_c \cap A_dC_d$.

The point

$$C_d = \left(\frac{1}{c\lambda}(a^2b^2c^2+ac+bc-ab), \frac{1}{c\lambda}(a^2bc+ab^2c-abc^2+1)\right)$$

is analogous to A_d from (16). It is incident to the line

$$c(a^3bcd+ab+ad-ac)x-c(a^2bc+a^2cd-a^2bd+1)y = \\ = (p-1)(a^2c^2+1),$$

and again because of symmetry on b and d, C_b is incident to it as well, so it is the line C_dC_b. This line is incident to the point

$$\Big(\frac{p-1}{2acd\lambda}(a^2bc+a^2bd-a^2cd+1), \\ -\frac{p-1}{2acd\lambda}(a^3bcd+ac+ad-ab)\Big),$$

and that point lies on the line D_cD_b because of the symmetry on c and d in the form of this point. Hence, this point is $C_dC_b \cap D_bD_c$. The obtained points $A_cD_c \cap A_dC_d$ and $C_dC_b \cap D_bD_c$ have the proportional coordinates. Homothety with the center O and coefficient $-\frac{1}{4p}(p-1)^2$ associates one point to another. As this coefficient is symmetric on parameters a,b,c,d then by cyclic permutation of b,c,d and B,C,D it follows that the same homothety associates the point $A_dB_d \cap A_bD_b$ to the point $D_bD_c \cap B_cB_d$, and the point $A_bC_b \cap A_cB_c$ to the point $B_cB_d \cap C_dC_b$, i.e. the mentioned homothety associates the triangle with vertices $A_cD_c \cap A_dC_d$, $A_dB_d \cap A_bD_b$, $A_bC_b \cap A_cB_c$ to the triangle formed by lines B_cB_d, C_dC_b, D_bD_c. It can be checked the following theorem and also three more analogous statements

Theorem 8 *Let A_b, A_c, A_d be pedal points and $\mathcal{P}_a$ pedal circle of A with respect to the triangle BCD. Let B_a, B_c, B_d, C_a, C_b, C_d, D_a, D_b, D_c be pedal points of B, C, D with respect to the triangle ACD, ABD, ABC, respectively. The points $A_cD_c \cap A_dC_d$, $A_dB_d \cap A_bD_b$ and $A_bC_b \cap A_cB_c$ are incident to $\mathcal{P}_a$.*

Because of the mentioned homothety, there is and the next result

Theorem 9 *The triangle formed by lines B_cB_d, C_dC_b, D_bD_c is inscribed to the circle that passes through the center O and at that point touches the circle $\mathcal{P}_a$.*

All of these results can be found in [1] and they are associated to Q.T. Bui.
In [1] the center of the quadrangle $ABCD'$ is studied as well. From Theorem 1 from [13] and Theorem 5 we know that the center O of the quadrangle $ABCD$ is incident to the Euler's circle $\mathcal{N}_d$ of the triangle ABC and to the pedal circle $\mathcal{P}_d$ of the point D with respect to that same triangle. So the center of the quadrangle $ABCD'$ is incident to the Euler's circle $\mathcal{N}_d$ of the triangle ABC and to the pedal circle of the point D' with respect to that triangle. The latter circle is the circle $\mathcal{P}_d$ because the isogonal points in the triangle have the same pedal circle. There is a question appearing: Is this center the center of the quadrangle O or the other intersection point of the circles $\mathcal{N}_d$ and $\mathcal{P}_d$? In the first case the point D' would lie on the hyperbola $\mathcal{H}$ and that is possible, but if it would be always like that then the same it should be valid for the points B', C' and D'. The point D' is incident to the hyperbola $\mathcal{H}$ under the condition that the equality $(d-a-b-c)(abd+acd+bcd-abc) = (p-1)^2$ is valid. The conditions for the points B', C' and D' look similarly. However, adding up these four conditions we get the equality $-16p = 4(p-1)^2 = 0$ i. e. $p = -1$ and the quadrangle $ABCD$ is the orthocentric. If we exclude this case, then we get the following statement.

Theorem 10 *The center of the quadrangle $ABCD'$ is the second intersection point of the circles $\mathcal{N}_d$ and $\mathcal{P}_d$ next to the center O.*

Three more analogous statements follow up.
The circle $\mathcal{P}_a$ with the equation (19) and the circle $\mathcal{P}_b$ with analogous equation

$$(p-1)(x^2+y^2) - [b(p+1)-s]x + \left(\frac{p+1}{b} - r\right)y = 0$$

have the radical axis with the equation $abx + y = 0$. The midpoint of the point C and the point H_d from (7) is the point $(\frac{1}{2}(c - \frac{1}{abc}), \frac{1}{2}(\frac{1}{c} - abc))$ and it is incident to the radical axis. The same is valid and for the midpoint of points D and H_c. Points C and H_c are incident to the line $abdx - cy = p - 1$ that passes through the point $(\frac{p-1}{ab(c+d)}, -\frac{p-1}{c+d})$. Because of symmetry on c and d, this point is also incident to DH_d. However, the intersection point $CH_c \cap DH_d$ is lying on the mentioned radical axis, see Figure 3. This result can be reached in [6] and [8]. The point M_{ab} from (21) is also incident to the mentioned radical axis with the equation $abx + y = 0$. The statement on the collinearity of these four points as well as five more such collinearities is given in [1]. Hence, the radical axis of the circles $\mathcal{P}_a$ and $\mathcal{P}_b$ bisects the segments CH_d, DH_c and $A'B'$. That radical axis is antiparallel to the line AB with respect the axes of the hyperbola $\mathcal{H}$, and the similar is valid for five more analogous radical axes. We have just proved the following theorem and five more analogous statements

Theorem 11 *Let H_c, H_d be orthocenters of ABD, ABC, respectively, and let A', B' be isogonal points of A, B and with respect to BCD, ACD respectively, and $\mathcal{P}_a, \mathcal{P}_b$ pedal circles of the points A, B with respect to the triangles BCD, ACD. Then the following four points lie on the radical axis of $\mathcal{P}_a$ and $\mathcal{P}_b$: midpoints of three segments $A'B'$, DH_c, CH_d and the intersection point $CH_c \cap DH_d$.*

The point M_{ab} obviously lies on the line CD as well as the points A_b and B_a. It is easy to check that the point M_{ab} is incident to the line

$$\begin{aligned}(a^2bc + ab^2d - abcd + 1)x + (a^2b^2cd + ac + bd - ab)y = \\ = (a^2b^2+1)(c+d),\end{aligned}$$

as well as the point A_c from (17). By substituting $a \leftrightarrow b$ and $c \leftrightarrow d$ in the previous equation one obtains the line incident to the point B_d. Hence, the point M_{ab} is incident to the line A_cB_d, and analogously to the line A_dB_c. It means that the point M_{ab} is the center of the perspectivity for triangles $A_bA_cA_d$ and $B_aB_cB_d$. Out of (17) it follows that the line OA_c has the slope

$$\frac{m'}{n'} = \frac{ab^2d + abd^2 - a^2bd + 1}{a^2b^2d^2 + ab + ad - bd},$$

and, analogously, the line OA_b has the slope

$$\frac{m}{n} = \frac{ac^2d + acd^2 - a^2cd + 1}{a^2c^2d^2 + ac + ad - cd}.$$

After some calculation we get

$$\begin{aligned}m'n - mn' &= (a^2d^2+1)(a-d)(b-c)(p-1),\\ mm' + nn' &= (a^2d^2+1)[(p-1)^2 + ad(b^2+c^2) + bc(a^2+d^2)],\end{aligned}$$

so due to (14) it follows

$$tg\angle A_bOA_c = \frac{(a-d)(b-c)(p-1)}{(p-1)^2 + ad(b^2+c^2) + bc(a^2+d^2)}.$$

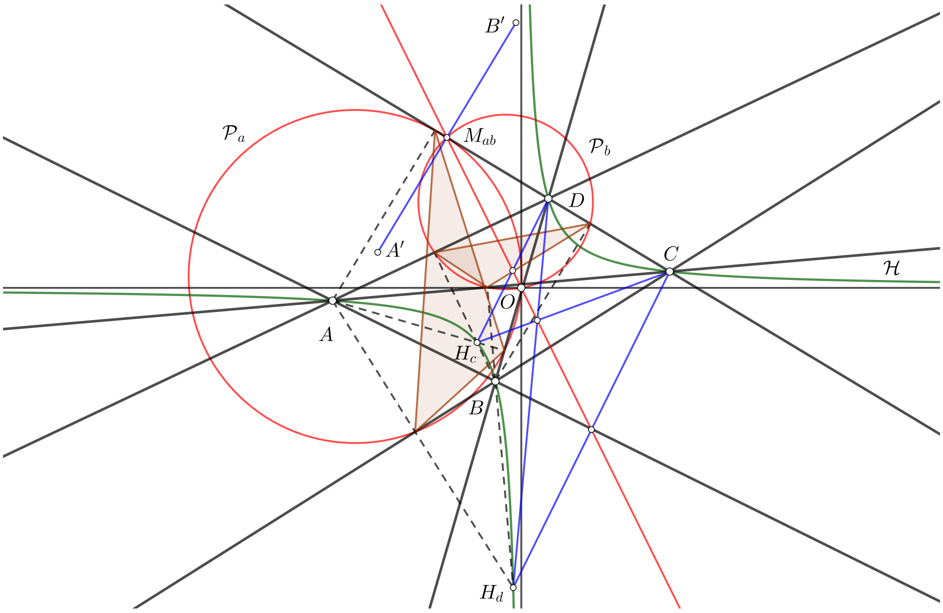

Figure 3: *Visualization of Theorem 11*

Substituting $a \leftrightarrow b$ and $c \leftrightarrow d$ the equality

$$tg\angle B_aOB_d = \frac{(a-d)(b-c)(p-1)}{(p-1)^2+ad(b^2+c^2)+bc(a^2+d^2)}$$

follows up. By this we achieved the equality of the oriented angles $\angle A_bOA_c = \angle B_aOB_d$, as well as $\angle A_bOA_d = \angle B_aOB_c$. However, out of these equalities the equality $\angle A_bOB_a = \angle A_cOB_d = \angle A_dOB_c$ is valid meaning that the center O is the center of the similarity of triangles $A_bA_cA_d$ and $B_aB_dB_c$. So, we have just proved the following result and five more analogous results that can be found in [6]:

Theorem 12 *The triangles $A_bA_cA_d$ and $B_aB_dB_c$ are similar and perspective where the center of the similarity is the center O, one intersection point of the circles $A_bA_cA_d$ and $B_aB_dB_c$, and the center of the perspectivity is their other intersection point M_{ab}.*

For the oriented segments $\overrightarrow{AB}$ and $\overrightarrow{P_aP_b}$ the following equalities are valid

$$\overrightarrow{AB} = \left(b-a, \frac{1}{b}-\frac{1}{a}\right) = \frac{b-a}{ab}(ab,-1),$$

$$\overrightarrow{P_aP_b} = \frac{1}{2(p-1)}\left(ab^2cd-a-a^2bcd+b, bcd-\frac{1}{b}-acd+\frac{1}{a}\right)$$
$$= \frac{(b-a)(p+1)}{2ab(p-1)}(ab,1).$$

As the vectors $[ab,-1]$ and $[ab,1]$ have the same square of the lengths equals to a^2b^2+1, then from previous mentioned two equalities it follows that the ratio of the lengths P_aP_b and AB equals to $\frac{p+1}{2(p-1)}$, the same is valid for the rest of the corresponding sides of $ABCD$ and $P_aP_bP_cP_d$. So, we can conclude

Theorem 13 *The quadrangles $ABCD$ and $P_aP_bP_cP_d$ are similar and the coefficient of the similarity is $\frac{p+1}{2(p-1)}$.*

This result can be reached in [8].

References

[1] Ayme, J.L., Le point d'Euler-Poncelet d'un quadrilatère, `jl.ayme.pagesperso-orange.fr`, *Geometry* **8** (2010), 133.

[2] Forder, H.G., Illustrations in the use of crosses, Note 2126, *Math. Gaz.* **34** (1950), 62–65.

[3] Ladd, C., Question 4335, *Educ. Times* **21** (1874), 62.

[4] Laisant, A., Question 1202, *Nouv. Ann. Math.* **15**(2) (1876), 191., solution par Paul et Maréchal, 286–287.

[5] Lawlor, J.H., Pedal circles, *Math. Gaz.* **9** (1917), 127–130.

[6] Lawlor, J.H., Some propositions relative to a tetrastigm, *Math. Gaz.* **10** (1920), 135–139.

[7] Lorieux, É. , Théorème proposé au concours général de 1849, *Nouv. Ann. Math.* **8** (1849), 369–376.

[8] MALLISON, H.V., Pedal circles and the quadrangle, *Math. Gaz.* **42** (1958), 17–20.

[9] NÉVROUZIAN, A., Démonstration du théorème donné au concours de mathématiques élémentaires en 1849, *Nouv. Ann. Math.* **11** (1852), 49–52.

[10] S., Solution de la question de géométrie proposée en mathématiques élémentaires, au concours général de 1849, *Nouv. Ann. Math.* **8** (1849), 401–408.

[11] TERRIER, P., Note sur la question 1202, *Nouv. Ann. Math.* **15**(2) (1876), 287.

[12] VOLENEC, V., JURKIN, E., ŠIMIĆ HORVATH, M., On Quadruples of Orthopoles, *J. Geom.* **114** (2023), 29, https://doi.org/10.1007/s00022-023-00692-4

[13] VOLENEC, V., ŠIMIĆ HORVATH, M., JURKIN, E., On some properties of a complete quadrangle, *AppliedMath*, submitted

Vladimir Volenec
orcid.org/0000-0001-7418-8972
e-mail: volenec@math.hr

University of Zagreb Faculty of Science
Bijenička cesta 30, HR-10000 Zagreb, Croatia

Ema Jurkin
orcid.org/0000-0002-8658-5446
e-mail: ema.jurkin@rgn.unizg.hr

University of Zagreb
Faculty of Mining, Geology and Petroleum Engineering
Pierottijeva 6, HR-10000 Zagreb, Croatia

Marija Šimić Horvath
orcid.org/0000-0001-9190-5371
e-mail: marija.simic@arhitekt.unizg.hr

University of Zagreb Faculty of Architecture
Kačićeva 26, HR-10000 Zagreb, Croatia

INSTRUCTIONS FOR AUTHORS

SCOPE. "KoG" publishes scientific and professional papers from the fields of geometry, applied geometry and computer graphics.

SUBMISSION. Scientific papers submitted to this journal should be written in English, professional papers should be written in Croatian or English. The papers have not been published or submitted for publication elsewhere.
The manuscript should be sent in PDF format via e-mail to the editor:

Ema Jurkin
ema.jurkin@rgn.unizg.hr

The first page should contain the article title, author and coauthor names, affiliation, a short abstract in English, a list of keywords and the Mathematical subject classification.

UPON ACCEPTANCE. After the manuscript has been accepted for publication authors are requested to send its LaTex file via e-mail to the address:

ema.jurkin@rgn.unizg.hr

Figures should be titled by the figure number that match to the figure number in the text of the paper.

The corresponding author and coauthors will receive hard copies of the issue free of charge.

How to get KoG?

The easiest way to get your copy of KoG is by contacting the editor's office:

Marija Šimić Horvath
marija.simic@arhitekt.unizg.hr
Faculty of Architecture
Kačićeva 26, 10 000 Zagreb, Croatia
Tel: (+385 1) 4639 176

The price of the issue is €15 + mailing expenses €5 for European countries and €10 for other parts of the world.

The amount is payable to:

ACCOUNT NAME:	Hrvatsko društvo za geometriju i grafiku Kačićeva 26, 10000 Zagreb, Croatia
IBAN:	HR8623600001101517436